

PUBLICATIONS OF
THE UNIVERSITY OF EASTERN FINLAND



UNIVERSITY OF
EASTERN FINLAND

**Dissertations in Science,
Forestry and Technology**

XUDAN ZHU

**The mechanisms
behind aquatic
browning in
boreal catchments**

**The mechanisms behind aquatic browning
in boreal catchments**

Xudan Zhu

The mechanisms behind aquatic browning in boreal catchments

Publications of the University of Eastern Finland
Dissertations in Science, Forestry and Technology
No 41

University of Eastern Finland
Joensuu
2024

Academic dissertation

To be presented by permission of the Faculty of Science, Forestry and
Technology for public examination in the Auditorium N100 in the Natura
Building at the University of Eastern Finland, Joensuu, on 10th of May 2024,
at 10 o'clock noon

PunaMusta Oy
Joensuu, 2024
Editor: Raine Kortet

ISBN: 978-952-61-5175-5 (nid.)

ISBN: 978-952-61-5176-2 (PDF)

ISSNL: 2954-131X

ISSN: 2954-131X (nid.)

ISSN: 2954-1484 (PDF)

Author's address: Xudan Zhu
University of Eastern Finland
Depart. of Environmental and Biological Sciences
P.O. Box 111
80101 JOENSUU, FINLAND
email: xudan.zhu@uef.fi

Supervisors: Professor Frank Berninger, Ph.D.
University of Eastern Finland
Depart. of Environmental and Biological Sciences
P.O. Box 111
80101 JOENSUU, FINLAND
email: frank.berninger@uef.fi

Professor Jukka Pumpanen, Ph.D.
University of Eastern Finland
Depart. of Environmental and Biological Sciences
P.O. Box 111
70211 KUOPIO, FINLAND
email: jukka.pumpanen@uef.fi

Professor Christina Biasi, Ph.D.
University of Eastern Finland
Depart. of Environmental and Biological Sciences
P.O. Box 111
70211 KUOPIO, FINLAND
email: christina.biasi@uef.fi

Reviewers: Professor emerita Leena Finér, Ph.D.
Natural Resources Institute Finland
Yliopistokatu 6
80100 JOENSUU, FINLAND
email: leena.finer@gmail.com

Docent Aida BARGUES TOBELLA, Ph. D
Swedish University of Agricultural Sciences
Depart. of Forest Ecology and Management
90183 Umeå, Sweden
email: aida.bargues.tobella@slu.se

Opponent:

Professor William H. McDowell, Ph.D.
University of New Hampshire
Depart. of Natural Resources & the Environment,
NH 03824 Durham, United State
email: Bill.McDowell@unh.edu

Zhu, Xudan

The mechanisms behind aquatic browning in boreal catchments

Joensuu: University of Eastern Finland, 2024

Publications of the University of Eastern Finland

Dissertations in Science, Forestry and Technology; 41

ISBN: 978-952-61-5175-5 (nid.)

ISBN: 978-952-61-5176-2 (PDF)

ISSNL: 2954-131X

ISSN: 2954-131X (nid.)

ISSN: 2954-1484 (PDF)

ABSTRACT

Increases in dissolved organic carbon (DOC) concentrations, or browning, have occurred in many freshwater ecosystems across Europe and North America in recent decades, giving the water a brownish color. Several mechanisms have been proposed to explain aquatic browning, but consensus regarding the relative importance of recovery from acid deposition, climate change, and land management remains elusive. Meanwhile, elevated CO₂, longer growing seasons and permafrost thaw induced by climate change have increased terrestrial productivity, which may alter the export of DOC from terrestrial to aquatic ecosystems. Although the link between terrestrial greening and aquatic browning has recently gained more attention, it is not yet well established. Moreover, heterogeneities of browning across space and time have been observed, but the reasons behind these differences are still unclear.

The objectives of this thesis are to understand how varied factors affect short-term variations and long-term trends of DOC concentrations in boreal catchments, focusing especially on the nexus between terrestrial carbon (C)

export and stream DOC concentrations, and the causes of spatial and temporal heterogeneity in browning across boreal catchments. The thesis is based on three studies. **Study I** developed methods to predict real-time high-frequency DOC concentrations in catchments using in-situ UV-Vis spectrophotometers, which can be applied especially in remote areas to save time and money. **Study II** used the methods developed by Study I to predict high-resolution time series DOC concentrations and analysed the relationship between terrestrial productivity and short-term DOC variations across boreal catchments. **Study III** extended the analysis to longer time periods and wider range catchments by integrated mechanisms (recovery from acid deposition, climate change, and site characteristics), quantified the contributions of multiple drivers on long-term DOC trends and provided an explanation for the spatiotemporal heterogeneity of browning.

Collectively, this thesis revealed that increased terrestrial productivity induced by climate change can alter terrestrial DOC exports to aquatic ecosystems through priming effect. Whereas no single mechanism can fully explain long-term DOC trends; instead, recovery from sulfate deposition, terrestrial productivity, discharge, and temperature jointly shaped DOC trends. Site characteristics (catchment size and land cover type) can affect the response rate of DOC to these drivers leading to the spatial heterogeneity of browning across sub-catchments. Moreover, browning has weakened in the last decade as sulfate deposition has fully recovered and other current drivers are insufficient to sustain the long-term DOC trends. My work improves our mechanistic understanding of surface water DOC regulation in boreal catchments, confirms the importance of DOC fluxes in regulating ecosystem C budgets and highlights the significance of considering multifaceted, spatially structured, and nonstationary drivers when predicting long-term DOC trends in the future.

Keywords: Water quality; UV-Vis spectrophotometer; spectral absorbance; dissolved organic carbon; discharge; terrestrial productivity; sulfate deposition; temperature; landscape; catchment size; boreal catchments; integrated mechanisms.

Acknowledgements

I am extremely grateful to my main supervisor, Prof. Frank Berninger, for his support, encourage and guidance. At certain points in our lives, we may encounter individuals who have the power to completely reshape our life course. Frank is such a person for me. He is like a lighthouse that guides me when I am lost, gives me complete freedom, trust, and inspiration. And the most crucial lesson I have learned from Frank is that we never know what will happen if we do not take the chance and try. Thank you for leading me to Joensuu, a truly marvellous place where I have met so many wonderful people, encountered numerous delightful experiences and gotten closer to whom I want to be.

I would like to express my sincerely thanks and appreciation for my other supervisors, Prof. Jukka Pumpanen and Prof. Christina Biasi for their kindly help, advice, and comments throughout my PHD. I especially appreciate Jukka for his kindness and generosity to support me financially during my gap months and covered all the fee when I took a course in SLU. We had so many happy times together for fieldwork, conference, and hiking in different places. I also appreciate Prof. Hjalmar Laudon for his hospitality during my visit in Umeå and for providing me with so many chances for cooperation. I extend my sincere gratitude to Prof. Chunyang Li, who has an indelible impact on my career. I wish to be as powerful, wise, generous, and selfless as Professor Li and to inspire more people with this spirit in the future!

It has been amazing to be able to work with people who are passionate about their work. Therefore, I would like to thank my group members and collaborator, Xuan Zhou, Kajar Köster, Egle Köster, Niko Kinnunen, Taija Saarela, Tiina Kolari, Teemu Tahvanainen, Markku Keinänen, Anne Ojala, Jessenia Polack Huaman and Mathilde Rebiffé. Your presence has made my research life much easier and more colourful.

My deepest thanks to my dear colleague friends, Tuula Toivanen, Sarita Keski-Saari, Jaakko Haverinen, Marja Noponen, Sari Kontunen-Soppela, Bhabishya Gurung and Mika Pajari. Your kindness, patience and support

make Joensuu as my second hometown. Because of you, I feel more connected to Finnish culture and have adapted more rapidly to the life here.

I would also like to express my gratitude to my lovely friends: Manqing Tian, Fangfang Li, Yaxin Ren, Fanglei Wu, Chengmin Zhou, Mengwen Guo and Meilan Luo. Thanks to you, my spare time is never boring and full of laughter and joy. We play badminton, go hiking, running, skiing, shopping, and sightseeing together. Every festive season, we gather to comfort each other with delicious food and ease homesickness with companionship. Those sweaty and foody times will shine in my memories and never fade! Special thanks to my bestie Tingting Zhu, who travelled all the way from China to Joensuu carrying the best wishes of my Chinese friends by the end of my PHD. This visit was a great inspiration and comfort to me.

My family has always motivated and supported me in pursuing my goals. It has meant a great deal in pursuit of my PHD. No matter where or whom I will be, their love and support always follow me and drive me forward. I am sincerely grateful to my parents who respect all my decisions, and my sister who always pushes me to achieve my best as well as my lovely nieces who are never stinted to show their love by video calls.

I owe a dearest thanks to my darling boyfriend--Liang Chen. Rewind to 2018 when I was running several restaurants in China, Liang brought a bright light into my chaotic, repetitive life. He gave me the strength and company to step out of the life that had trapped me and encouraged me to follow my inner voice. Then I quit my business and picked up research again. Thereafter, my dream became our dreams, and we came together to Finland for a new life. Doctoral study is never an easy task, but as we teamed up, covered each other, and rejoiced every achievement, the whole journey was enjoyable albeit challenging. Hope we will have more wonderful and new experiences.

Finally, this work could not happen without the financial support from CIMO Fellowship and Kone Foundation. 🌻 🧡 🌻

Joensuu, December 2023
Xudan Zhu

LIST OF ABBREVIATIONS

C	carbon
CO ₂	carbon dioxide
DOC	dissolved organic carbon
DOM	dissolved organic matter
SOC	soil organic carbon
SOM	soil organic matter
UV-Vis	ultraviolet-visible
S	sulfur
SO ₄	sulfate
NDVI	Normalized Difference Vegetation Index
MSR	multiple stepwise regression
PLS	partial least-squares regression
PCR	principal component regression
DLMs	distributed-lag linear models
EC	eddy covariance
GPP	gross primary productivity
NEP	net ecosystem production
RE	ecosystem respiration
MODIS	the Moderate Resolution Imaging Spectroradiometer
MGPP	GPP from moderate resolution imaging spectroradiometer
NDVI	normalized difference vegetation index
AIC	Akaike information criterion
R	the correlation coefficient
R ²	the explanatory power
RMSD	root-mean-square deviation
STD	standard deviation
DEM	digital elevation model

LIST OF ORIGINAL PUBLICATIONS

This thesis is based on data presented in the following articles, referred to by the Roman Numerals I–III.

- I Zhu, X., Chen, L., Pumpanen, J., Keinänen, M., Laudon, H., Ojala, A., Palviainen, M., Kiirikki, M., Neitola, K., & Berninger, F. (2021). Assessment of a portable UV–Vis spectrophotometer's performance for stream water DOC and Fe content monitoring in remote areas. *Talanta*, 224, 121919.
- II Zhu, X., Chen, L., Pumpanen, J., Ojala, A., Zobitz, J., Zhou, X., Laudon, H., Palviainen, M., Neitola, K., & Berninger, F. (2022). The role of terrestrial productivity and hydrology in regulating aquatic dissolved organic carbon concentrations in boreal catchments. *Global Change Biology*, 28(8), 2764–2778.
- III Zhu, X., Berninger, F., Chen, L., Larson, J., Sponseller, R. A., & Laudon, H. (2024). Several mechanisms drive the heterogeneity in browning across a boreal stream network. Submitted manuscript.

The above publications have been included at the end of this thesis with their copyright holders' permission.

AUTHOR'S CONTRIBUTION

- I) Author planned the experiments together with Frank Berninger. Author performed the data collection, lab work, statistical analysis, and the interpolation of the results. Author wrote the original draft and reviewed the paper with the comments from other co-authors.

- II) Author was responsible for the conceptualization in collaboration with Frank Berninger. Author performed the data collection, lab work, statistical analysis, and the interpolation of the results. Author wrote the original draft and reviewed the paper with the comments from other co-authors.

- III) Author was responsible for the conceptualization in collaboration with Hjalmar Laudon and Frank Berninger. Author performed the data collection and interpolation, statistical analysis, and the visualization of the results. Author wrote the original draft and reviewed the paper with the comments from other co-authors.

Table of Contents

ABSTRACT	7
Acknowledgements	9
1 Introduction	17
1.1 Aquatic browning	17
1.1.1 Composition of DOC.....	18
1.1.2 Source of DOC.....	18
1.1.3 Impacts of browning.....	19
1.2 Potential mechanisms behind browning	20
1.2.1 Sulfate deposition.....	20
1.2.2 Land use change	21
1.2.3 Climate change	22
1.3 Spatiotemporal heterogeneity of browning	23
1.3.1 Browning over space	23
1.3.2 Browning over time	24
1.4 How to monitor browning.....	25
2 Aims of the thesis	27
3 Materials and methods	29
3.1 Study sites and sampling.....	29
3.1.1 Study sites	29
3.1.2 Sampling and DOC measurement.....	31
3.2 Build the absorbance–DOC prediction models (I).....	32
3.2.1 Spectral absorbance measurement.....	33
3.2.2 Multilinear regressions.....	33
3.3 Lag effect of terrestrial productivity on DOC (II).....	35
3.3.1 High–frequency DOC prediction.....	36
3.3.2 Environmental factors.....	36
3.3.3 Lag–effect models.....	37
3.4 Mechanisms drive the heterogeneity in browning (III)	39

3.4.1 Environmental trends.....	40
3.4.2 Data collection and interpolation.....	40
3.4.3 Statistical analysis	42
4 Results and discussion	45
4.1 Performance of absorbance–DOC prediction models (I).....	45
4.2 Link terrestrial greening with aquatic browning (II)	50
4.3 Integrated mechanisms to reveal variations in DOC (III)	57
4.4 Drivers of long-term DOC trends over time and space (III)	61
5 Conclusions and future perspectives.....	67
Bibliography	69

1 Introduction

1.1 Aquatic browning

Browning, also known as brownification, indicates a notable darkening color of the water (Fig.1). This phenomenon has been documented in a substantial number of northern freshwater environments in recent decades (Evans et al., 2006; Clark et al., 2010; Lawrence & Roy, 2021). The change in the color of water has primarily been attributed to elevated levels of dissolved organic carbon (DOC) from terrestrial sources (Weyhenmeyer et al., 2014). The presence of DOC, particularly in the form of humic and fulvic acids (Wilken et al., 2018), enhances the capacity of water to absorb radiant light (Worrall & Burt, 2010). Although browning could also be caused by an increase in iron concentrations (Weyhenmeyer et al., 2014), this study mainly focuses on the role of DOC in browning.



Figure 1. Aquatic browning in boreal catchments (Photo: Xudan Zhu)

1.1.1 Composition of DOC

Dissolved organic matter (DOM) is commonly discussed in studies on dissolved organic substances. However, in the literature, DOM is frequently interchanged with DOC, even though DOC constitutes only a portion of the overall DOM composition (Pagano et al., 2014). DOC is composed of various carbon (C)-containing molecules, such as lignin, humic acids, fulvic acids, and other complex organic substances (Thurman, 1985). These organic compounds are typically small enough to pass through a 0.45µm filter, enabling them to remain in a dissolved form in water (McDonald et al., 2004). Based on its composition, DOC can be categorized into humic and non-humic fractions (Leenheer & Croué, 2003). The humic fraction can be subdivided into humic acids, fulvic acids, and humin based on solubility properties at specific pH levels (McDonald et al., 2004) and molecular weight (Malcolm, 1990) (Fig.2).

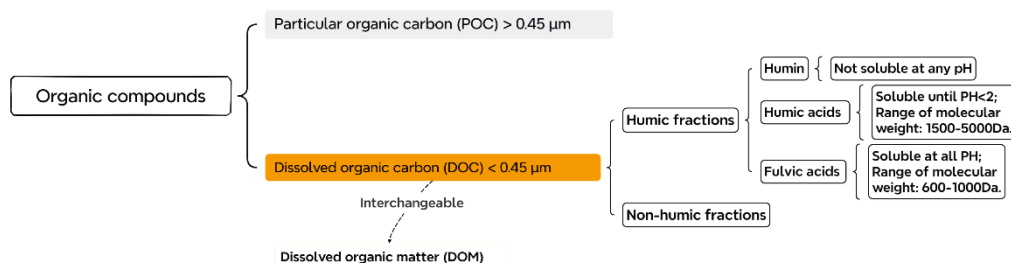


Figure 2. Composition of dissolved organic carbon (DOC)

1.1.2 Source of DOC

Aquatic ecosystems are linked to surrounding terrestrial ecosystems via material and energy transfers. Nearly 2 Pg of terrestrial organic C is transported or stored by streams and rivers globally on annual basis, which represents a significant portion of the global annual terrestrial net ecosystem production (Battin et al., 2008; Tranvik et al., 2009). Allochthonous DOC with terrestrial origins is primarily produced as a result of C assimilation via primary production in higher order plants. The DOC production process is mostly dependent on the subsequent microbial degradation or the leaching of partially decomposed plant litter in soils

(Kalbitz et al., 2000) (Fig. 3). Plants may contribute to DOC production via biotic and abiotic pathways. Through biotic pathways, plant material can directly introduce organic matter into its surroundings via root exudates which can be transformed into DOC through enzyme-catalyzed reactions (Kalbitz et al., 2000). Through abiotic pathways, the process of DOC leaching from the tree canopy is very important in forest ecosystems (Ukonmaanaho et al., 2014). Part of plant biomass is consumed by herbivores, and their dead residues and subsequent manure constitute secondary sources of net DOC (Findlay and Sinsabaugh, 2003). The release of organic matter through the breakdown of microbial biomass can also contribute to DOC production (Kalbitz et al., 2000) (Fig.3).

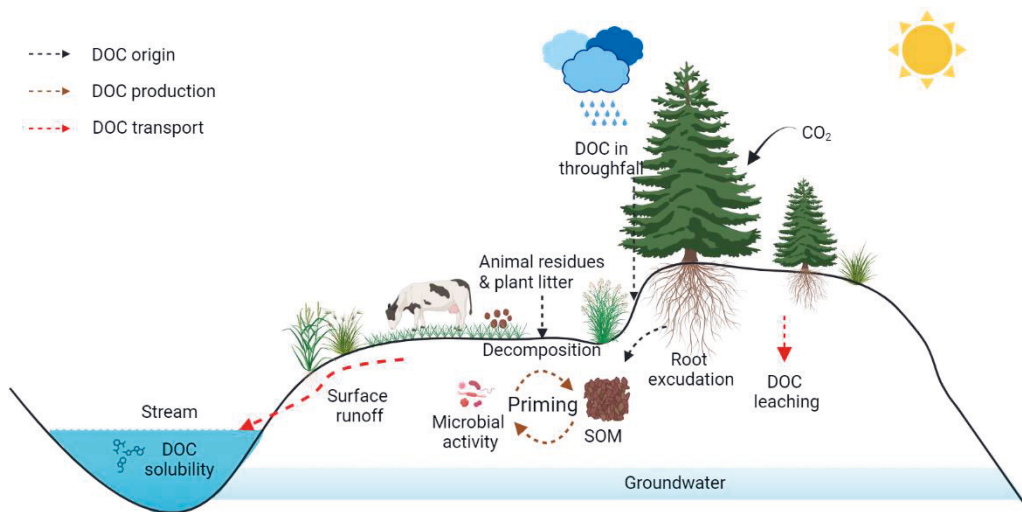


Figure 3. Simplified view of dissolved organic carbon (DOC) transfer from terrestrial to aquatic ecosystems. SOM is soil organic matter.

1.1.3 Impacts of browning

The concentration and flux of DOC hold significant importance, due to their profound effects on various aspects of aquatic ecology (Findlay & Sinsabaugh, 2003). First, increased coloration of water caused by elevated DOC supply affects light penetration and thermal regimes which can alter predator-prey interactions and food webs of aquatic ecosystems (Conley et al., 2011; Leach et al., 2019; Kritzberg et al., 2020). Second, it may contribute to eutrophication in coastal ecosystems, leading to hypoxia (Conley et al.,

2011) and the loss of biodiversity (Villnäs & Norkko, 2011). Furthermore, increasing DOC reduces the value of aquatic landscapes from recreational and aesthetic aspects and boosts the cost of purifying drinking water (Freeman et al., 2004; Ekström, 2013). Finally, the DOC flux from terrestrial to aquatic ecosystems is an important aspect of the global C cycle (Aitkenhead & McDowell, 2000). Globally, riverine DOC fluxes account for approximately 25–50% of the total C exports to oceans (Ciais et al., 2008; Huang et al., 2012; Drake et al., 2018). Increased DOC has the potential to mobilize large terrestrial C pools and affect C fluxes in both the atmosphere and the ocean (Mann et al., 2012; Öquist et al., 2014).

1.2 Potential mechanisms behind browning

The past few decades have witnessed an increase in DOC concentrations across many catchments in the Northern Hemisphere. Potential drivers have been proposed to explain this phenomenon, include recovery from acidification (Kang et al., 2018; Meyer-Jacob et al., 2019), land use change (Meyer-Jacob et al., 2015; Wilson & Xenopoulos, 2008) and climate change (Asmala et al., 2019; Finstad et al., 2016). The following sections explain the mechanisms by which these distinct factors may affect the production, transport, and solubility of DOC from surrounding soils.

1.2.1 Sulfate deposition

Sulfate (SO_4) deposition has exhibited significant fluctuations over the past century, with a notable rise following the Second World War, and a subsequent marked reduction as a result of international legislation curbing emissions (Kritzberg et al., 2020). Recovery from sulfur (S) deposition after its peak in the 1970s is a widely recognized driver of browning (Monteith et al., 2007; Pagano et al., 2014; Lawrence & Roy, 2021). Acidity and ionic strength play significant roles in the mechanism of recovery from S deposition, contributing to an increase in DOC. A increase of 0.5 pH units can result in an approximately 50% proportional rise in DOC release and can affect the microbial-mediated production of DOC (Tipping & Woof, 1990). Increased pH can also stimulate DOC mobilization due to enhanced enzyme

activities (Pind et al., 1994). Meanwhile, decreasing ionic strength enhances colloidal dispersion and organic matter disaggregation by expanding the diffuse double layer. This, in turn, increases the solubility and transport of DOC and affects its lateral export from soils (Evans et al., 2012; Lawrence & Roy, 2021).

Negative correlation between DOC concentration and SO₄ deposition has been widely reported. Previous studies also documented instances where declining S deposition is not accompanied by an increase in DOC levels (Hudson et al., 2003; Worrall & Burt, 2007), or areas with low acid deposition still experienced an increase in DOC (Laudon & Sponseller, 2018). Apparently, recovery from acid deposition alone cannot fully explain browning on a long-term scale (Johansson et al., 2010; Kritzberg, 2017). Hence, a more complex combination of drivers should be considered to improve our understanding of the mechanism behind increasing DOC.

1.2.2 Land use change

Land-use change such as reforestation, forest management and agricultural expansion, can have significant impacts on ecosystems, hydrology, and biogeochemical cycling. Recently, there has been mounting evidence that land-use change can also drive increases in aquatic DOC, either by enhancing the input of terrestrial organic C or by altering DOC routing from soils to streams (Kritzberg, 2017; Härkönen et al., 2023). For instance, during the last century southern Sweden has shifted from an open landscape largely shaped by agriculture and dominated by grasses and deciduous trees to a landscape marked by extensive forestry practices that is dominated by conifers (Lindbladh et al., 2014). Since coniferous forests tend to accumulate more soil organic carbon (SOC) than open land and deciduous forests, afforestation is also an important factor in browning over time (Sobek et al., 2007). However, recent research showed that agricultural expansion is positively related to stream DOC concentrations (Graeber et al., 2012). Agricultural practices such as tillage, particularly plowing disrupt the physical structure of organo-mineral aggregates resulting in a loss of soil organic matter (SOM), of which a part is potentially lost as DOC (Ogle et al., 2005; Ewing et al., 2006). Moreover, Härkönen et al., (2023) highlighted that

conventional forest management involving clear-cutting, site preparation, and drainage maintenance leads to increased organic C leaching and elevated C-rich runoff. The effects are attributed to variations in hydrology, peat decomposition, and peat exposure. Although the conclusions regarding land-use change are inconsistent, its importance as a factor behind browning should not be underestimated.

1.2.3 Climate change

Climate change-related impacts, such as higher temperature (Keller et al., 2008), altered hydrology (Tiwari et al., 2022), permafrost thaw (Tank et al., 2016) and elevated atmospheric CO₂ (Schlesinger & Andrews, 2000), have also been suggested as drivers of browning. Especially in Arctic zone with high peatlands cover, increasing precipitation events and permafrost destruction can degrade peatlands and promote DOC export (Minayeva et al., 2017). Freeman et al. (2004), however, claimed that there is insufficient evidence to support warming, increased discharge, or changing precipitation patterns. Instead, CO₂-mediated stimulation of primary productivity could be responsible for the rise in exported DOC from peatlands. Many northern and alpine regions have witnessed a prominent “greening” trend, which has led to a rise in vegetation, biomass C stores, and forest cover. This trend has been variously attributed to climate change, CO₂ fertilization, nitrogen deposition, decreased grazing activity, and less intense forestry harvesting (Guay et al., 2014; de Wit et al., 2015).

Meanwhile, the link between terrestrial greening (Myers-Smith et al., 2020) and aquatic browning export has garnered more attention (Larsen et al., 2011; Mzobe et al., 2018; Phoenix & Treharne, 2022), which could be particularly important in regions not exposed to high rates of acid deposition or major land use changes. Increases in vegetation productivity could increase DOC via increases in SOM, or via a process called priming effect (He et al., 2020). Priming alters the decomposition of SOM after the input of new C. These shifts in decomposition can result in either positive or negative effects on DOC production, depending upon the conditions (Linkosalmi et al., 2015; Dijkstra et al., 2013; Kuzyakov, 2002). Priming accelerates DOC fluctuations because microbial biomass and functions

continue to change over days to weeks after a change in the supply of easily available C.

Previous studies have examined the role of direct priming on DOC concentrations by proxy measurements (Finstad et al., 2016; Pumpanen et al., 2014). Finstad et al. (2016) demonstrated a positive correlation between increasing the Normalized Difference Vegetation Index (NDVI), an indicator derived from remote sensing that reflects plant leaf area and productivity, and DOC concentrations. Pumpanen et al. (2014) demonstrated that the average annual DOC concentration was influenced by the forest productivity of the preceding year. Though both studies point to the importance of priming, the evidence is on a yearly scale, which is longer than the response time (days to weeks) of microbial communities to resource changes. Additionally, the delivery of fresh photosynthates to the roots, changes in microbial biomass and the decomposition following a change in root exudation, and hydraulic delays necessary to transport DOC from the soil to water bodies can lead to a delay of several days to several weeks (Wen et al., 2020). Hence, the connections between primary production and DOC concentrations in surface waters are not easy to detect, and direct regressions of DOC concentrations and photosynthetic production are not plausible. Therefore, resolving these challenges requires high-frequency time series data that simultaneously capture chemical, hydrological, and terrestrial ecosystem parameters, but also new analytical tools that can isolate potentially non-stationary causal connections.

1.3 Spatiotemporal heterogeneity of browning

Besides the tentatively established link between terrestrial greening and aquatic browning, another major challenge to understanding the mechanisms behind browning is that multiple drivers can co-occur, interact, and even shift in importance over space and time.

1.3.1 Browning over space

The regional heterogeneity in historical acid deposition may be the origin of certain variations in the suggested drivers of browning across studies (Clark

et al., 2010). For example, at regional scales, variable deposition history may determine the potential for other factors, including climate warming and changes in hydrology, to drive DOC increases (Räike et al., 2016). However, even closely co-located streams with identical deposition histories can exhibit highly variable DOC trends (Fork et al., 2020), suggesting that local catchment properties can mediate responses to broader-scale drivers. In boreal landscapes, small-scale differences in mire versus forest cover appear to play this role, with DOC trends being far stronger in forest-dominated streams than in mire-dominated streams (Fork et al., 2020). The mechanistic basis for these patterns remains unresolved but such distinct DOC trends suggest fundamental differences in how different types of land cover affect the response to historical acid inputs. Moreover, moving beyond headwater systems, increases in catchment size can lead to greater supplies of deep, DOC-poor groundwater (Tiwari et al., 2018), and these inputs can also regulate and/or dampen DOC trends for larger streams and rivers (Fork et al., 2020). Overall, while broad-scale environmental changes are clearly influencing DOC production and supply from catchment soils, predicting the extent of browning in catchment networks also requires that we consider catchment size and landcover type as modulating factors.

1.3.2 Browning over time

These differences in temporal scales may also give rise to distinct drivers of browning, particularly regarding the pace of acid deposition recovery. Based on the long-term monitoring programs in the northern hemisphere, most regions are exhibiting browning trends (Lapierre et al., 2021; Lepistö et al., 2021; Redden et al., 2021). de Wit et al., (2016) observed positive trends of DOC in 474 boreal and subarctic catchments across Europe from 1990 to 2013 and concluded that future changes in precipitation are likely to promote continued browning. Conversely, Eklöf et al. (2021) reported that the widespread increases in DOC concentrations across Sweden between 1990 and 2010 ceased a decade ago, coinciding with the culmination of acidification recovery. These conflicting findings cast doubt on the hypothesis that ongoing pressures, such as climate change, are driving widespread browning. Therefore, understanding the relative contributions

of each of the proposed mechanisms above on different spatial and temporal scales remains critical for generating accurate predictions about future browning trends.

1.4 How to monitor browning

Traditionally, to detect browning, researchers must visit the sites, collect water samples, and filter, freeze, and transfer the samples before they can measure DOC contents with a desktop analyser in the lab. However, DOC is often exported during extreme rainfall or snowmelt events, which are usually of short duration and challenge the capture of DOC exports by physical water sampling (Raymond et al., 2016). Therefore, high-frequency monitoring of pulse events is critical. Advancements in technology and reduced costs have led to the growing adoption of in-situ sensors for monitoring purposes, particularly in remote areas where physical sampling can be costly (Langergraber et al., 2003; Avagyan et al., 2014). Ultraviolet-visible (UV-Vis) spectrophotometry is an emerging technology for measuring and monitoring DOC concentrations in situ. It can determine real-time spectral absorbance in waterbodies (Avagyan et al., 2014) and capture rapid changes in response to environmental conditions. Thereafter, algorithms calculate DOC concentrations based on absorbance at a specific wavelength or multiple wavelengths. Different wavelengths (e.g., 254, 255, 350, 400 nm) have been used to estimate DOC concentration from spectral absorbances (Laudon et al., 2004; Wallage & Holden, 2010; Waterloo et al., 2006). The performance in predicting DOC concentrations varied by method (Laudon et al., 2004; Wallage & Holden, 2010). A previous study suggested using absorbance from 2–5 wavelengths as a proxy for DOC concentration (Avagyan et al., 2014). The increasing prevalence of UV-Vis spectrophotometers, complicated by conflicting conclusions regarding absorbance and DOC prompted the question of how to establish and calibrate relationships between spectral absorbances and DOC concentrations in water.

2 Aims of the thesis

Overall, my thesis aims to enhance knowledge of the mechanisms behind aquatic browning in the northern hemisphere. To accomplish this, I will address three key objectives. First, I aim to develop an improved method for predicting high-frequency DOC concentrations in aquatic ecosystems. Second, I will link aquatic browning with increased terrestrial productivity by priming effect. Last, my study will provide a comprehensive analysis of the factors influencing DOC patterns in boreal catchments, encompassing both spatial variation across different catchments and temporal variations over an extended period. By accomplishing these goals, my thesis will contribute significant insight into the mechanisms governing the release of DOC into natural waters and may improve our capacity to predict and model forthcoming alterations in the chemistry and functioning of aquatic environments. This knowledge becomes particularly crucial in the context of impending climate change, since understanding DOC dynamics can aid in anticipating and managing potential impacts on aquatic ecosystems.

- 1) Study I compared the performance of an in-situ UV-Vis spectrophotometer (S::can) to a laboratory benchtop instrument (UV1800) in measuring water absorbance and then analyzed various calibration strategies for estimating high-frequency DOC concentrations by spectral absorbance from S::can.
- 2) Study II tested the delay effects of terrestrial productivity (from eddy covariance tower) on short-term DOC variations using high-frequency time series data.
- 3) Study III combined multiple potential mechanisms to reveal the underlying drivers of DOC variations and then quantified the contributions of the identified drivers to long-term DOC trends from both spatial and temporal perspectives.

3 Materials and methods

3.1 Study sites and sampling

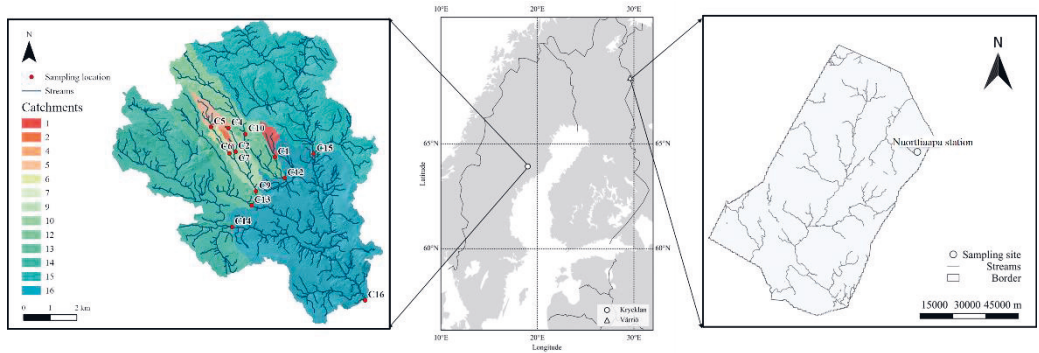


Figure 4. Study sites in Krycklan, Sweden and Nuorttiaapa measuring station, Finland.

3.1.1 Study sites

In northern Sweden, Krycklan sub-catchments (C1–C16) are situated in the boreal landscape, approximately 50 km northwest of the city of Umeå (64° 14'N, 19°46'E; Fig. 4). The site characteristics of all sub-catchments are shown in Table 1. Underlying bedrock in the catchment consists of 94% metasediments/metagraywacke, 4% acid and intermediate metavolcanic rocks, and 3% basic metavolcanic rocks. Above the highest postglacial coastline across Krycklan (257 m asl), glacial till dominates quaternary deposits, while post-glacial sedimentary deposits dominate the soils below it (Laudon et al., 2013). Forests cover 87% of the area and are predominantly Scots pine (*Pinus sylvestris*, 63%) and Norway spruce (*Picea abies*, 26%) with 9% deciduous forest. Peatlands cover 9% of the catchment and are dominated by Sphagnum species. The climate is characterized as a cold temperate humid type with persistent snow cover during the winter season. The 30-year mean annual precipitation (1981–2010) was 614 mm of which 35% was as snow during winter (December to April), average annual runoff was 311 mm, giving an annual average evapotranspiration of 303 mm. The

mean annual temperature was 1.8 °C, January -9.5°C and July +14.7 °C. The average snow water equivalent for the last 40 years of record was 180 mm, ranging from 64 mm (1996) to 321 mm (1988). The 40-year average duration of winter snow cover was 167 days (Laudon et al., 2021a).

In Finland, Yli-Nuortti is a catchment near the Nuorttiaapa measuring station in Värriö (67°44'N, 29°27'E), about 120 km north of the Arctic Circle (Fig. 4). The watershed covers about 40 km² above the measurement point of which 25% is peatlands and 5% is covered by alpine vegetation on the top of the fells while the rest of the catchment is dominated by pine forests on glacial tills (Table 1). There are no lakes above the measurement station. According to the statistics of the Finnish Meteorological Institute (1981–2012), the mean annual air temperature was -0.5°C. The mean temperature in January was -11.4°C and in July was 13.1°C. The mean annual precipitation was 601 mm, mean annual runoff 212 mm and annual average evapotranspiration 389 mm. The average number of days with snow cover was 205–225 days (Pohjonen et al., 2008).

Study I focused on C4 and C5 in Krycklan, Sweden (2016–2019) and Nuorttiaapa measuring station (NT) in Värriö, Finland (2018–2019) due to the availability of spectral absorbance data from the in-situ UV-Vis probes (spectro:lyser, S:CAN Messtechnik GmbH, Austria).

Study II applied data from four catchments of different sizes and land cover types. C2, C4, C6 (2016–2018) and NT (2018–2020) were selected because of their fit for the site characteristics and the accessibility of C flux data from the nearby eddy covariance (EC) tower. In the later part of Study II, the size and landscape of each catchment were noted after the site name (C2[S-forest], C4[S-mire], C6[M-mix], and NT[L-mix]) to aid comparison. The letters 'S', 'M' and 'L' indicate for the small, medium, and large catchment size, respectively, while the symbols 'forest', 'mire' and 'mix' describe the different types of landscapes (forest, mire, and forest-mire mixed).

Study III was conducted in all 13 sub-catchments in Krycklan with varied sizes (12 to 6790 ha) and landscape types under long-term monitoring (2003–2021). Due to equipment failure, the data for 2019 – 2021 are missing in C12, C14, and C15.

Table 1. Study site information in Sweden and Finland.

Site ^a	Country	Size [ha]	Lake [%]	Forest [%]	Mire [%]	Open land [%]	Arable [%]	Alpine vegetation [%]	Land cover ^b	Study I	Study II	Study III
C1	Sweden	48	0	98	0	0	0	0	forest			✓
C2	Sweden	12	0	100	0	0	0	0	forest		✓	✓
C4	Sweden	18	0	56	44	0	0	0	mire	✓	✓	✓
C5	Sweden	65	6	54	40	0	0	0	mire	✓		✓
C6	Sweden	110	4	72	24	0	0	0	mix		✓	✓
C7	Sweden	47	0	82	18	0	0	0	mix			✓
C9	Sweden	288	2	84	14	0	0	0	mix			✓
C10	Sweden	336	0	74	26	0	0	0	mix			✓
C12	Sweden	544	0	83	17	0	0	0	mix			✓
C13	Sweden	700	1	88	10	0	1	0	mix			✓
C14	Sweden	1410	1	90	5	1	3	0	mix			✓
C15	Sweden	1913	2	83	14	1	0	0	mix			✓
C16	Sweden	6790	1	87	9	1	2	0	mix			✓
NT	Finland	4000	0	70	25	0	0	5	mix	✓	✓	

^a C5 is the outlet to a headwater humic lake, NT is Nuorttiaapa measuring station in Värriö, Finland.

^b Landcover type was defined by percent mire coverage, with <2% mire as “forest”, 2–30% mire as “mix”, and >30% mire as “mire”.

3.1.2 Sampling and DOC measurement

All water samples were collected from the surface water (depth of 25cm) at each site by acid-washed, high-density polyethylene bottles. In Finland, the sampling frequency was monthly from fall to winter, biweekly in spring and weekly in summer. In Sweden, we typically took samples from each site on the same day, monthly during the winter, fortnightly from summer to fall, and every third day during the snow-melting season. There were also several samples from each site for different measurements (e.g., absorbance, DOC, SO₄, pH). All samples were filtered the day after collection (0.45µm MCE membrane, Millipore) and frozen at -21°C. Before analysis, water samples were moved to 4°C for melting (not reused).

Following acidification to remove inorganic compounds, DOC concentration was detected by heat oxidation and infrared detection (Multi N/C 2100, Analytik Jena, Germany) in Finland and, by catalytic oxidation combustion (Shimadzu TOC-5000, Kyoto, Japan) in Sweden (Laudon et al., 2011).

3.2 Build the absorbance–DOC prediction models (I)

Building Study I’s absorbance–DOC prediction models required the following three steps. 1) Field work: collect and filter water samples, measure real-time absorbance by in-situ S::CAN; 2) Lab work: analyze the water samples for spectral absorbance and DOC concentrations; 3) Validation and Modelling: apply multilinear regressions to the combined data set from in-situ monitoring and lab measurements (Fig.5).

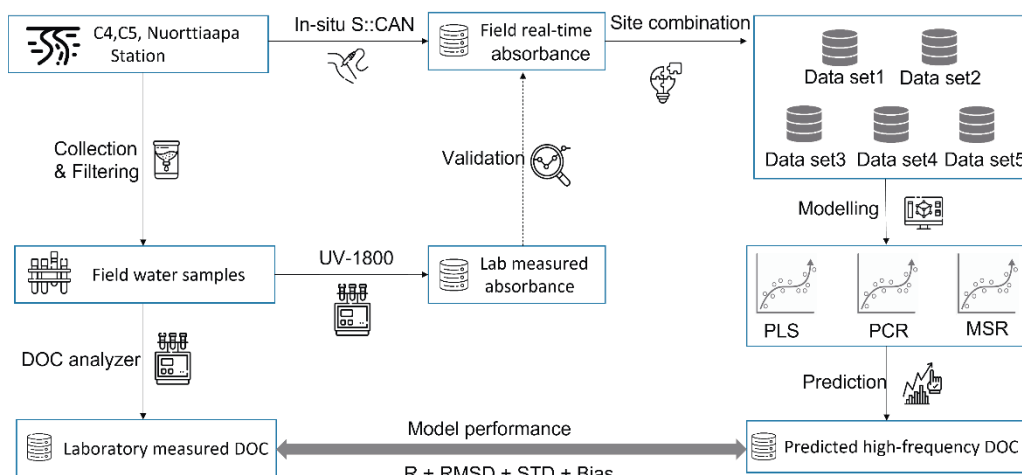


Figure 5. The schematic presentation of Study I—Building absorbance – DOC prediction models, including fieldwork, lab measurements, validation, and modeling. PCR = principal component regression; PLS = partial least-squares regression; MSR = multiple stepwise regression.

3.2.1 Spectral absorbance measurement

In-situ UV-Vis probes (spectro:lyser, S::CAN Messtechnik GmbH, Austria) were installed in Krycklan catchments (C4 and C5) on May 9, 2016 and in Yli-Nuortti river (NT) on June 12, 2018. Real-time spectral absorbance was measured hourly cross wavelength from 220 to 732.5 nm (at 2.5 nm intervals with a path length of 35 mm) and the results were saved in an internal datalogger.

Laboratory spectral absorbance was analyzed with a UV1800 UV-Vis spectrophotometer (Shimadzu, Kyoto, Japan) between 200 and 800 nm with a 10 mm pathlength quartz cell (acquisition step: 1 nm; scan speed: slow).

3.2.2 Multilinear regressions

The data sets included collinear variables with a greater number of independent variables than observations, which led to the use of the following regression methods: principal component regression (PCR), partial least-squares regression (PLS), and multiple stepwise regression (MSR). In contrast to MSR, which only selects the strongest predictors, PCR and PLS construct latent linear variables to reduce the number of data dimensions (Varmuza & Filzmoser, 2009). However, there is a difference between PCR and PLS regarding how the linear combinations are created. When generating the principal components to characterize the maximum variation in the predictors, the strength of the link between the independent and dependent variables is considered in PLS but not in PCR (Miller & Miller, 2010).

Using various data sets, a series of calibrations based on these three multilinear regressions were conducted to test for an optimum estimation of DOC by spectral absorbance. Daily absorbance values from 250 nm to 732.5 nm at 2.5 nm intervals (194 variables) were used as the independent variables (Tipping et al., 1988) while laboratory measured DOC concentration was set as the dependent variable. Absorbances from wavelengths of 220 to 250 nm were omitted to prevent interference from inorganic substances at the lower end of the UV-Vis spectrum. The data set was split into training and test data sets for the purpose of calibration. Five different combinations of datasets were prepared for calibration: (1) The

training (75%) and testing (25%) sets were randomly selected from all observations (C4, C5 & NT); (2) The training set consisted of observations from C4 and C5, while the testing set included observations from NT; (3) The training (75%) and testing (25%) sets were randomly selected from observations in C4 and C5; (4) The training (75%) and testing (25%) sets were randomly selected from observations in C4 and NT; (5) The training (75%) and testing (25%) were randomly selected from observations in C5 and NT.

MSR were performed by '*caret*' package (Wing et al., 2019) in R (R Core Team, 2019). The '*pls*' package (Mevik et al., 2019) in R (R Core Team, 2019) was used to run PCR and PLS models, and the jackknife T-test method ('*jack.test*' function) was used to estimate coefficients and p values. The model performance was evaluated using the correlation coefficient (R), root-mean-square deviation (RMSD), standard deviation (STD), and bias.

3.3 Lag effect of terrestrial productivity on DOC (II)

The purpose of Study II was to link terrestrial greening with aquatic browning which was accomplished in four steps: 1) Prediction of high-frequency DOC concentrations based on the absorbance-DOC model developed in Study I; 2) Data acquisition of environmental variables (discharge and C flux data) by monitoring or open-access sources; 3) Identification of the relationship between DOC and environmental variables by wavelet coherence analysis; 4) Quantification of the contributions of terrestrial productivity and discharge by distributed-lag linear models (Fig. 6).

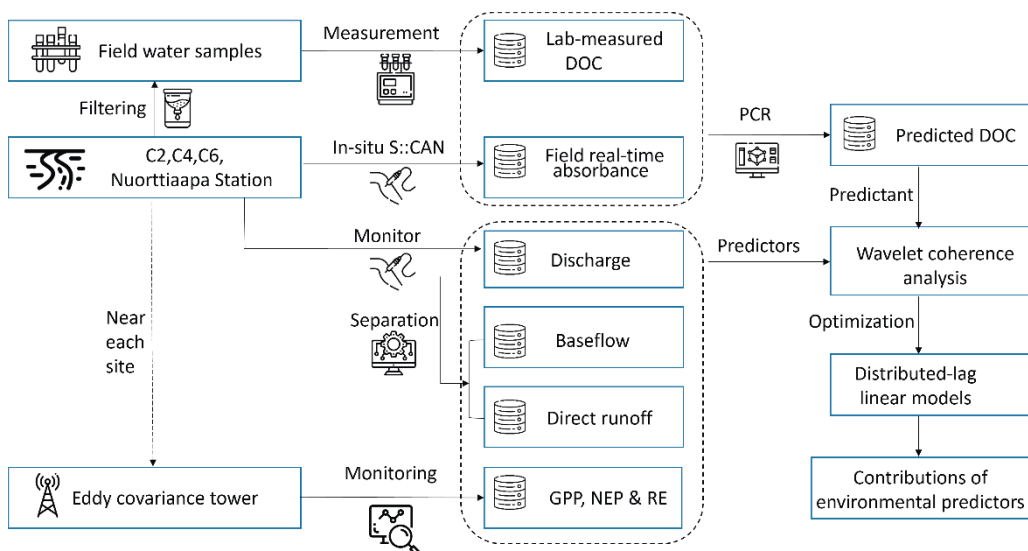


Figure 6. The schematic presentation of Study II—Linking terrestrial greening with aquatic browning, including the prediction of high-frequency DOC concentrations, data collection of environmental variables, and attribution of DOC variations to factors. GPP, NEP, and RE mean gross primary productivity, net ecosystem productivity and ecosystem respiration, respectively.

3.3.1 High-frequency DOC prediction

The absorbance–DOC prediction model developed in Study I was employed to estimate high-frequency DOC concentrations (PCR was chosen for its top performance) during the experimental period. In this case, training (75%) and testing (25%) sets were randomly chosen from all observations in (C2[S–forest], C4[S–mire], C6[M–mix], and NT [L–mix]). Hourly real-time spectral absorbances were used as inputs into the PCR model to estimate hourly DOC concentrations. For further analysis, the hourly predicted DOC concentrations were aggregated into daily data. The outliers were automatically detected and corrected by the '*tsclean*' function of the '*forecast*' package (Hyndman & Khandakar, 2008) in R (R Core Team, 2019).

3.3.2 Environmental factors

Water discharge. Water discharge was calculated according to water level measurements. In Finland, water level was detected by a pressure sensor (Levellogger, Solinst, Georgetown, Canada) and then converted to flow rates using channel cross-section, water depth and manual flow rate measurements (Flow Tracker Handheld ADV, SonTek, CA, USA). In Sweden, we measured water level via pressure transducers connected to Campbell Scientific dataloggers (USA) or duplicate WT–HR water height data loggers. Thereafter, salt dilution or time–volume approaches were used to create rating curves from discharge measurements (Laudon et al., 2011). Based on discharge, baseflow and direct runoff were derived using the base flow separation method (Gonzales et al., 2009).

Terrestrial productivity. The C exchange between the terrestrial ecosystem and the atmosphere was continuously measured by EC tower in the measuring station next to each catchment (Medlyn et al., 2005). In Sweden, EC data from Rosinedalsheden (64°10'N, 19°45'E, 145 m asl) were utilized to C2[S–forest] and C6[M–mix] while Degerö (64°11'N, 19°33'E, 270 m asl) was used for C4[S–mire]. In Finland, flux data from SMEAR I (67°45'N, 29°36'E, 390 m asl) were applied to NT [L–mix]. Day–time measurements were used to derive gross primary productivity (GPP) and ecosystem respiration (RE) (Aubinet et al., 2012), while net ecosystem productivity (NEP) was calculated as the negative value of net ecosystem exchange (Black et al., 2007). C flux

data from Rosinedalsheden and Degerö are available from the ICOS data portal (Drought 2018 Team and ICOS Ecosystem Thematic Centre, 2020). The ONEFlux processing pipeline was used to apply standardized quality control to the data. More details about the ONEFlux processing pipeline can be found in Pastorello et al., (2020). The flux data from SMEAR I was obtained via the Dynamic Ecological Information Management System. Due to the polar day (24-hour sunlight) during the growing season, the processing pipeline was different from the two Swedish sites. Kulmala et al., (2019) provide more details on the complete procedure for data quality control.

3.3.3 Lag-effect models

Wavelet coherence analysis. Wavelet coherence analysis attempts to quantify the variance of specific time series and correlations between different time-series across multiple frequencies (Grinsted et al., 2004). It can determine if two time series tend to rise and fall concurrently, in phase (without time lags), or out of phase (with time lags) during a certain time period (Vargas et al., 2011). With good localization properties in the time and frequency domain, wavelet analysis has been widely employed in the geosciences and ecology (Grinsted et al., 2004; Kumar & Foufoula-Georgiou, 1997; Vargas et al., 2011). By applying wavelet coherence analysis during the entire experimental period, specifically in the growing season, we explored the temporal correlation between discharge, terrestrial productivity (GPP, NEP, and RE) and DOC concentration. A 95% confidence level for wavelet analysis was conducted through a Monte Carlo Simulation. Wavelet analysis was done using the '*WaveletComp*' package (Schmidbauer & Roesch, 2018) in R (R Core Team, 2019).

Distributed-lag linear model. Distributed-lag linear models (DLMs) are linear regressions between the weighted lagged values of independent variables and dependent variables (Gasparrini, 2011). We applied DLMs to separately quantify the lag effects of discharge and terrestrial productivity on DOC at each site (C2[S-forest], C4[S-mire], C6[M-mix] and NT [L-mix]). First, the lag time for each variable was set based on the results of wavelet coherence analysis. Thus, the lag time was 0–7 days for discharge and 4–30 days for terrestrial productivity. Next, a so-called cross-basis function was

built to specify the values of the weights using polynomial transformations of the lags of each independent variable. Fourth-degree polynomial cross-basis functions were chosen for GPP, RE and NEP and second-degree polynomials for discharge. Additionally, we added 'year' as a factor variable since our variables had an annual cycle and there were other drivers that were not included in this study. Finally, DOC variations were predicted by linear combinations of cross-basis and year. The modelling was run using the 'DLNM' package (Gasparrini, 2011) in R (R Core Team, 2019). The best DLM model across each site was chosen using the Akaike information criterion (AIC) and explanatory power (R^2). The following are the definitions of DLMs (DLM1.1–1.6) used at all sites:

$$DLM1.1: DOC = \beta_1 DIS_{lag} + \alpha Year \quad (1)$$

$$DLM1.2: DOC = \beta_1 GPP_{lag} + \alpha Year \quad (2)$$

$$DLM1.3: DOC = \beta_1 \mathfrak{R}_{lag} + \alpha Year \quad (3)$$

$$DLM1.4: DOC = \beta_1 NEP_{lag} + \alpha Year \quad (4)$$

$$DLM1.5: DOC = \beta_1 DIS_{lag} + \beta_2 GPP_{lag} + \alpha Year \quad (5)$$

$$DLM1.6: DOC = \beta_1 DIS_{lag} + \beta_2 GPP_{lag} + \beta_3 \mathfrak{R}_{lag} + \alpha Year \quad (6)$$

where β is the lag effect of discharge (DIS), GPP, RE, and NEP on DOC concentrations, DIS_{lag} , GPP_{lag} , \mathfrak{R}_{lag} and NEP_{lag} are the cross-basis of discharge, GPP, RE and NEP, respectively. Additionally, we examined the impacts of discharge, baseflow, and direct runoff on DOC variations by DLM 1.1 across the sites. Since the analysis indicated that discharge was more closely linked to DOC, discharge was used to illustrate the impact of hydrology on DOC in DLM 1.5 and 1.6.

3.4 Mechanisms drive the heterogeneity in browning (III)

Study II built a nexus between terrestrial productivity and browning, and Study III introduced more potential drivers, e.g., recovery from acid deposition, climate related factors and site characteristics to reveal the long-term DOC trends. Moreover, we extended the study period (19 years) and increased the number of catchments (12 sites) to detect the heterogeneity of browning over time and space (Fig. 7).

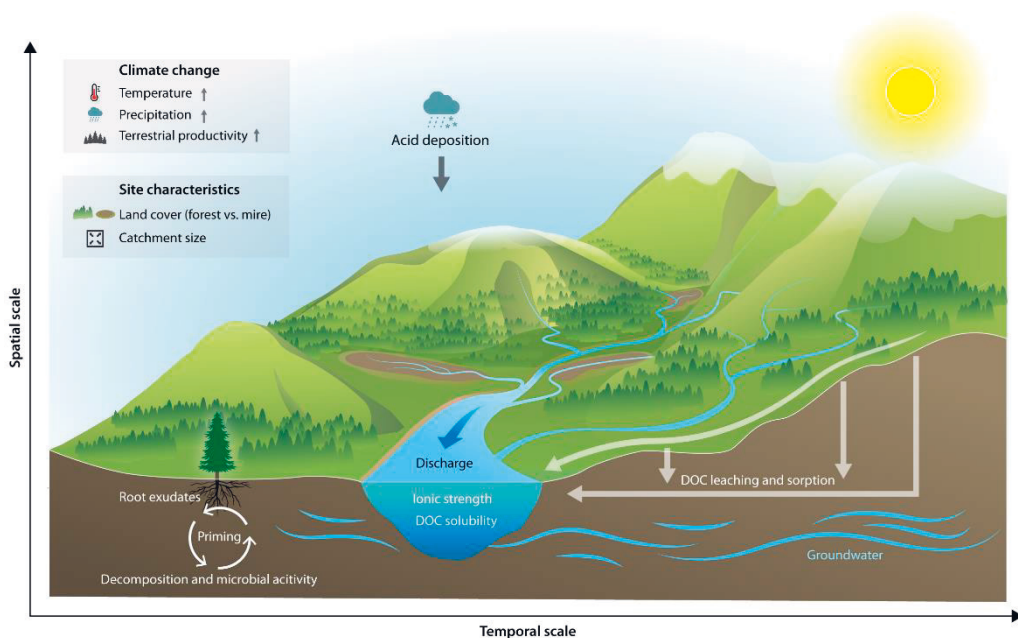


Figure 7. The schematic presentation of Study III—Multiple mechanisms (including recovery from sulfate deposition, climate change, and site characteristics) drive the spatiotemporal heterogeneity in browning across a boreal stream network.

3.4.1 Environmental trends

Trend of sulfate deposition. In Krycklan, sulfate deposition peaked ($4 \text{ kg S ha}^{-1} \text{ yr}^{-1}$) in the 1980s. Since then, the amount of sulfate deposited through snowfall and rainfall has steadily decreased, reaching a value ($0.8 \text{ kg S ha}^{-1} \text{ yr}^{-1}$) comparable to that recorded during the pre-industrial period (Laudon et al., 2021b).

Trend of climate change. A strong trend for global warming was observed in the long-term air temperature record at Svartberget in central Krycklan (1980–2020). The average annual increase in air temperature since 1891 was about $3.0 \text{ }^{\circ}\text{C}$. However, a major rise of $2.5 \text{ }^{\circ}\text{C}$ has taken place in the past four decades, with 2020 standing out as the warmest year in history (Laudon et al., 2021a). The average annual precipitation has not shown any statistical trend over the past 40 years; however, the average length of winter snow cover has exhibited a significant decline (Laudon et al., 2021a).

Trend of land use. Direct human disturbance on Krycklan has been quite minimal. The dominant land use is forestry, and the most prevalent management practice is traditional rotation forestry, generally even-aged, primarily artificially regenerated, and thinned. In Krycklan, the most central catchments have been shielded from forest management for nearly a century, yet on average, about 0.6% of the entire catchment area is clearcut annually.

3.4.2 Data collection and interpolation

Site characteristic. Catchment areas were delineated from a LiDAR derived digital elevation model (DEM) using Deterministic-8 (O'Callaghan & Mark, 1984). The DEM (2 m resolution) was created from a point cloud with a point density of $15\text{--}25 \text{ points m}^{-2}$ and hydrologically corrected by burning streams and culverts across roads (Lidberg et al., 2017). The land cover type was calculated according to the Swedish property map (1:12500, Lantmäteriet Gävle, Sweden) (Table 1).

Climate data. Air temperature and soil temperature at 20 cm were measured in the central part of Krycklan at the Svartberget research station

(Laudon et al., 2021a). Climate data from the station were assumed to be representative of the broader catchment area.

Chemistry data. Sulfate (SO_4) concentration in stream water was measured by a Dionex DX-300 or DX-320 ion chromatography system (Fork et al., 2020). More information about field sampling can be found in Laudon et al. (2013) and Winterdahl et al. (2014). Daily DOC and SO_4 concentrations of stream water from 2003 to 2021 were interpolated using '*Random Forest*' by package '*missForest*' (Stekhoven & Buhlmann, 2012) in R (R Core Team, 2019).

Water discharge. Daily stream discharge of the 13 catchments from 2003 to 2021 was predicted by an ensemble version of a bucket-type, semi-distributed hydrological (HBV) model (Karimi et al., 2022). A more detailed description of this type of model can be found in Karimi et al. (2022).

MODIS GPP. Due to the absence of EC towers near most of the sites, GPP derived from the Moderate Resolution Imaging Spectroradiometer (MODIS) was utilized to represent terrestrial productivity. We used three different approaches (point, line and area) to extract MODIS GPP (MGPP) of each site from Google Earth Engine (Gorelick et al., 2017): 1) by the coordinate; 2) by the riparian zone (50 meters on both side); 3) by the watershed (Fig. 8). By comparing MGPP with GPP generated from EC towers at sites where both were available, we determined that MGPP derived from the riparian zone performed best. MGPP from the riparian zone was used for further analysis.

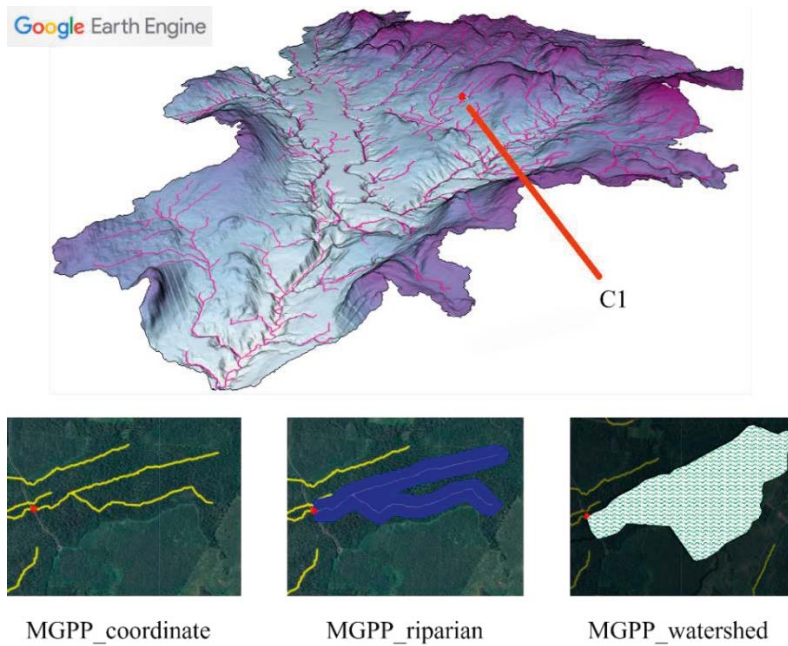


Figure 8. Extraction of MGPP (gross primary productivity derived from the Moderate Resolution Imaging Spectroradiometer) from coordinate, riparian zone, and watershed by Google Earth Engine.

3.4.3 Statistical analysis

Linear regression. For each site, the long-term trend of DOC concentrations (or discharge, sulfate, MGPP, and soil temperature) between 2003 and 2021 was calculated as the slope of the simple linear regression of mean DOC (or environmental drivers) values against the year. The mean slope of each catchment was used to compute the long-term trend of each variable.

Distributed-lag linear model. Based on Study II, more potential drivers were introduced to DLMs. The cross-basis for the lag factors were created in the same way. Fourth-degree polynomial cross-basis functions with 4–30 days delay was built for MGPP and second degree with 0–7 days delay for discharge. Thereafter, DOC concentrations were predicted using linear combinations of sulfate (SO_4), soil temperature (T_{soil}), catchment size ($Area$), mire coverage ($Mire\%$), and the cross-basis of both discharge and MODIS GPP ($MGPP$). The models (DLM2.1–7) were defined as follows:

$$DLM2.1: DOC = \beta_1 Dis_{lag} \quad (7)$$

$$DLM2.2: DOC = \beta_1 MGPP_{lag} \quad (8)$$

$$DLM2.3: DOC = \beta_1 Dis_{lag} + \beta_2 MGPP_{lag} \quad (9)$$

$$DLM2.4: DOC = \beta_1 Dis_{lag} + \beta_2 MGPP_{lag} + \alpha_1 SO_4 \quad (10)$$

$$DLM2.5: DOC = \beta_1 Dis_{lag} + \beta_2 MGPP_{lag} + \alpha_1 SO_4 + \alpha_2 T_{soil} \quad (11)$$

$$DLM2.6: DOC = \beta_1 Dis_{lag} + \beta_2 MGPP_{lag} + \alpha_1 SO_4 + \alpha_2 T_{soil} + \alpha_3 Area \quad (12)$$

$$DLM2.7: DOC = \beta_1 Dis_{lag} + \beta_2 MGPP_{lag} + \alpha_1 SO_4 + \alpha_2 T_{soil} + \alpha_3 Area + \alpha_4 Mire\% \quad (13)$$

where β is the lag effect of discharge (Dis) and MODIS GPP ($MGPP$) on DOC concentrations, and α is the impact of sulfate (SO_4), soil temperature (T_{soil}), catchment size ($Area$) and mire coverage ($mire\%$). Dis_{lag} and $MGPP_{lag}$ are the mean cross basis of discharge and MGPP during their lag times, respectively.

Total differential equation. To evaluate spatial patterns, we quantified the contributions of environmental drivers (sulfate, discharge, MGPP, and soil temperature) to observed DOC trend during 2003–2021 across each site. This quantification was achieved by decomposing the 19-year linear trend of DOC at each site into the additive contributions of the four components. To focus more on temporal patterns, we quantified the contributions of environmental drivers to 10-year DOC trends across each period. A 10-year moving window was used to cut the 19-year dataset at 1-year interval to obtain 10 datasets. Thereafter, we decomposed the 10-year linear trend of DOC across each period into the additive contributions of four components.

$$\begin{aligned} \frac{d DOC}{dt} &= \frac{\partial DOC}{\partial Dis} * \frac{d Dis}{dt} + \frac{\partial DOC}{\partial SO_4} * \frac{d SO_4}{dt} + \frac{\partial DOC}{\partial MGPP} * \frac{d MGPP}{dt} + \frac{\partial DOC}{\partial T_{soil}} * \frac{d T_{soil}}{dt} \\ &= \Delta DOC^{Dis} + \Delta DOC^{SO_4} + \Delta DOC^{MGPP} + \Delta DOC^{T_{soil}} \end{aligned} \quad (14)$$

where $\frac{\partial DOC}{\partial X}$ represents the sensitivity of DOC to an explanatory variable X (discharge, sulfate, MGPP, or soil temperature). These sensitivities were estimated as the regression coefficients of a multiple linear regression performed with DOC against all listed explanatory variables at a certain

period. $\frac{dDOC}{dt}$ (Or $\frac{dX}{dt}$) represents the linear trend of *DOC* (or *X*) at a certain period. For each site at a certain period, this trend was calculated as the slope of the simple linear regression of the mean *DOC* (or *X*) values against the year. Here, the *DOC* trend at a certain period ($\frac{dDOC}{dt}$) was decomposed into the contribution of each variable *X* (ΔDOC^X), which was represented as the product of the partial derivative against that variable *X* as $\frac{\partial DOC}{\partial X}$ and the concurrent trend of *X* itself as $\frac{dX}{dt}$. Note that discharge and sulfate were displayed as *Dis* and *SO₄*, respectively. The approach given by Eq. (14) was conducted for each site, and the total areal-averaged contribution of each factor to the trend of *DOC* over each period was calculated by averaging the decomposed contribution of factors (ΔDOC^X) across all catchments.

4 Results and discussion

4.1 Performance of absorbance–DOC prediction models (I)

In-situ S::CAN uses different technologies to measure spectral absorbance than benchtop spectrophotometers. The main differences are that in-situ instruments measure unfiltered water and are sensitive to variations in temperature and ambient sunlight. Additionally, the reliability of the power supply is lower in situ than in the lab. Linear regression showed that S::CAN-measured absorbances encompassed 96% of the absorbances from UV1800 though the slope of absorbance ratios varied between days (Fig. 9a). Further analysis also indicated that the variations in slopes were not caused by the temperature, water level or voltage. According to Avagyan et al. (2014), in-situ and ex-situ measurements should be done on the same day to prevent a slight change in spectrophotometric features during storage. In our case, storage of the samples was unavoidable due to the remote locations; thus, water samples were frozen at -21°C to prevent microbial decomposition. There were a few instances of non-linear correlations from February to April (Fig. 9b) that can be attributed to ice formation on the instruments or the particles on the lenses. Collectively, in-situ spectral measurements were found to be reliable, although more care is needed during winter.

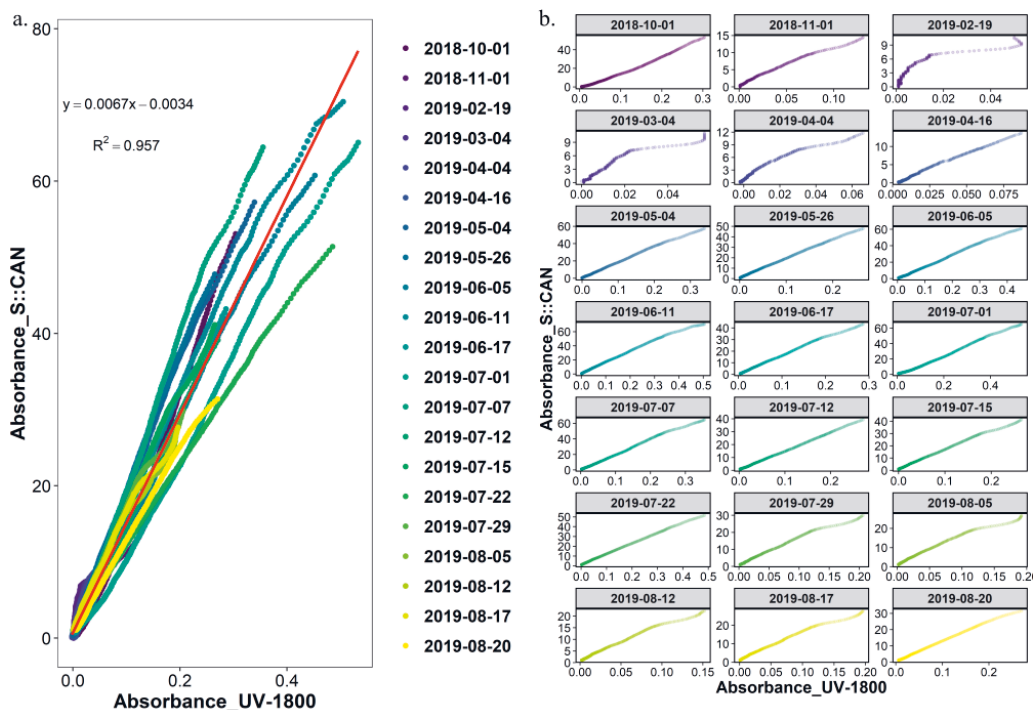


Figure 9. Relationship between the spectral absorbances measured by UV-1800 and by S::CAN

Since DOC primarily controls UV absorbance in aquatic systems, the goal of Study I was to produce accurate, broad, and unbiased reconstructions of DOC prediction by spectral absorbance analysis. We evaluated how well the three multivariate approaches (PCR, PLS and MSR) work by comparing the model performance (Fig 10). It turned out that MSR produced a model with the highest explanatory power and RMSD (or bias) the lowest (Fig 10). In contrast to Avagyan et al. (2014) that failed to produce accurate estimates by PCR, the three methods all exhibited good performance in our study, with only relatively minor differences. The absorbance–DOC prediction models explained more than 95% of lab-measured DOC. Various wavelengths have been used as proxies of DOC concentration including 254 nm (Baker et al., 2008; Tipping et al., 2009), 272 nm (Baker et al., 2008), 320 nm (Pastor et al., 2003), 340 nm (Baker & Spencer, 2004; Grayson & Holden, 2012; Wallage & Holden, 2010), 365 nm (Baker et al., 2008), 400 nm (Grayson & Holden, 2012;

Wallage & Holden, 2010) and 410 nm (Baker et al., 2008). The incorporation of absorbance data at 600 nm and 740 nm wavelengths may greatly improve DOC estimation accuracy (Avagyan et al., 2014). In our case, the most significant wavelength ranges covered most of the wavelengths extensively used in previous studies, as determined by PCR and PLS loadings (Fig. 11).

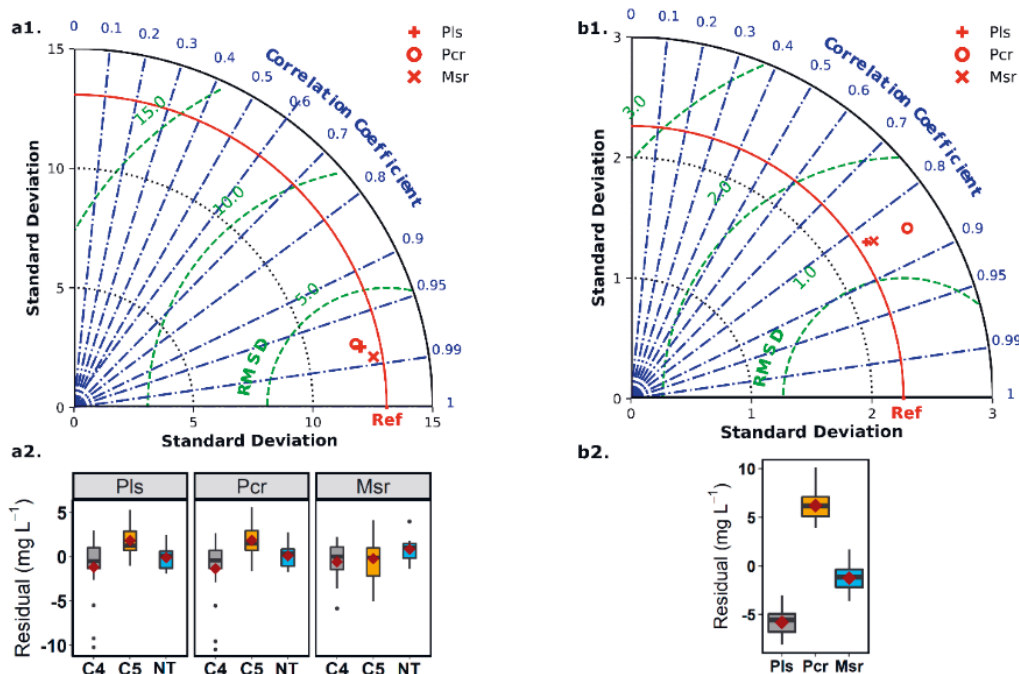


Figure 10. Statistical parameters (testing sets) of partial least-squares (PLS), principal component (PCR) and multiple stepwise regressions (MSR) of estimating DOC concentration by spectral absorbance, “Ref” shows the standard deviation of the laboratory-measured DOC concentration; the diamond symbol in each box plot represents the bias. Models a1&2 are based on data set 1, in which the training set was 75% of all observations (n=140), and the testing set contains the rest 25% (n=43). Models b1&2 are based on data set 2 where the training set contains observations from C4 & C5 (n=150), and the testing set contains observations from NT (n=33).

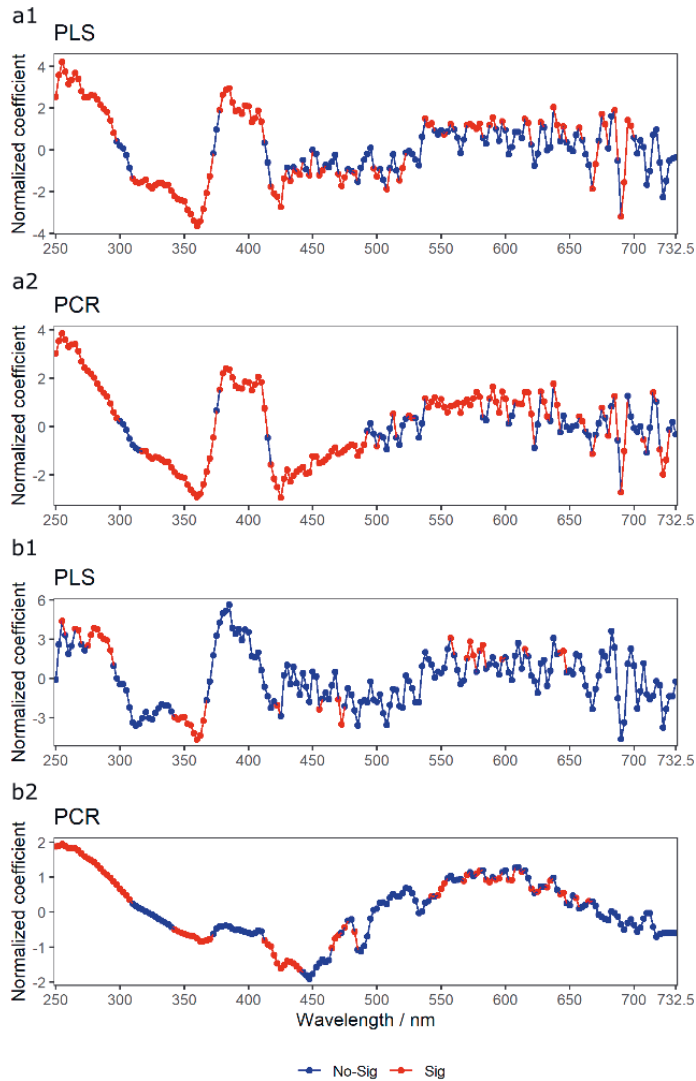


Figure 11. The effects of absorbances (wavelengths between 250 and 732.5 nm) on DOC by normalized regression coefficients of partial least-squares (PLS) and principal component (PCR) models. Models a1&2 are based on data set 1, in which 75% of all observations are training set (n=140), the rest 25% is testing set (n=43). Models b1&2 are based on data set 2, in which the training set are observations from C4 & C5 (n=150), the testing set are observations from NT (n=33). “Sig”, $p < 0.05$; “No-sig”, $p > 0.05$.

Additionally, when tested with observations from the Varriö river (NT), the PLS, PCR, and MSR models that we trained using data from the Kryklan rivers (C4&C5) still performed well (Fig. 10b). Moreover, the good performance was stable when we applied MSR to different combination of datasets (Table 2). The results indicated our success in building accurate and unbiased models for DOC prediction across multiple watersheds. The models were, at a certain loss of precision, appropriate for extrapolation from one watershed to another even without site-specific calibration for DOC. This achievement can help to ease the requirement of physical water sampling for calibrating new sensors. However, application is restricted in Northern Fennoscandia as the relation between absorbance and DOC may be variable in areas with different pH or turbidity. Future research will calibrate the absorbance-DOC prediction models in temperate and tropical regions and reunite all the data and models to provide free access to researchers worldwide.

Table 2. When applying multiple stepwise regressions (MSR) to different data sets for DOC prediction, the goodness of fit statistics of MSR models, and Wavelengths used in MSR.

Data sets	Training set		Training set			Number of wavelengths	Wavelengths (nm)
	r ²	RMSE (mg l ⁻¹)	r ²	RMSE (mg l ⁻¹)	Bias (mg l ⁻¹)		
Data set 1 (C4, C5&NT): Training set = 75% (n=140) Testing set = 25% (n=43)	0.96	2.61	0.97	2.35	-0.14	7	250, 290, 307.5, 437.5, 447.5, 630, 645
Data set 2 (C4&C5; NT): Training set = C4&C5 (n=150) Testing set = NT (n=33)	0.93	2.90	0.7	1.45	-1.24	5	305, 307.5, 632.5, 645, 692.5
Data set 3 (C4&C5): Training set = 75% (n=114) Testing set = 25% (n=36)	0.90	3.24	0.94	2.80	-0.29	5	252.5, 255, 257.5, 447.5, 645
Data set 4 (C4&NT): Training set = 75% (n=86) Testing set = 25% (n=28)	0.97	2.60	0.98	2.42	-0.20	4	255, 260, 692.5, 722.5
Data set 5 (C5&NT): Training set = 75% (n=72) Testing set = 25% (n=24)	0.96	1.80	0.8	4.18	1.37	4	257.5, 260, 420, 722.5

4.2 Link terrestrial greening with aquatic browning (II)

All study sites showed seasonal fluctuations in DOC concentrations. Compared to the growing season, snow-cover periods always had lower and more stable DOC concentrations (Fig. 12). This phenomenon has been attributed to several reasons. First, there is a relatively limited amount of litterfall during winter (Jutras et al., 2011; Liu et al., 2014). This assumption was supported by the report of a pulse in DOC from senescing vegetation at the end of the growing season (Worrall et al., 2004). Second, biological activity, degradability of organic matter, and DOC solubility reduced under lower temperature in winter (Dawson et al., 2008). Finally, the flow of terrestrial organic matter from upland and riparian zones to streams may be slowed down during the winter by frozen soil, leading to substantial DOC fluctuations during the snowmelt season (Pacific et al., 2010).

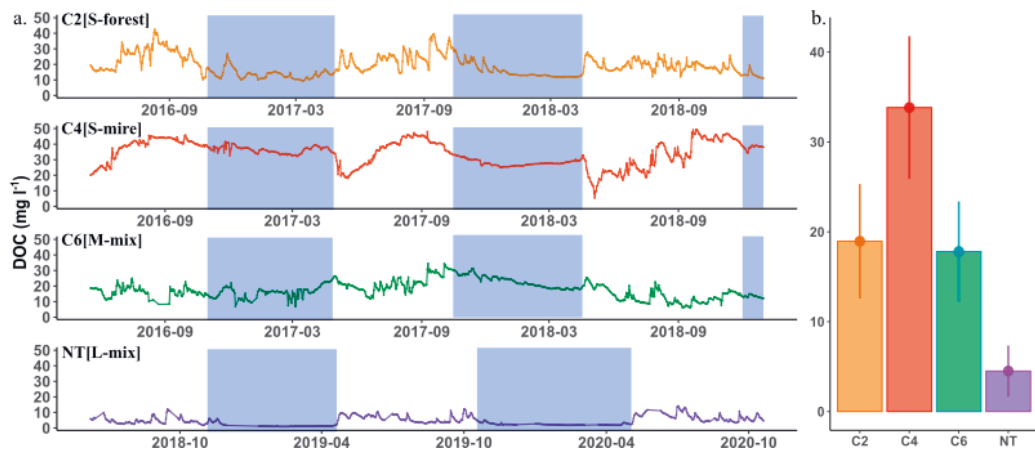


Figure 12. Daily DOC variations (predicted by PCR model) between 2016 and 2018 in C2[S-forest], C4[S-mire], and C6[M-mix], between 2018 and 2020 in NT[L-mix] (a); and the mean DOC concentration with standard deviation at each site during the entire experimental period (b). The blue shades represent the snow-cover periods.

Wavelet coherence analysis indicated that temporal synchrony existed between discharge (Fig. 13a) and DOC concentrations with a time lag of 1 to 30 days, as well as between GPP (Fig. 13b), NEP (Fig. 13c), and RE (Fig. 13d) and DOC from 4 to 30 days. These findings supported the delayed impacts of discharge and terrestrial productivity on DOC. The delay was contributed by the delivery of photosynthates, microbial activities, decomposition of SOM, and hydraulic transport of DOC from soil to water (Wen et al., 2020).

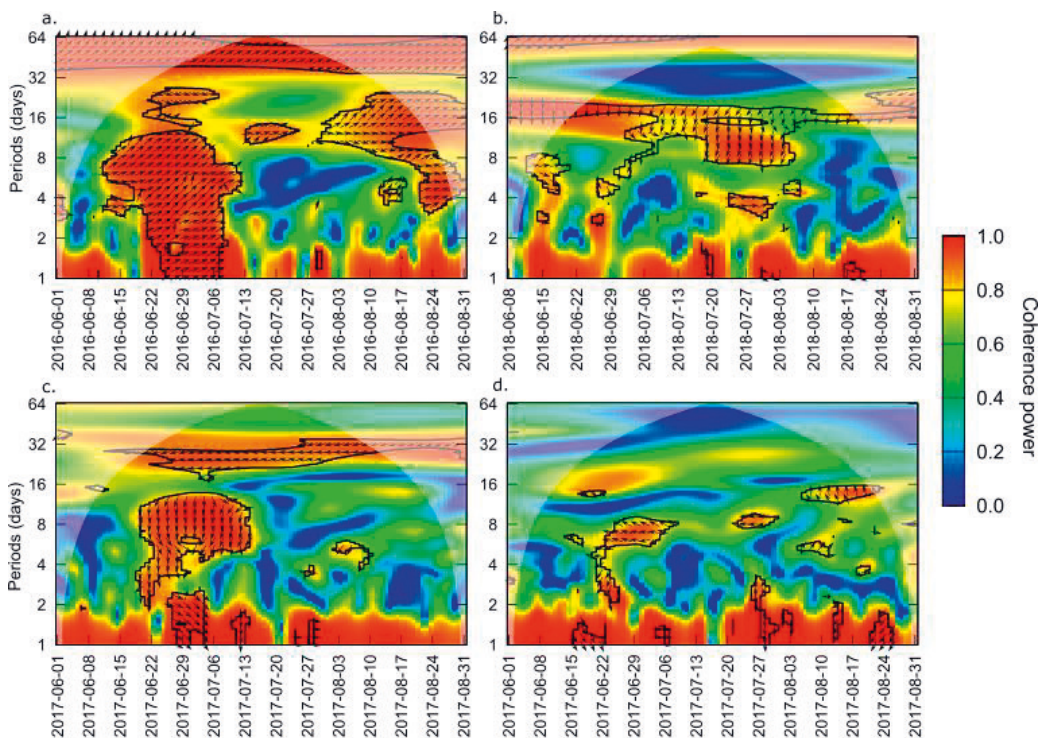


Figure 13. Wavelet coherence analysis of the relationship between DOC concentrations and discharge (a), GPP (b), NEP (c), RE (d) in summer 2016, 2018, 2017, and 2017, respectively. The colors of the power values range from blue (low values) to green (intermediate) to red (high values). The red parts inside the black border indicate significant temporal coherence between the studied parameters ($p < 0.05$). The arrows show the leading and lagging relationships between the variables. The y-axis indicates the length of the time window in the wavelet coherence analysis (in days).

Table 3. Performance of distributed-lag linear models (DLM1.1–1.6) showing the relationship between DOC and environmental predictors across C2[S-forest], C4[mire], C6[mix] and NT [mix]. DOC concentrations were predicted by PCR model; DIS means discharge. DIS_{lag} , GPP_{lag} , NEP_{lag} and RE_{lag} represent the mean cross basis of discharge, GPP, NEP and RE, respectively.

DLMs	C2[S-forest]		C4[S-mire]		C6[M-mix]		NT [L-mix]	
	AIC	R ²	AIC	R ²	AIC	R ²	AIC	R ²
DLM1.1: DOC= DIS _{lag} + year	6051.4	0.22	6374.8	0.25	5339.5	0.36	2693.6	0.72
DLM1.2: DOC= GPP _{lag} + year	5464.7	0.52	5980.9	0.41	5337.2	0.28	3387.6	0.17
DLM1.3: DOC= RE _{lag} + year	5415.3	0.55	5807.8	0.51	5352.8	0.26	3390.8	0.17
DLM1.4: DOC= NEP _{lag} + year	5712.6	0.38	6187.3	0.27	5325.2	0.28	3405.0	0.15
DLM1.5: DOC= DIS _{lag} + GPP _{lag} + year	5130.6	0.67	5778.1	0.53	5201.9	0.38	2621.4	0.72
DLM1.6: DOC= DIS _{lag} + GPP _{lag} + RE _{lag} + year	5069.0	0.69	5531.9	0.65	5155.3	0.42	2608.6	0.73

As evidenced by an increase in R² and a decrease in AIC across all sites, the performances of DLMs improved as more time-lag environmental factors were considered (Table 3). This result demonstrated the importance of terrestrial productivity and discharge in regulating DOC concentrations though with delay. In general, 62% of aquatic DOC variations across the four catchments could be explained by the best distributed-lag linear model (DLM1.6). Discharge, GPP and RE accounted for 26%, 22% and 3% of DOC variations, respectively (Table 4).

The relationship between GPP and DOC concentration might be controlled by the priming effect (Guenet et al., 2010). We primarily focused on priming in soil since a meta-analysis revealed little potential for significant priming in water (Bengtsson et al., 2018; Catalán et al., 2015). In boreal habitats, where nitrogen is typically limited, plants primarily rely on mycorrhiza to acquire nutrients. Increased forest productivity stimulates more root exudates and further encourages the growth of mycorrhizal fungi, which increases the nutrients supply available to trees (Pumpanen et al., 2009; Heinonsalo et al., 2010). Additionally, riparian zones with high SOC and water content are the predominant links between aquatic and terrestrial ecosystems in most northern headwaters (Laudon & Sponseller 2018; Wen et al. 2020). Although the riparian organic C pool may support DOC export

at the current pace for several hundred years without supplement (Ledesma et al., 2015), our findings showed that fresh C input due to increased GPP did alter the export of DOC from riparian zones to aquatic systems.

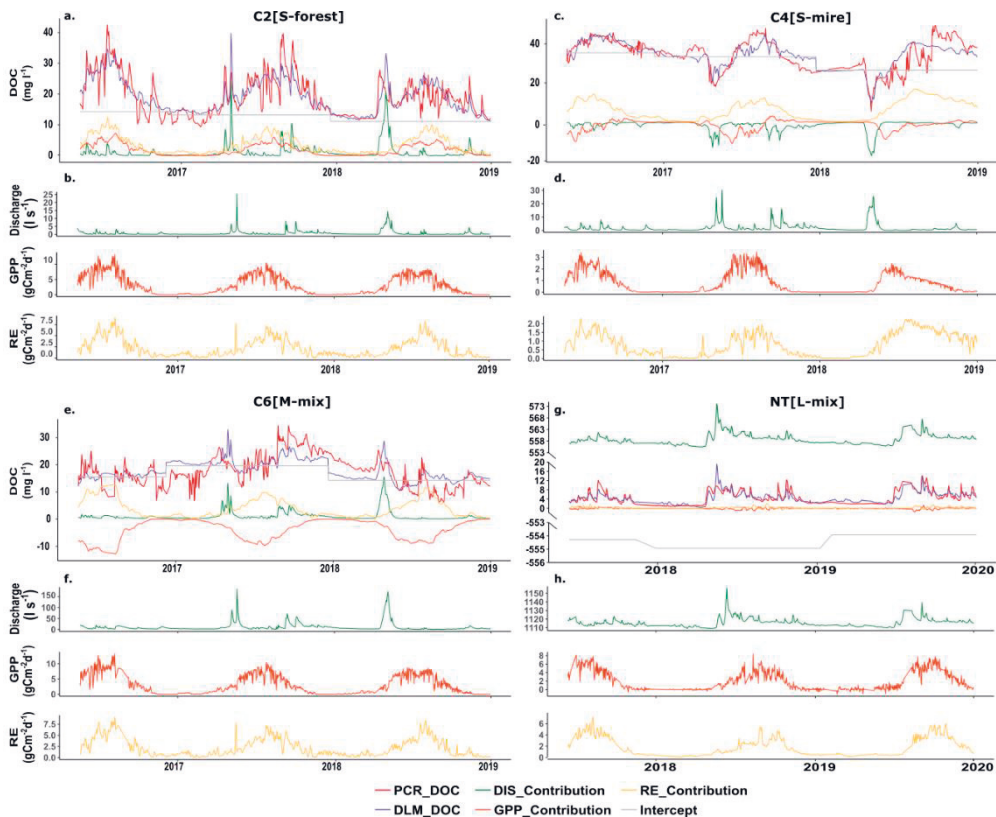


Figure 14. The independent contributions of discharge, gross primary production (GPP) and ecosystem respiration (RE) to DOC based on DLM 1.6 in C2[S-forest] (a), C4[S-mire] (c), C6[M-mix] (e), and NT[L-mix] (g). PCR_DOC and DLM_DOC was predicted by the PCR and DLM 1.6 model. Time-series environmental predictors (discharge, GPP and RE) across years in C2[S-forest] (b), C4[S-mire] (d), C6[M-mix] (f), and NT[L-mix] (h).

Table 4. Mean values of discharge, GPP and RE during the experimental period, and their contributions to DOC concentrations across four catchments based on DLM1.6. The plus and minus signs indicate positive or negative relations with DOC concentrations, respectively.

Site	Size (km ²)	Discharge (l s ⁻¹)		GPP (g C m ⁻² d ⁻¹)		RE (g C m ⁻² d ⁻¹)		Year	R ²			
		Mean	Contribution	Mean	Contribution	Mean	Contribution					
C2[S-forest]	0.14	0.73±1.67	9.9 %	+	3.01±3.11	53.2 %	+	2.19±2.00	2.5 %	+	3.6 %	69.3 %
C4[S-mire]	0.19	1.87±3.24	14.3 %	-	0.78±0.91	30.8 %	-	0.79±0.66	3.9 %	+	15.6 %	64.5 %
C6[M-mix]	1.3	10.88±19.95	15.0 %	+	2.94±3.10	2.2 %	-	2.13±1.97	6.1 %	+	18.6 %	41.9 %
NT [L-mix]	40	1115.71±4.99	68.7 %	+	1.94±2.25	1.0 %	ns	1.83±1.65	1.1 %	ns	2.3 %	73.1 %
Average			26.9 %			21.8 %			3.4 %		10.0 %	62.2 %

Interestingly, DOC variations were dominated by GPP in small catchments (C2[S-forest] and C4[S-mire]) but not in larger catchments (C6[M-mix] and NT [L-mix]) (Table 4). There could be several causes for the faded influence of GPP within larger catchments. First, most biogeochemical processes take place within a few meters of the riparian zone as ground water travels from upland mineral soil through the riparian zone (Laudon & Sponseller, 2018). Therefore, smaller catchments must be more prominent in DOC dynamics than larger ones for a given amount of DOC export. Additionally, the increased relative contribution of deep groundwater inflow with increased drainage area mediates biogeochemical transitions from small to mesoscale catchments (Tiwari et al., 2017). In smaller streams, the dominant hydrological pathway primarily involves surface flow routes carrying rich SOM, whereas in larger-scale catchments, it shifts toward deeper groundwater with lower organic content. The alterations in the flow route also clarify why the influence of GPP was concealed by discharge in C6[M-mix] and NT [L-mix]. Moreover, it is notable that more than 60% of DOC is exported annually from soil to water during the snow-melt period (May to June) (Mann et al., 2012). Thus, large-scale rivers receive a significant portion of their flow from groundwater, resulting in their DOC concentrations being less susceptible to variations in DOC inputs from soils (Shanley et al., 2002; Strohmeier et al., 2021). These distinctions provide additional insight into why the proportion of DOC influenced by GPP diminishes with larger catchment sizes.

However, GPP can contribute to DOC concentrations either positively or negatively (Table 4). Comparing the two small-scale catchments (C2[S-forest] and C4[S-mire]), the forest GPP had a positive effect on DOC, while that of the mire had a negative impact (Fig 14). Priming was altered from negative or absent at low C input to strongly positive at high C input (Liu et al., 2017). In our case, the mean GPP values in C2[S-forest] ($3.01 \text{ g C m}^{-2} \text{ d}^{-1}$) were significantly higher than in C4[S-mire] ($0.78 \text{ g C m}^{-2} \text{ d}^{-1}$) (Table 4) which is one reason for the opposite direction of the priming in these two small-scale catchments. According to Bastida et al. (2019), priming effects are generally positive in dryer, lower-SOC sites and negative in more mesic, higher-SOC sites. Our study agrees with this finding: The wetland site (C4[S-mire]) was rich in SOC and humidity compared to the forest site (C2[S-forest]). The huge difference in aboveground biomass between the sites may also have influenced the outcomes, since it has been observed that the level of rhizosphere priming effect positively corresponds with aboveground plant biomass (Huo et al., 2017).

In contrast to GPP, RE showed a consistent positive correlation with DOC exports (Table 4 & Fig.14). These correlations align with the concept that complex organic substances decompose into monomers because of below-ground microbial activity, which forms the bulk of DOC (Schimel et al., 1994). The catchment effectively retains the generated DOC within soil water and on soil surfaces, causing a gradual buildup of DOC until the subsequent precipitation event occurs, flushing out the stored DOC. Therefore, when hydrological connectivity is low, there is a delay in the export of DOC. Low hydrological connectivity therefore suggests a delay in DOC export, with the result that the DOC present in the stream today can often be the DOC created some time ago (Wen et al., 2020).

Meanwhile, it is fundamental to acknowledge the role of discharge in transporting DOC from terrestrial to aquatic ecosystems. Around 80% of watersheds in both USA and France exhibit notable associations between stream DOC concentration and discharge, with either positive or negative correlations (Wen et al., 2020). Dawson et al. (2002) reported that discharge could predict DOC values by 58% to 81% depending on the seasons. According to Clark et al., (2007), discharge could account for 72% of DOC

concentrations during autumn storm events, while the other seasons exhibited a weaker correlation. Rather than organizing the data into seasonal groups to eliminate this aspect of the yearly variation (Clark et al., 2007; Dawson et al., 2008), our DLM models incorporated 'year' as a factor variable without data segmentation (Table 3). This approach aimed to maintain continuity while addressing the delayed impact of discharge on DOC concentration. In our case, discharge explained from 9.9% to 68.7% of DOC variations across year among sites, in either a positive or negative pattern (Fig 14 & Table 4).

The dynamic of DOC concentrations in soil and stream water is ultimately determined by the hydrological connection to the stream vs the distribution of SOC, resulting in distinct discharge–DOC patterns (Covino, 2017; Wen et al., 2020). The discharge–DOC patterns switched from dilution in a wetland catchment (C4[S–mire]) to flushing in forested and mixed sites (C2[S–forest], C6[M–mix], and NT [L–mix]) (Fig 14). This result agrees with Laudon et al., (2011). Different flow pathways can illustrate how hydrological functioning differs among sites. It has been established that the movement of DOC losses from bulk soil is influenced by hydrological processes in response to precipitation events and changing flow pathways through different soil horizons varying in the amount of organic matter (Dawson et al., 2008; Hinton et al., 1998). In the mire dominated catchment (C4[S–mire]), during the initial stages of rising hydrograph runoff, event water occurs as overland flow due to either a frozen wetland surface or high saturation. This results in a dilution effect on DOC concentrations (Laudon et al., 2004). On the other hand, SOC is rich in uplands of the other three sites (C2[S–forest], C6[M–mix] and NT [L–mix]), and most runoff from forested areas travels over subsurface flow pathways carrying freshly activated SOC to streams (Bishop et al., 2004).

4.3 Integrated mechanisms to reveal variations in DOC (III)

Over the period between 2003 and 2021, all catchments in Krycklan experienced an upward trend in DOC concentrations, although the slope of this increase varied among sites (Fig. 15a). Oni et al. (2012) studied the DOC trends in C2, C4, and C7 from 1993 to 2010, and only C2 showed a significant annual increasing trend during that time. There were decreasing trends in stream sulfate concentrations (SO_4) and pH (Fig. 15f) throughout all catchments (Fig. 15b). Soil temperature and MGPP demonstrated an increasing trend from 2003 to 2021, though the former's increase was not significant ($p > 0.5$) (Fig. 15c & e). Discharge at each site also displayed an increasing trend which was strongly affected by the last two years of the record (Figure 15d). Our study indicated that no single mechanism alone could account for the variations in DOC concentrations over space and time (Table 5). Instead, we showed that a combination of factors, including sulfate deposition (31%), terrestrial productivity (3%), discharge (4%), soil temperature (0.2%), and properties of the catchment such as size (13%) and land cover type (2%) govern the variation of DOC trends (Fig. 16).

Table 5. The performances of the distributed-lag linear models (DLM2.1–2.7) show the relationship between DOC variations and potential environmental drivers across 13 boreal catchments in Krycklan. MGPP_{lag} means the cross basis of MODIS GPP from riparian zone; DIS_{lag} represents the cross basis of discharge; T_{soil} is soil temperature at 20cm; Area means the size of catchment. Mire% is the proportion of mire according to the landscape of catchment.

Distributed-lag linear Models (DLMs)	Discharge	MGPP	Performance	
	Lag\day	Lag\day	AIC	R ²
DLM2.1: $\text{DOC} = \text{DIS}_{\text{lag}}$	0–7	–	241681.3	0.04
DLM2.2: $\text{DOC} = \text{MGPP}_{\text{lag}}$	–	4–30	243021.7	0.02
DLM2.3: $\text{DOC} = \text{DIS}_{\text{lag}} + \text{MGPP}_{\text{lag}}$	0–7	4–30	239037.2	0.07
DLM2.4: $\text{DOC} = \text{DIS}_{\text{lag}} + \text{MGPP}_{\text{lag}} + \text{SO}_4$	0–7	4–30	203457.9	0.38
DLM2.5: $\text{DOC} = \text{DIS}_{\text{lag}} + \text{MGPP}_{\text{lag}} + \text{SO}_4 + T_{\text{soil}}$	0–7	4–30	202970.3	0.38
DLM2.6: $\text{DOC} = \text{DIS}_{\text{lag}} + \text{MGPP}_{\text{lag}} + \text{SO}_4 + T_{\text{soil}} + \text{Area}$	0–7	4–30	183503.3	0.51
DLM2.7: $\text{DOC} = \text{DIS}_{\text{lag}} + \text{MGPP}_{\text{lag}} + \text{SO}_4 + T_{\text{soil}} + \text{Area} + \text{Mire}\%$	0–7	4–30	179979.3	0.53

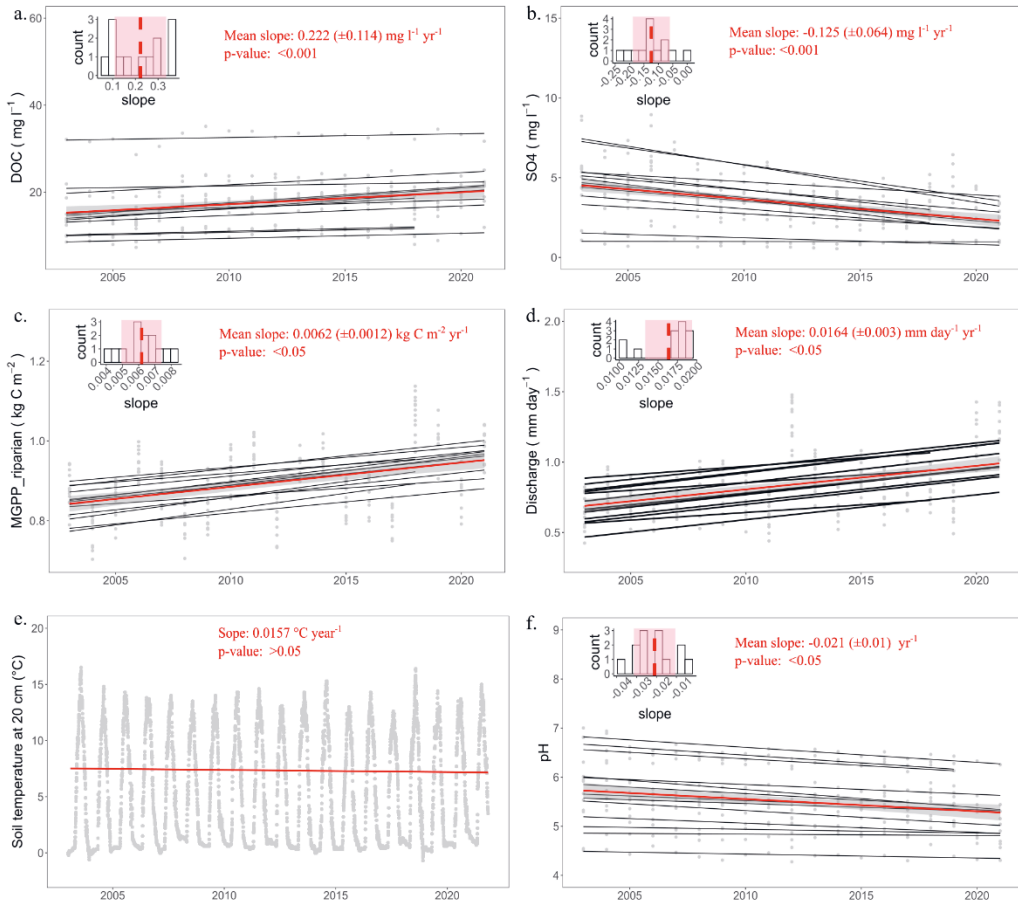


Figure 15. The long-term trends of DOC concentration (a), sulfate (SO₄) (b), MGPP(c), discharge (d), soil temperature at 20 cm (e) and pH (f) across the Krycklan Catchments from 2003 to 2021. The annual changes of all variables were calculated using daily data across all sites. The red line represents the mean trend across all sites over 19 years. The grey area highlights trends within one standard deviation of the mean trend. Individual site observations and trends are given as grey dots and black lines, respectively. The inset shows the distribution of the rate of change in DOC across the Krycklan catchments. The dashed red line represents the mean slope. The red shaded area represents the mean slope \pm standard deviation.

Whereas our modeling approach identified multiple drivers of DOC variations, stream SO_4 concentrations emerged as by far the most important (Fig. 16). This is consistent with past studies in Krycklan that assessed DOC- SO_4 relationships in soil water (Oni et al., 2012; Ledesma et al., 2016). S-deposition can alter DOC solubility by changing either the acidity of soils or (and) the ionic strength of soil solutions (Monteith et al., 2007). In contrast to expectations, annual pH did not recover during the study period; instead, declined slightly at all sites (Fig. 15f). Thus, we suggest that, regarding stream pH, the rise in DOC and associated organic acidity, overwhelm the trends in S-deposition (Laudon et al., 2021b). Strikingly, Krycklan catchments have similarly undergo a large decline in the sum of base cations (BC), primarily Ca^{2+} and Mg^{2+} , which from a charge perspective is comparable to the decline in SO_4 concentration (Laudon et al., 2021b). This concurrent decrease in SO_4 and BC decreased ionic strength, which consequently enhanced the colloidal dispersion and organic matter disaggregation in soil solution by expanding the diffuse double layer. Such changes, in turn, can increase the solubility of DOC in soil water and promote its lateral export to streams (Lawrence & Roy, 2021). Therefore, the decline in ionic strength rather than recovery from acidification seems to be the main driver of the increasing DOC trends across Krycklan catchments. It is noteworthy that the large DOC trends occurred despite the relatively low sulfate deposition in Krycklan, peaking at $4 \text{ kg S ha}^{-1} \text{ yr}^{-1}$ around 1980 (Laudon et al., 2021b), more than 5 times lower than the most affected parts of Sweden (Ferm et al., 2019).

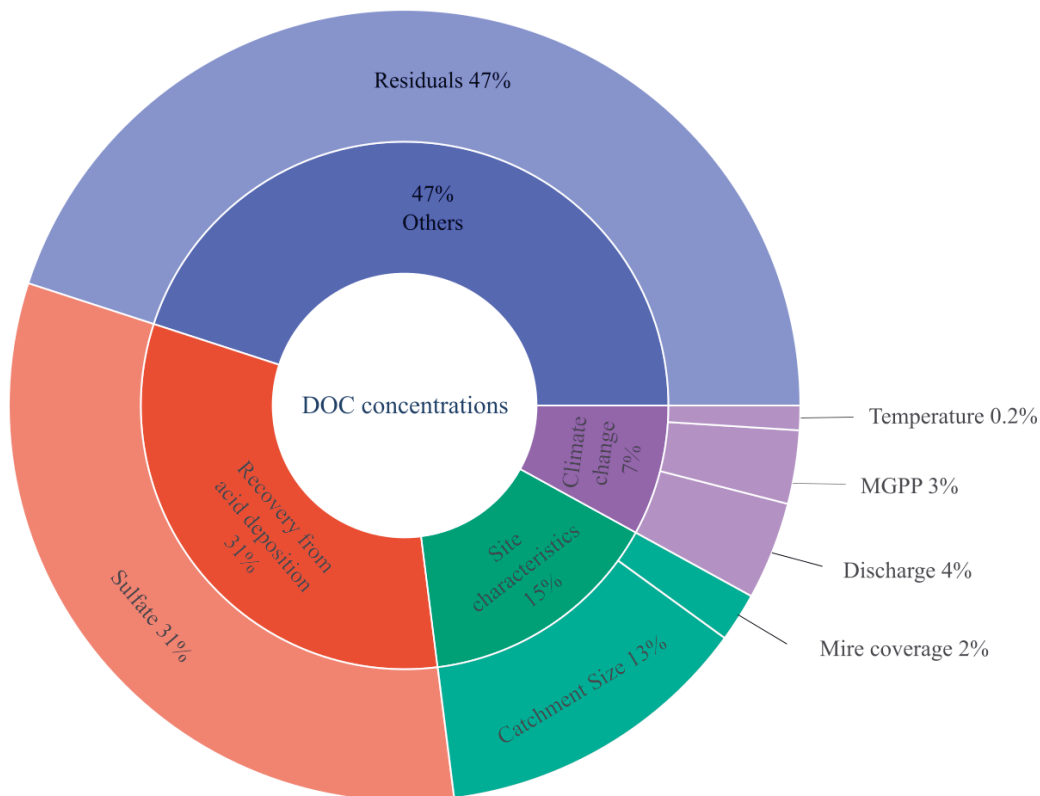


Figure 16. The contribution of the proposed mechanisms and site characteristics to the variations in DOC concentrations in Krycklan catchments from 2003 to 2021 according to the best distributed-lag linear model (DLM 2.7).

Our results also revealed important impacts of climate related factors, including increases in forest productivity and changes in discharge. Previous studies have also linked increased production and mobilization of terrestrial organic C from soils to browning (Finstad et al., 2016). There have been obvious increases in forest growth in and around the Krycklan Catchment over the last 60 years (Laudon et al., 2021a), and this trend has likely increased the size of soil organic matter pools that can be mobilized to streams (Jansson et al., 2008). Further, previous work in Krycklan revealed the lag-effects of terrestrial productivity on soil DOC production through priming (Zhu et al., 2022); the current study confirmed these findings across a larger number of catchments and over an extended period. Finally, while

the relationship between increasing discharge and elevated DOC concentrations is in line with theory (Wit et al., 2016), this pattern should be interpreted with caution as the discharge time series is weighted by the final two years in the record. Indeed, there is increasing evidence that hydrological patterns in northern landscapes are becoming more variable with climate change (Teutschbein & Seibert, 2012) and that more severe summer droughts in Krycklan can have large influences on DOC; lower concentrations during low flow, followed by elevated concentrations during rewetting phases (Tiwari et al., 2022). Regardless, our analysis illustrates how multiple, climate-related features can operate concurrently with deposition recovery to shape stream DOC trends.

4.4 Drivers of long-term DOC trends over time and space (III)

After detecting the potential drivers of DOC variations, we attributed the long-term increased DOC trends of all Krycklan catchments from 2003 to 2021 to these drivers by the total differential equation. When considering all sites together, the primary correlates of the long-term trend (spanning 19 years) in DOC concentrations were the concurrent declines in sulfate concentrations (78%), followed by increases in terrestrial productivity (8%), soil temperature (8%), and discharge (6%) (Fig 17b). Catchment properties also mediated the response of DOC to these environmental drivers (Fig 17a), leading to a five-fold variance in DOC trends across the sub-catchments within the Krycklan network (Table 6). Briefly, the increase in long-term DOC concentrations was more pronounced in catchments with higher forest and lower mire cover (i.e., forest > mixed > mire sites), but the rate of increase tended to slow as catchment size increased (Table 6).

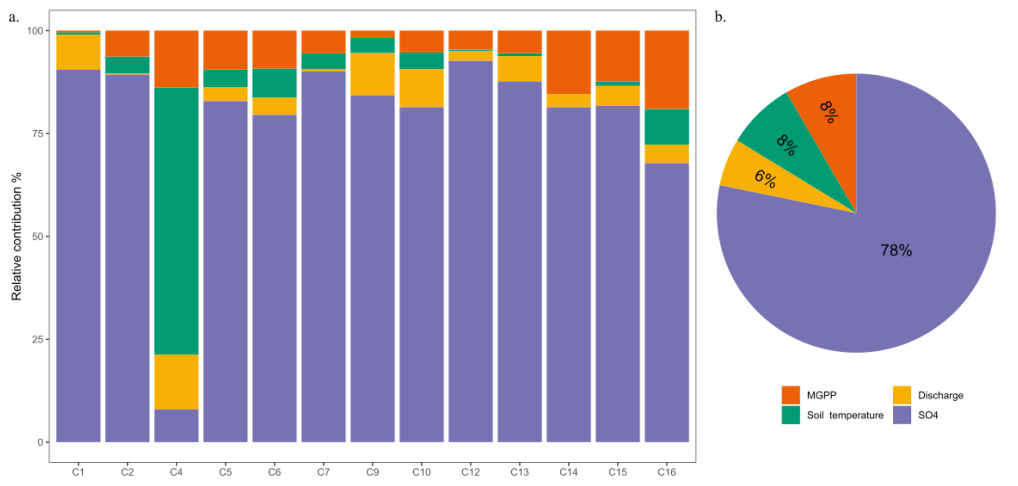


Figure 17. The relative contribution (%) of each driver to long-term DOC trends across 13 catchments in Krycklan from 2003 to 2021 (a). The mean relative contribution of each driver to long-term DOC trends in Krycklan from 2003 to 2021 (b).

Land cover type can further regulate the patterns between discharge, SO₄, terrestrial productivity and DOC concentrations. First, there is substantial heterogeneity in the hydrological pathways that connect soils and streams in different landscapes (Laudon & Sponseller, 2018). For sites with high mire cover, a larger proportion of water travels overland, due to frozen surfaces or within deep preferential flow paths that can be diluted during high flows (Peralta-Tapia et al., 2015a). By comparison, runoff from forest hillslopes entering streams through subsurface flow pathways can carry newly activated SOC to the catchment (Laudon et al., 2004). Therefore, more DOC is flushed into forested catchments, while dilution is more common for mire catchments, resulting in decreased concentrations during rain events (Bishop et al., 2004; Oni et al., 2012). This may account for the fact that, despite similar discharge patterns across catchments during the study period (Table. 6), the response rates of DOC were higher in sites with greater forest cover. Simultaneously, SO₄ imported to the mire sites has been washed out and diluted because of the much higher hydrological connectivity and greater contribution of overland flow (Peralta-Tapia et al.,

2015a). Additionally, mires are known to promote sulfate reduction processes (Pester et al., 2012), as persistent anaerobic conditions allow sulfate-reducing bacteria to remove SO_4 from the system by converting it to sulfide (Porowski et al., 2019; Taketani et al., 2010). Thus, we observed lower mean concentrations and weaker trends for SO_4 (Table 6) in sites with higher mire coverage. Our results highlighted the dilution and buffer functions of mires, such that greater peat coverage dampens the response rate of DOC to S-deposition. Moreover, terrestrial productivity and stand biomass increased with higher forest and lower mire cover, which led to higher loads of fresh organic matter from terrestrial to aquatic ecosystems, consequently, a higher response rate of DOC concentrations (Crapart et al., 2023).

Table 6. The long-term trends of DOC concentrations, MODIS GPP (MGPP), discharge, sulfate, soil temperature and pH from 2003 to 2021 across sites. The measured period was 2003 to 2018 for C12, C14, and C15.

Site	Size (ha)	Land cover	DOC		MGPP		Discharge		Sulfate		Soil temperature		Stream pH	
			Slope	p value	Slope	p value	Slope	p value	Slope	p value	Slope ^a	p value	Slope	p value
C1	48	forest	0.371	<0.001	0.006	NS	0.018	<0.05	-0.234	<0.001	0.016	NS	-0.015	<0.05
C2	12	forest	0.378	<0.001	0.006	NS	0.018	<0.05	-0.206	<0.001	0.016	NS	-0.019	<0.01
C4	18	mire	0.090	<0.001	0.006	NS	0.019	<0.05	-0.001	NS	0.016	NS	-0.008	NS
C5	65	mire	0.082	<0.001	0.004	NS	0.019	<0.05	-0.042	<0.01	0.015	NS	-0.003	NS
C6	110	mixed	0.174	<0.001	0.006	<0.05	0.019	<0.05	-0.082	<0.01	0.016	NS	-0.019	<0.05
C7	47	mixed	0.278	<0.001	0.006	<0.05	0.018	<0.05	-0.132	<0.001	0.016	NS	-0.008	NS
C9	288	mixed	0.215	<0.001	0.005	NS	0.018	<0.05	-0.126	<0.001	0.016	NS	-0.020	<0.01
C10	336	mixed	0.282	<0.001	0.007	<0.05	0.017	<0.05	-0.115	<0.001	0.016	NS	-0.028	<0.01
C12	544	mixed	0.309	<0.001	0.004	NS	0.011	NS	-0.184	<0.001	-0.006	NS	-0.026	<0.05
C13	700	mixed	0.366	<0.001	0.007	<0.05	0.017	<0.05	-0.134	<0.001	0.016	NS	-0.037	<0.001
C14	1410	mixed	0.110	<0.001	0.008	NS	0.011	NS	-0.157	<0.001	-0.006	NS	-0.027	<0.01
C15	1913	mixed	0.121	<0.001	0.008	NS	0.012	NS	-0.123	<0.001	-0.006	NS	-0.032	<0.001
C16	6790	mixed	0.113	<0.001	0.007	<0.05	0.017	<0.05	-0.083	<0.01	0.016	NS	-0.031	<0.001

^a Soil temperature trends in C12, C14 and C15 were from 2003 to 2018 to match DOC data, as records from 2018 to 2021 were missing at these three sites.

Meanwhile, catchment size can also regulate DOC response rates through changes in the dominant course of water supporting stream flow. Accordingly, for larger catchments, the contribution of deeper, DOC-poor groundwater to streams is usually larger, reducing the significance of DOC inputs from near-surface soils, which are dominant sources in the headwaters (Shanley et al., 2002; Peralta-Tapia et al., 2015b; Strohmenger et al., 2021). This hydrological pattern appears widespread in the region (Tiwari et al., 2018), and the increasing supply of deeper groundwater likely buffers against the changes in DOC mobilization that are generated in shallower soils. By modifying the importance of different water sources, increased catchment sizes could moderate the response of DOC to environmental drivers.

Among the more novel results of our analysis is the resolution of non-stationary drivers of DOC export over time (Fig. 18). The observed decline in browning (Fig. 18e) across Krycklan catchments aligns with the findings of Eklöf et al., (2021) who showed that increases in DOC that were prevalent throughout Sweden from 1991 to 2010 ended a decade ago. The fact that browning trends have weakened during the last ten years in Krycklan suggests that recovery from sulfate deposition was strong in the early 2000s and began to fully recover in the second decade (Fig. 18a). This argument supports both the hypothesis that recovery from sulfate deposition was the primary cause of increasing DOC trends in most areas of Sweden and that this recovery is approaching an end point (Eklöf et al., 2021). Despite this, as the contribution of SO_4 has diminished over time (Fig. 18a1), the relative importance of terrestrial productivity (Fig.18b1) and soil temperature have increased (Fig.18d1). However, the absolute contributions of these factors to DOC trends has remained roughly consistent, suggesting that these emergent drivers are weaker than the deposition recovery response. Indeed, the contribution of terrestrial productivity to variations in DOC concentrations can be either positive or negative, according to the direction of priming effect under different landscapes and the C input (Zhu et al., 2022). In addition, the importance of discharge across time was quite stable (Fig.18 c1); discharge may decrease DOC concentrations via dilution or increase DOC concentrations via flushing based on the predominate

hydrological pathways in different landscapes (Tiwari et al. 2022; Zhu et al., 2022). Finally, although soil temperature has made a relatively greater contribution during the last decade, it is unlikely to generate a substantial upward trend of DOC by itself (Freeman et al., 2001; Pastor et al., 2003). Therefore, in the recent decade since the driving force of sulfate weakened, other factors have been insufficient to maintain the long-term trend.

The ongoing browning observed in many sites in Sweden can be attributed to either the high impact of land use changes (Lindbladh et al., 2014; Kritzberg, 2017; Škerlep et al., 2020) or to the areas that received the most acid deposition, particularly in the southern region, which may take a longer time to recover (Eklöf et al., 2021). Thus, our findings largely concur with Evans et al. (2006), in that rising DOC in freshwaters may to a large extent reflect recovery from S-deposition, rather than ecosystem responses to climate change, and future predictions of dramatic intensification of C export from terrestrial ecosystem may perhaps be overly pessimistic, at least in the shorter term. However, we acknowledge that variables we test likely have very different response times on DOC increases (e.g., a change in SO_4 or temperature could be instantaneous, while building up a large humus layer could result in a DOC increase decades later), and any delayed responses are not readily detected.

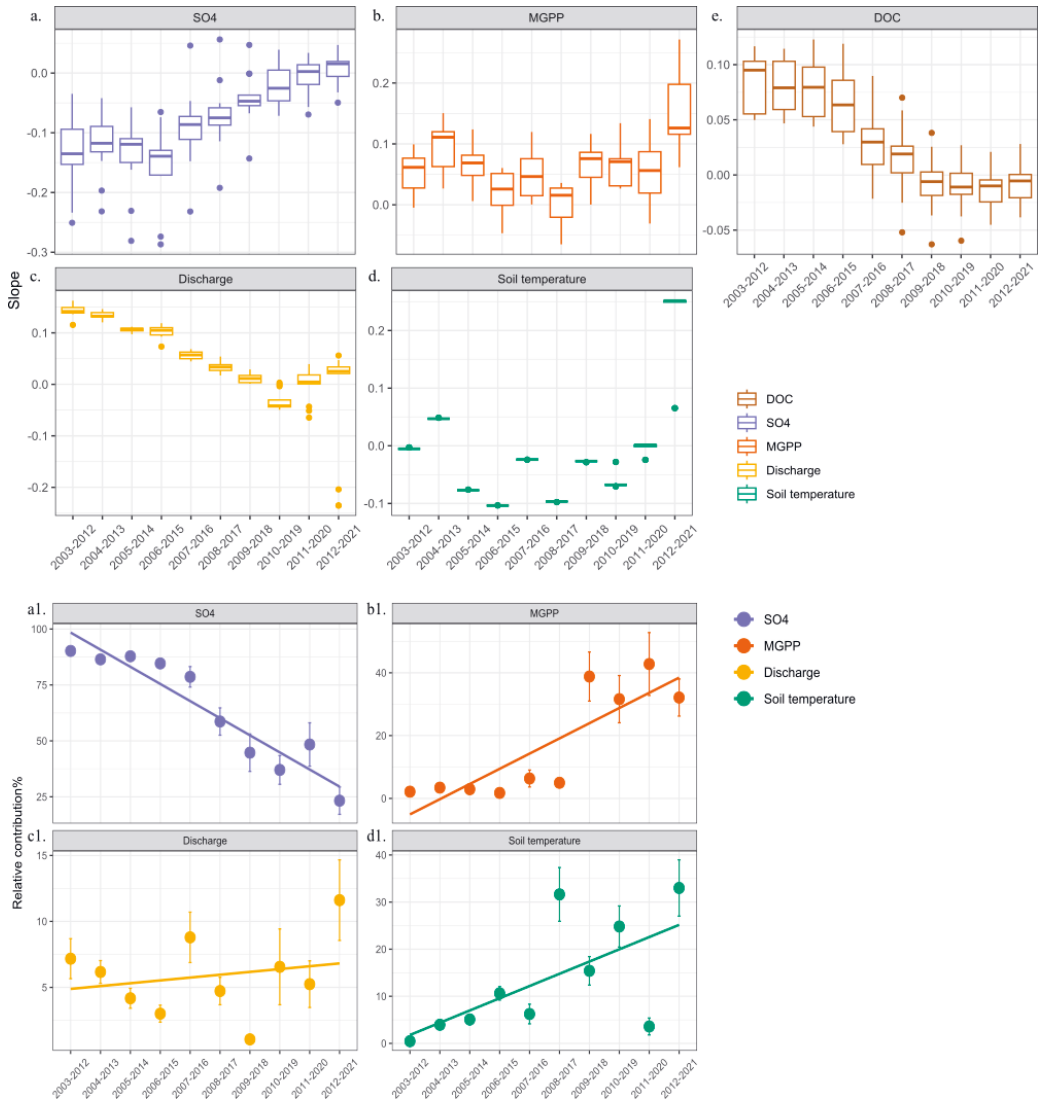


Figure 18. The slope of sulfate (SO₄) (a), MODIS GPP (MGPP) (b), discharge (c), soil temperature (d) and DOC (e) trends across all periods (a 10-year moving window from 2003 to 2021) in Krycklan catchments. Meanwhile, the relative contribution (%) of SO₄ (a1), MGPP (b1), discharge (c1) and soil temperature (d1) to long-term DOC trends across all periods.

5 Conclusions and future perspectives

Study I indicated that the in-situ S::CAN works well, although during February to April ice formation on the instruments may somehow reduce accuracy. However, this did not affect the successful creation of accurate and unbiased models for DOC across multiple watersheds, and these models could be extrapolated from one watershed to another, even without site-specific calibration. This means that the remote DOC sensors based on spectrophotometry could be calibrated with a low number of samples. Comparison of the performance of the three multivariate methods (PCR, PLS and MSR) indicated that MSR lead to the best model for predictions of DOC concentrations. In the future, the same research could be conducted in regions around the world to improve the versatility of our proposed models.

Study II demonstrated the importance of the interaction between terrestrial productivity and discharge in controlling variations of DOC concentrations in boreal catchments. Forest productivity dramatically promotes DOC contents in small catchments (< 1 km²), while the importance of GPP is masked by discharge in larger catchments. Moreover, priming effect and land cover type (proportion of mire) should be included in process-based DOC models. Overall, our investigation revealed that terrestrial greening and altering hydrology following climate change may have a major impact on DOC concentration in aquatic ecosystems, as well as reaffirmed the importance of DOC fluxes in controlling ecosystem C budgets, which is generally disregarded. In the future, to firmly establish the link between terrestrial greening and aquatic browning, we need to extend our modelling approach to different climatic regions.

Study III provided evidence that large (five-fold) variations in browning trends among northern streams can reflect the outcome of interactions among multiple factors, including recovery from SO₄ deposition, climate-related factors, and catchment properties. Our results further suggest that recovery from SO₄ rather than from acidification per se has been the main driver of DOC change, despite the low deposition history in this region. Additionally, our modelling approach revealed the important lag-effects of

terrestrial production and discharge on stream DOC, albeit with weaker influences on overall DOC trends when compared to SO_4 declines. This also helps to explain why browning has weakened in the last decade: stream sulfate levels have plummeted, and other drivers were insufficient to sustain the ongoing long-term trend of DOC. However, given the unexplained variations in our model performance and the heterogeneity in the inherent DOC dynamics among catchments, a critical evaluation is needed when extrapolating our models to other regions or predicting the future trends.

My future research on browning will expand the scope from cold zones to tropical regions, delve from DOC quantity into DOC quality, trace the entire cycle of DOC from its origin, and finally enhance comprehension of the broader C cycle across terrestrial, aquatic, and atmospheric ecosystems.

Bibliography

- Aitkenhead, J.A. & McDowell, W.H. 2000. Soil C:N ratio as a predictor of annual riverine DOC flux at local and global scales. *Global Biogeochemical Cycles* 14: 127–138.
- Asmala, E., Carstensen, J. & Raibe, A. 2019. Multiple anthropogenic drivers behind upward trends in organic carbon concentrations in boreal rivers. *Environ. Res. Lett.* 14: 124018.
- Aubinet, M., Vesala, T. & Papale, D. 2012. *Eddy Covariance: A Practical Guide to Measurement and Data Analysis*. Springer Science & Business Media.
- Avagyan, A., Runkle, B.R.K. & Kutzbach, L. 2014. Application of high-resolution spectral absorbance measurements to determine dissolved organic carbon concentration in remote areas. *Journal of Hydrology* 517: 435–446.
- Baker, A., Bolton, L., Newson, M. & Spencer, R.G.M. 2008. Spectrophotometric properties of surface water dissolved organic matter in an afforested upland peat catchment. *Hydrological Processes* 22: 2325–2336.
- Baker, A., Spencer & R.G.M. 2004. Characterization of dissolved organic matter from source to sea using fluorescence and absorbance spectroscopy. *Science of The Total Environment* 333: 217–232.
- Bastida, F., Garca, C., Fierer, N., Eldridge, D.J., Bowker, M.A., Abades, S., Alfaro, F.D., Asefaw Berhe, A., Cutler, N.A., Gallardo, A., Garca-Velazquez, L., Hart, S.C., Hayes, P.E., Hernandez, T., Hseu, Z.-Y., Jehmlich, N., Kirchmair, M., Lambers, H., Neuhauser, S., Pena-Ramirez, V.M., Perez, C.A., Reed, S.C., Santos, F., Siebe, C., Sullivan, B.W., Trivedi, P., Vera, A., Williams, M.A., Luis Moreno, J. & Delgado-Baquerizo, M. 2019. Global ecological predictors of the soil priming effect. *Nat Commun* 10: 3481.
- Battin, T.J., Kaplan, L.A., Findlay, S., Hopkinson, C.S., Marti, E., Packman, A.I., Newbold, J.D. & Sabater, F. 2008. Biophysical controls on organic carbon fluxes in fluvial networks. *Nature Geosci* 1: 95–100.
- Bengtsson, M.M., Attermeyer, K. & Catalan, N. 2018. Interactive effects on organic matter processing from soils to the ocean: are priming effects relevant in aquatic ecosystems? *Hydrobiologia* 822: 1–17.

- Bishop, K., Seibert, J., Köhler, S. & Laudon, H. 2004. Resolving the Double Paradox of rapidly mobilized old water with highly variable responses in runoff chemistry. *Hydrological Processes* 18:185–189.
- Black, K., Bolger, T., Davis, P., Nieuwenhuis, M., Reidy, B., Saiz, G., Tobin, B. & Osborne, B. 2007. Inventory and eddy covariance-based estimates of annual carbon sequestration in a Sitka spruce (*Picea sitchensis* (Bong.) Carr.) forest ecosystem. *Eur J Forest Res* 126: 167–178.
- Catalán, N., Kellerman, A.M., Peter, H., Carmona, F. & Tranvik, L.J. 2015. Absence of a priming effect on dissolved organic carbon degradation in lake water. *Limnology and Oceanography* 60: 159–168.
- Ciais, P., Schelhaas, M.J., Zaehle, S., Piao, S.L., Cescatti, A., Liski, J., Luysaert, S., Le-Maire, G., Schulze, E.-D., Bouriaud, O., Freibauer, A., Valentini, R. & Nabuurs, G.J. 2008. Carbon accumulation in European forests. *Nature Geosci* 1: 425–429.
- Clark, J.M., Bottrell, S.H., Evans, C.D., Monteith, D.T., Bartlett, R., Rose, R., Newton, R.J. & Chapman, P.J. 2010. The importance of the relationship between scale and process in understanding long-term DOC dynamics. *Science of The Total Environment* 408: 2768–2775.
- Clark, J.M., Lane, S.N., Chapman, P.J. & Adamson, J.K. 2007. Export of dissolved organic carbon from an upland peatland during storm events: Implications for flux estimates. *Journal of Hydrology* 347: 438–447.
- Conley, D.J., Carstensen, J., Aigars, J., Axe, P., Bonsdorff, E., Eremina, T., Haahti, B.-M., Humborg, C., Jonsson, P., Kotta, J., Lännegren, C., Larsson, U., Maximov, A., Medina, M.R., Lysiak-Pastuszek, E., Remeikaitė-Nikienė, N., Walve, J., Wilhelms, S. & Zillén, L. 2011. Hypoxia Is Increasing in the Coastal Zone of the Baltic Sea. *Environ. Sci. Technol.* 45: 6777–6783.
- Covino, T. 2017. Hydrologic connectivity as a framework for understanding biogeochemical flux through watersheds and along fluvial networks. *Geomorphology, Connectivity in Geomorphology from Binghamton* 2016. 277: 133–144.
- Crapart, C., Finstad, A.G., Hessen, D.O., Vogt, R.D. & Andersen, T. 2023. Spatial predictors and temporal forecast of total organic carbon levels in boreal lakes. *Science of The Total Environment* 870: 161676.
- Dawson, J.J.C., Billett, M.F., Neal, C. & Hill, S. 2002. A comparison of particulate, dissolved and gaseous carbon in two contrasting upland streams in the UK. *Journal of Hydrology* 257: 226–246.

- Dawson, J.J.C., Soulsby, C., Tetzlaff, D., Hrachowitz, M., Dunn, S.M. & Malcolm, I.A. 2008. Influence of hydrology and seasonality on DOC exports from three contrasting upland catchments. *Biogeochemistry* 90: 93–113.
- de Wit, H.A., Austnes, K., Hysten, G. & Dalsgaard, L. 2015. A carbon balance of Norway: terrestrial and aquatic carbon fluxes. *Biogeochemistry* 123: 147–173.
- de Wit, H.A., Valinia, S., Weyhenmeyer, G., Futter, M., Kortelainen, P., Austnes, K., Hessen, D.O., Raike, A., Laudon, H. & Vuorenmaa, J. 2016. Current Browning of Surface Waters Will Be Further Promoted by Wetter Climate. *Environmental Science and Technology Letters* 3: 430–435.
- Dijkstra, F., Carrillo, Y., Pendall, E. & Morgan, J. 2013. Rhizosphere priming: a nutrient perspective. *Frontiers in Microbiology* 4: 216.
- Drake, T.W., Raymond, P.A., Spencer & R.G.M. 2018. Terrestrial carbon inputs to inland waters: A current synthesis of estimates and uncertainty. *Limnology and Oceanography Letters* 3: 132–142.
- Drought 2018 Team, ICOS Ecosystem Thematic Centre, 2020. Drought-2018 ecosystem eddy covariance flux product for 52 stations in FLUXNET-Archive format.
- Eklöf, K., von Brömssen, C., Amvrosiadi, N., Fölster, J., Wallin, M.B. & Bishop, K. 2021. Brownification on hold: What traditional analyses miss in extended surface water records. *Water Research* 203: 117544.
- Ekström, S. 2013. Brownification of freshwaters - the role of dissolved organic matter and iron (thesis/doccomp). Lund University.
- Evans, C., Chapman, P., Clark, J.M., Monteith, D. & Cresser, M.S. 2006. Alternative explanations for rising dissolved organic carbon export from organic soils. *Global Change Biology* 12: 2044–2053.
- Ewing, S.A., Sanderman, J., Baisden, W.T., Wang, Y. & Amundson, R. 2006. Role of large-scale soil structure in organic carbon turnover: Evidence from California grassland soils. *Journal of Geophysical Research: Biogeosciences* 111.
- Ferm, M., Granat, L., Engardt, M., Pihl Karlsson, G., Danielsson, H., Karlsson, P.E. & Hansen, K. 2019. Wet deposition of ammonium, nitrate and non-sea-salt sulphate in Sweden 1955 through 2017. *Atmospheric Environment: X* 2: 100015.
- Findlay, S. & Sinsabaugh, R.L. 2003. *Aquatic Ecosystems: Interactivity of Dissolved Organic Matter*. Academic Press.

- Finstad, A.G., Andersen, T., Larsen, S., Tominaga, K., Blumentrath, S., de Wit, H.A., Tømmervik, H. & Hessen, D.O. 2016. From greening to browning: Catchment vegetation development and reduced S-deposition promote organic carbon load on decadal time scales in Nordic lakes. *Sci Rep* 6: 31944.
- Fork, M.L., Sponseller, R.A. & Laudon, H. 2020. Changing Source-Transport Dynamics Drive Differential Browning Trends in a Boreal Stream Network. *Water Resources Research* 56: e2019WR026336.
- Freeman, C., Evans, C.D., Monteith, D.T., Reynolds, B. & Fenner, N. 2001. Export of organic carbon from peat soils. *Nature* 412: 785–785.
- Freeman, C., Fenner, N., Ostle, N.J., Kang, H., Dorrick, D.J., Reynolds, B., Lock, M.A., Sleep, D., Hughes, S. & Hudson, J. 2004. Export of dissolved organic carbon from peatlands under elevated carbon dioxide levels. *Nature* 430: 195–198.
- Gasparrini, A. 2011. Distributed Lag Linear and Non-Linear Models in R: The Package *dlm*. *Journal of Statistical Software* 43: 1–20.
- Gonzales, A., J, N., J, H. & Uhlenbrook, S. 2009. Comparison of different base flow separation methods in a lowland catchment. *Hydrology and Earth System Sciences* 6.
- Gorelick, N., Hancher, M., Dixon, M., Ilyushchenko, S., Thau, D. & Moore, R. 2017. Google Earth Engine: Planetary-scale geospatial analysis for everyone. *Remote Sensing of Environment, Big Remotely Sensed Data: tools, applications and experiences* 202: 18–27.
- Graeber, D., Gelbrecht, J., Pusch, M.T., Anlanger, C. & von Schiller, D. 2012. Agriculture has changed the amount and composition of dissolved organic matter in Central European headwater streams. *Science of The Total Environment* 438: 435–446.
- Grayson, R. & Holden, J. 2012. Continuous measurement of spectrophotometric absorbance in peatland streamwater in northern England: implications for understanding fluvial carbon fluxes. *Hydrological Processes* 26: 27–39.
- Grinsted, A., Moore, J.C. & Jevrejeva, S. 2004. Application of the cross wavelet transform and wavelet coherence to geophysical time series. *Nonlinear Processes in Geophysics* 11: 561–566.
- Guay, K.C., Beck, P.S.A., Berner, L.T., Goetz, S.J., Baccini, A. & Buermann, W. 2014. Vegetation productivity patterns at high northern latitudes: a multi-sensor satellite data assessment. *Global Change Biology* 20: 3147–3158.

- Guenet, B., Danger, M., Abbadie, L. & Lacroix, G. 2010. Priming effect: bridging the gap between terrestrial and aquatic ecology. *Ecology* 91: 2850–2861.
- Härkönen, L.H., Lepistö, A., Sarkkola, S., Kortelainen, P. & Räike, A. 2023. Reviewing peatland forestry: Implications and mitigation measures for freshwater ecosystem browning. *Forest Ecology and Management* 531: 120776.
- He, Y., Cheng, W., Zhou, L., Shao, J., Liu, H., Zhou, H., Zhu, K. & Zhou, X. 2020. Soil DOC release and aggregate disruption mediate rhizosphere priming effect on soil C decomposition. *Soil Biology and Biochemistry* 144: 107787.
- Heinonsalo, J., Pumpanen, J., Rasilo, T., Hurme, K.-R. & Ilvesniemi, H. 2010. Carbon partitioning in ectomycorrhizal Scots pine seedlings. *Soil Biology and Biochemistry* 42: 1614–1623.
- Hinton, M.J., Schiff, S.L. & English, M.C. 1998. Sources and flowpaths of dissolved organic carbon during storms in two forested watersheds of the Precambrian Shield. *Biogeochemistry* 41: 175–197.
- Huang, T.-H., Fu, Y.-H., Pan, P.-Y. & Chen, C.-T.A. 2012. Fluvial carbon fluxes in tropical rivers. *Current Opinion in Environmental Sustainability, Carbon and nitrogen cycles* 4: 162–169.
- Hudson, J.J., Dillon, P.J. & Somers, K.M. 2003. Long-term patterns in dissolved organic carbon in boreal lakes: the role of incident radiation, precipitation, air temperature, southern oscillation and acid deposition. *Hydrology and Earth System Sciences* 7: 390–398.
- Huo, C., Luo, Y. & Cheng, W. 2017. Rhizosphere priming effect: A meta-analysis. *Soil Biology and Biochemistry* 111: 78–84.
- Hyndman, R.J. & Khandakar, Y. 2008. Automatic Time Series Forecasting: The forecast Package for R. *J. Stat. Soft.* 27.
- Jansson, M., Hickler, T., Jonsson, A. & Karlsson, J. 2008. Links between Terrestrial Primary Production and Bacterial Production and Respiration in Lakes in a Climate Gradient in Subarctic Sweden. *Ecosystems* 11: 367–376.
- Johansson, L., Temnerud, J., Abrahamsson, J. & Kleja, D.B. 2010. Variation in Organic Matter and Water Color in Lake Mälaren during the Past 70 Years. *AMBIO* 39: 116–125.
- Jutras, M.-F., Nasr, M., Castonguay, M., Pit, C., Pomeroy, J.H., Smith, T.P., Zhang, C., Ritchie, C.D., Meng, F.-R., Clair, T.A. & Arp, P.A. 2011. Dissolved organic carbon concentrations and fluxes in forest

- catchments and streams: DOC-3 model. *Ecological Modelling* 222: 2291–2313.
- Kalbitz, K., Solinger, S., Park, J.-H., Michalzik, B. & Matzner, E. 2000. CONTROLS ON THE DYNAMICS OF DISSOLVED ORGANIC MATTER IN SOILS: A REVIEW. *Soil Science* 165: 277–304.
- Kang, H., Kwon, M.J., Kim, S., Lee, S., Jones, T.G., Johncock, A.C., Haraguchi, A. & Freeman, C. 2018. Biologically driven DOC release from peatlands during recovery from acidification. *Nat Commun* 9: 3807.
- Karimi, S., Seibert, J. & Laudon, H. 2022. Evaluating the effects of alternative model structures on dynamic storage simulation in heterogeneous boreal catchments. *Hydrology Research* 53: 562–583.
- Keller, W. (Bill), Paterson, A.M., Somers, K.M., Dillon, P.J., Heneberry, J. & Ford, A. 2008. Relationships between dissolved organic carbon concentrations, weather, and acidification in small Boreal Shield lakes. *Can. J. Fish. Aquat. Sci.* 65: 786–795.
- Köhler, S.J., Buffam, I., Laudon, H. & Bishop, K.H. 2008. Climate's control of intra-annual and interannual variability of total organic carbon concentration and flux in two contrasting boreal landscape elements. *Journal of Geophysical Research: Biogeosciences* 113.
- Kritzberg, E.S. 2017. Centennial-long trends of lake browning show major effect of afforestation. *Limnology and Oceanography* 2: 105–112.
- Kritzberg, E.S., Hasselquist, E.M., Škerlep, M., Löfgren, S., Olsson, O., Stadmark, J., Valinia, S., Hansson, L.-A. & Laudon, H. 2020. Browning of freshwaters: Consequences to ecosystem services, underlying drivers, and potential mitigation measures. *Ambio* 49: 375–390.
- Kulmala, L., Pumpanen, J., Kolari, P., Dengel, S., Berninger, F., Köster, K., Matkala, L., Vanhatalo, A., Vesala, T. & Bäck, J. 2019. Inter- and intra-annual dynamics of photosynthesis differ between forest floor vegetation and tree canopy in a subarctic Scots pine stand. *Agricultural and Forest Meteorology* 271: 1–11.
- Kumar, P. & Foufoula-Georgiou, E. 1997. Wavelet analysis for geophysical applications. *Reviews of Geophysics* 35: 385–412.
- Kuzyakov, Y., 2002. Review: Factors affecting rhizosphere priming effects. *Journal of Plant Nutrition and Soil Science* 165: 382–396.
- Malcolm, R. L. 1990. The uniqueness of humic substances in each of soil, stream and marine environments. *Analytica Chimica Acta* 232: 19–30.
- Langergraber, G., Fleischmann, N. & Hofstädter, F. 2003. A multivariate calibration procedure for UV/VIS spectrometric quantification of

- organic matter and nitrate in wastewater. *Water Science and Technology* 47: 63–71.
- Lapierre, J.-F., Collins, S.M., Oliver, S.K., Stanley, E.H. & Wagner, T. 2021. Inconsistent browning of northeastern U.S. lakes despite increased precipitation and recovery from acidification. *Ecosphere* 12: e03415.
- Larsen, S., Andersen, T. & Hessen, D.O. 2011. Predicting organic carbon in lakes from climate drivers and catchment properties. *Global Biogeochemical Cycles* 25.
- Laudon, H., Berggren, M., Ågren, A., Buffam, I., Bishop, K., Grabs, T., Jansson, M. & Köhler, S. 2011. Patterns and Dynamics of Dissolved Organic Carbon (DOC) in Boreal Streams: The Role of Processes, Connectivity, and Scaling. *Ecosystems* 14: 880–893.
- Laudon, H., Hasselquist, E.M., Peichl, M., Lindgren, K., Sponseller, R., Lidman, F., Kuglerová, L., Hasselquist, N.J., Bishop, K., Nilsson, M.B. & Ågren, A.M. 2021a. Northern landscapes in transition: Evidence, approach and ways forward using the Krycklan Catchment Study. *Hydrological Processes* 35: e14170.
- Laudon, H., Köhler, S. & Buffam, I. 2004. Seasonal TOC export from seven boreal catchments in northern Sweden. *Aquatic Sciences - Research Across Boundaries* 66: 223–230.
- Laudon, H. & Sponseller, R.A. 2018. How landscape organization and scale shape catchment hydrology and biogeochemistry: insights from a long-term catchment study. *WIREs Water* 5: e1265.
- Laudon, H., Sponseller, R.A. & Bishop, K. 2021b. From legacy effects of acid deposition in boreal streams to future environmental threats. *Environ. Res. Lett.* 16: 015007.
- Laudon, H., Taberman, I., Ågren, A., Futter, M., Ottosson-Löfvenius, M. & Bishop, K. 2013. The Krycklan Catchment Study—A flagship infrastructure for hydrology, biogeochemistry, and climate research in the boreal landscape. *Water Resources Research* 49: 7154–7158.
- Lawrence, G.B. & Roy, K.M. 2021. Ongoing increases in dissolved organic carbon are sustained by decreases in ionic strength rather than decreased acidity in waters recovering from acidic deposition. *Science of The Total Environment* 766: 142529.
- Leach, T.H., Winslow, L.A., Hayes, N.M. & Rose, K.C. 2019. Decoupled trophic responses to long-term recovery from acidification and associated browning in lakes. *Global Change Biology* 25: 1779–1792.

- Ledesma, J.L.J., Futter, M.N., Laudon, H., Evans, C.D. & Köhler, S.J. 2016. Boreal forest riparian zones regulate stream sulfate and dissolved organic carbon. *Science of The Total Environment* 560–561: 110–122.
- Ledesma, J.L.J., Grabs, T., Bishop, K.H., Schiff, S.L. & Köhler, S.J. 2015. Potential for long-term transfer of dissolved organic carbon from riparian zones to streams in boreal catchments. *Global Change Biology* 21: 2963–2979.
- Leenheer, J.A. & Croué, J.-P. 2003. Peer Reviewed: Characterizing Aquatic Dissolved Organic Matter. *Environ. Sci. Technol.* 37: 18A-26A.
- Lepistö, A., Räike, A., Sallantausta, T. & Finér, L. 2021. Increases in organic carbon and nitrogen concentrations in boreal forested catchments — Changes driven by climate and deposition. *Science of The Total Environment* 780: 146627.
- Lidberg, W., Nilsson, M., Lundmark, T. & Ågren, A.M. 2017. Evaluating preprocessing methods of digital elevation models for hydrological modelling. *Hydrological Processes* 31: 4660–4668. 5
- Lidman, F., Boily, Å., Laudon, H. & Köhler, S.J. 2017. From soil water to surface water – how the riparian zone controls element transport from a boreal forest to a stream. *Biogeosciences* 14: 3001–3014.
- Lindbladh, M., Axelsson, A.-L., Hultberg, T., Brunet, J. & Felton, A. 2014. From broadleaves to spruce – the borealization of southern Sweden. *Scandinavian Journal of Forest Research* 29: 686–696.
- Linkosalmi, M., Pumpanen, J., Biasi, C., Heinonsalo, J., Laiho, R., Lindén, A., Palonen, V., Laurila, T. & Lohila, A. 2015. Studying the impact of living roots on the decomposition of soil organic matter in two different forestry-drained peatlands. *Plant Soil* 396: 59–72.
- Liu, W., Xu, X., McGoff, N.M., Eaton, J.M., Leahy, P., Foley, N. & Kiely, G. 2014. Spatial and Seasonal Variation of Dissolved Organic Carbon (DOC) Concentrations in Irish Streams: Importance of Soil and Topography Characteristics. *Environmental Management* 53: 959–967.
- Liu, X.-J.A., Sun, J., Mau, R.L., Finley, B.K., Compson, Z.G., van Gestel, N., Brown, J.R., Schwartz, E., Dijkstra, P. & Hungate, B.A. 2017. Labile carbon input determines the direction and magnitude of the priming effect. *Applied Soil Ecology* 109: 7–13.
- Mann, P.J., Davydova, A., Zimov, N., Spencer, R.G.M., Davydov, S., Bulygina, E., Zimov, S. & Holmes, R.M. 2012a. Controls on the composition and lability of dissolved organic matter in Siberia's Kolyma River basin. *Journal of Geophysical Research: Biogeosciences* 117.

- McDonald, S., Bishop, A.G., Prenzler, P.D. & Robards, K. 2004. Analytical chemistry of freshwater humic substances. *Analytica Chimica Acta* 527: 105–124.
- McGlynn, B.L., McDonnell, J.J., Shanley, J.B. & Kendall, C. 1999. Riparian zone flowpath dynamics during snowmelt in a small headwater catchment. *Journal of Hydrology* 222: 75–92.
- Medlyn, B.E., Robinson, A.P., Clement, R. & McMurtrie, R.E. 2005. On the validation of models of forest CO₂ exchange using eddy covariance data: some perils and pitfalls. *Tree Physiology* 25: 839–857.
- Mevik, B.-H., Wehrens, R. & Liland, K.H. 2019. pls: Partial Least Squares and Principal Component Regression.
- Meyer-Jacob, C., Michelutti, N., Paterson, A.M., Cumming, B.F., Keller, W. (Bill) & Smol, J.P. 2019. The browning and re-browning of lakes: Divergent lake-water organic carbon trends linked to acid deposition and climate change. *Sci Rep* 9: 16676.
- Meyer-Jacob, C., Tolu, J., Bigler, C., Yang, H. & Bindler, R. 2015. Early land use and centennial scale changes in lake-water organic carbon prior to contemporary monitoring. *PNAS* 112: 6579–6584.
- Miller, J.N. & Miller, J.C. 2010. *Statistics and Chemometrics for Analytical Chemistry*, 6th Edition.
- Minayeva, T., Sirin, A., Kershaw, P. & Bragg, O. 2017. Arctic Peatlands, in: Finlayson, C.M., Milton, G.R., Prentice, R.C., Davidson, N.C. (Eds.), *The Wetland Book: II: Distribution, Description and Conservation*. Springer Netherlands, Dordrecht, pp. 1–15.
- Monteith, D.T., Stoddard, J.L., Evans, C.D., de Wit, H.A., Forsius, M., Høgåsen, T., Wilander, A., Skjelkvåle, B.L., Jeffries, D.S., Vuorenmaa, J., Keller, B., Kopáček, J. & Vesely, J. 2007. Dissolved organic carbon trends resulting from changes in atmospheric deposition chemistry. *Nature* 450: 537–540.
- Myers-Smith, I.H., Kerby, J.T., Phoenix, G.K., Bjerke, J.W., Epstein, H.E., Assmann, J.J., John, C., Andreu-Hayles, L., Angers-Blondin, S., Beck, P.S.A., Berner, L.T., Bhatt, U.S., Bjorkman, A.D., Blok, D., Bryn, A., Christiansen, C.T., Cornelissen, J.H.C., Cunliffe, A.M., Elmendorf, S.C., Forbes, B.C., Goetz, S.J., Hollister, R.D., de Jong, R., Loranty, M.M., Macias-Fauria, M., Maseyk, K., Normand, S., Olofsson, J., Parker, T.C., Parmentier, F.-J.W., Post, E., Schaepman-Strub, G., Stordal, F., Sullivan, P.F., Thomas, H.J.D., Tømmervik, H., Treharne, R., Tweedie, C.E.,

- Walker, D.A., Wilking, M. & Wipf, S. 2020. Complexity revealed in the greening of the Arctic. *Nat. Clim. Chang.* 10: 106–117.
- Mzobe, P., Berggren, M., Pilesjö, P., Lundin, E., Olefeldt, D., Roulet, N.T. & Persson, A. 2018. Dissolved organic carbon in streams within a subarctic catchment analysed using a GIS/remote sensing approach. *PLOS ONE* 13: e0199608.
- O'Callaghan, J.F. & Mark, D.M. 1984. The Extraction of Drainage Networks from Digital Elevation Data.
- Ogle, S.M., Breidt, F.J. & Paustian, K. 2005. Agricultural management impacts on soil organic carbon storage under moist and dry climatic conditions of temperate and tropical regions. *Biogeochemistry* 72: 87–121.
- Oni, S.K., Futter, M.N., Bishop, K., Köhler, S.J., Ottosson-Löfvenius, M. & Laudon, H. 2012. Long term patterns in dissolved organic carbon, major elements and trace metals in boreal headwater catchments: trends, mechanisms and heterogeneity (preprint). *Biogeochemistry: Rivers & Streams*.
- Öquist, M.G., Bishop, K., Grelle, A., Klemetsson, L., Köhler, S.J., Laudon, H., Lindroth, A., Ottosson Löfvenius, M., Wallin, M.B. & Nilsson, M.B., 2014. The Full Annual Carbon Balance of Boreal Forests Is Highly Sensitive to Precipitation. *Environ. Sci. Technol. Lett.* 1: 315–319.
- Pacific, V.J., Jencso, K.G. & McGlynn, B.L. 2010. Variable flushing mechanisms and landscape structure control stream DOC export during snowmelt in a set of nested catchments. *Biogeochemistry* 99: 193–211.
- Pagano, T., Bida, M. & Kenny, J.E. 2014. Trends in Levels of Allochthonous Dissolved Organic Carbon in Natural Water: A Review of Potential Mechanisms under a Changing Climate. *Water* 6: 2862–2897.
- Pastor, J., Solin, J., Bridgham, S.D., Updegraff, K., Harth, C., Weishampel, P. & Dewey, B. 2003. Global warming and the export of dissolved organic carbon from boreal peatlands. *Oikos* 100: 380–386.
- Pastorello, G., Trotta, C., Canfora, E., Chu, H., Christianson, D., Cheah, Y.-W., Poindexter, C., Chen, J., Elbashandy, A., Humphrey, M., Isaac, P., Polidori, D., Reichstein, M., Ribeca, A., van Ingen, C., Vuichard, N., Zhang, L., Amiro, B., Ammann, C., Arain, M.A., Ardö, J., Arkebauer, T., Arndt, S.K., Arriga, N., Aubinet, M., Aurela, M., Baldocchi, D., Barr, A., Beamesderfer, E., Marchesini, L.B., Bergeron, O., Beringer, J., Bernhofer, C., Berveiller, D., Billesbach, D., Black, T.A., Blanken, P.D., Bohrer, G., Boike, J., Bolstad, P.V., Bonal, D., Bonnefond, J.-M.,

Bowling, D.R., Bracho, R., Brodeur, J., Brümmer, C., Buchmann, N., Burban, B., Burns, S.P., Buysse, P., Cale, P., Cavagna, M., Cellier, P., Chen, S., Chini, I., Christensen, T.R., Cleverly, J., Collalti, A., Consalvo, C., Cook, B.D., Cook, D., Coursolle, C., Cremonese, E., Curtis, P.S., D'Andrea, E., da Rocha, H., Dai, X., Davis, K.J., Cinti, B.D., Grandcourt, A. de, Ligne, A.D., De Oliveira, R.C., Delpierre, N., Desai, A.R., Di Bella, C.M., Tommasi, P. di, Dolman, H., Domingo, F., Dong, G., Dore, S., Duce, P., Dufrêne, E., Dunn, A., Dušek, J., Eamus, D., Eichelmann, U., ElKhidir, H.A.M., Eugster, W., Ewenz, C.M., Ewers, B., Famulari, D., Fares, S., Feigenwinter, I., Feitz, A., Fensholt, R., Filippa, G., Fischer, M., Frank, J., Galvagno, M., Gharun, M., Gianelle, D., Gielen, B., Gioli, B., Gitelson, A., Goded, I., Goeckede, M., Goldstein, A.H., Gough, C.M., Goulden, M.L., Graf, A., Griebel, A., Gruening, C., Grünwald, T., Hammerle, A., Han, S., Han, X., Hansen, B.U., Hanson, C., Hatakka, J., He, Y., Hehn, M., Heinesch, B., Hinko-Najera, N., Hörtnagl, L., Hutley, L., Ibrom, A., Ikawa, H., Jackowicz-Korczynski, M., Janouš, D., Jans, W., Jassal, R., Jiang, S., Kato, T., Khomik, M., Klatt, J., Knohl, A., Knox, S., Kobayashi, H., Koerber, G., Kolle, O., Kosugi, Y., Kotani, A., Kowalski, A., Kruijt, B., Kurbatova, J., Kutsch, W.L., Kwon, H., Launiainen, S., Laurila, T., Law, B., Leuning, R., Li, Yingnian, Liddell, M., Limousin, J.-M., Lion, M., Liska, A.J., Lohila, A., López-Ballesteros, A., López-Blanco, E., Loubet, B., Loustau, D., Lucas-Moffat, A., Lüers, J., Ma, S., Macfarlane, C., Magliulo, V., Maier, R., Mammarella, I., Manca, G., Marcolla, B., Margolis, H.A., Marras, S., Massman, W., Mastepanov, M., Matamala, R., Matthes, J.H., Mazzenga, F., McCaughey, H., McHugh, I., McMillan, A.M.S., Merbold, L., Meyer, W., Meyers, T., Miller, S.D., Minerbi, S., Moderow, U., Monson, R.K., Montagnani, L., Moore, C.E., Moors, E., Moreaux, V., Moureaux, C., Munger, J.W., Nakai, T., Neiryneck, J., Nestic, Z., Nicolini, G., Noormets, A., Northwood, M., Noretto, M., Nouvellon, Y., Novick, K., Oechel, W., Olesen, J.E., Ourcival, J.-M., Papuga, S.A., Parmentier, F.-J., Paul-Limoges, E., Pavelka, M., Peichl, M., Pendall, E., Phillips, R.P., Pilegaard, K., Pirk, N., Posse, G., Powell, T., Prasse, H., Prober, S.M., Rambal, S., Rannik, Ü., Raz-Yaseef, N., Rebmann, C., Reed, D., Dios, V.R. de, Restrepo-Coupe, N., Reverter, B.R., Roland, M., Sabbatini, S., Sachs, T., Saleska, S.R., Sánchez-Cañete, E.P., Sanchez-Mejia, Z.M., Schmid, H.P., Schmidt, M., Schneider, K., Schrader, F., Schroder, I., Scott, R.L., Sedlák, P., Serrano-Ortíz, P., Shao, C., Shi, P., Shironya, I., Siebicke, L., Šigut, L., Silberstein,

- R., Sirca, C., Spano, D., Steinbrecher, R., Stevens, R.M., Sturtevant, C., Suyker, A., Tagesson, T., Takanashi, S., Tang, Y., Tapper, N., Thom, J., Tomassucci, M., Tuovinen, J.-P., Urbanski, S., Valentini, R., van der Molen, M., van Gorsel, E., van Huissteden, K., Varlagin, A., Verfaillie, J., Vesala, T., Vincke, C., Vitale, D., Vygodskaya, N., Walker, J.P., Walter-Shea, E., Wang, H., Weber, R., Westermann, S., Wille, C., Wofsy, S., Wohlfahrt, G., Wolf, S., Woodgate, W., Li, Yuelin, Zampedri, R., Zhang, J., Zhou, G., Zona, D., Agarwal, D., Biraud, S., Torn, M. & Papale, D. 2020. The FLUXNET2015 dataset and the ONEFlux processing pipeline for eddy covariance data. *Scientific Data* 7: 225.
- Peralta-Tapia, A., Sponseller, R.A., Tetzlaff, D., Soulsby, C. & Laudon, H. 2015a. Connecting precipitation inputs and soil flow pathways to stream water in contrasting boreal catchments. *Hydrological Processes* 29: 3546–3555.
- Peralta-Tapia, Andrés, Sponseller, R.A., Ågren, A., Tetzlaff, D., Soulsby, C. & Laudon, H. 2015b. Scale-dependent groundwater contributions influence patterns of winter baseflow stream chemistry in boreal catchments. *Journal of Geophysical Research: Biogeosciences* 120: 847–858.
- Pester, M., Knorr, K.-H., Friedrich, M., Wagner, M. & Loy, A. 2012. Sulfate-reducing microorganisms in wetlands – fameless actors in carbon cycling and climate change. *Frontiers in Microbiology* 3.
- Phoenix, G.K. & Treharne, R. 2022. Arctic greening and browning: Challenges and a cascade of complexities. *Global Change Biology* 28: 3481–3483.
- Pind, A., Freeman, C. & Lock, M.A. 1994. Enzymic degradation of phenolic materials in peatlands — measurement of phenol oxidase activity. *Plant Soil* 159: 227–231.
- Pohjonen, V., Mönkkönen, P. & Hari, P. 2008. Test of northern timber line. *Boreal forest and climate change* 472–475.
- Porowski, A., Porowska, D. & Halas, S. 2019. Identification of Sulfate Sources and Biogeochemical Processes in an Aquifer Affected by Peatland: Insights from Monitoring the Isotopic Composition of Groundwater Sulfate in Kampinos National Park, Poland. *Water* 11: 1388.
- Pumpanen, J., Lindén, A., Miettinen, H., Kolari, P., Ilvesniemi, H., Mammarella, I., Hari, P., Nikinmaa, E., Heinonsalo, J., Bäck, J., Ojala, A., Berninger, F. & Vesala, T. 2014. Precipitation and net ecosystem exchange are the most important drivers of DOC flux in upland boreal catchments. *Journal of Geophysical Research: Biogeosciences* 119: 1861–1878.

- Pumpanen, J.S., Heinonsalo, J., Rasilo, T., Hurme, K.-R. & Ilvesniemi, H. 2009. Carbon balance and allocation of assimilated CO₂ in Scots pine, Norway spruce, and Silver birch seedlings determined with gas exchange measurements and 14C pulse labelling. *Trees* 23: 611–621.
- R Core Team 2019. R: A Language and Environment for Statistical Computing. R Foundation for Statistical Computing, Vienna, Austria.
- Räike, A., Kortelainen, P., Mattsson, T. & Thomas, D.N. 2016. Long-term trends (1975–2014) in the concentrations and export of carbon from Finnish rivers to the Baltic Sea: organic and inorganic components compared. *Aquat Sci* 78: 505–523.
- Raymond, P.A., Saiers, J.E. & Sobczak, W.V. 2016. Hydrological and biogeochemical controls on watershed dissolved organic matter transport: pulse-shunt concept. *Ecology* 97: 5–16.
- Redden, D., Trueman, B.F., Dunnington, D.W., Anderson, L.E. & Gagnon, G.A. 2021. Chemical recovery and browning of Nova Scotia surface waters in response to declining acid deposition. *Environ. Sci.: Processes Impacts* 23: 446–456.
- Schlesinger, W.H. & Andrews, J.A. 2000. Soil respiration and the global carbon cycle. *Biogeochemistry* 48: 7–20.
- Schmidbauer, H. & Roesch, A. 2018. WaveletComp 1.1: A guided tour through the R package.
- Shanley, J.B., Kendall, C., Smith, T.E., Wolock, D.M. & McDonnell, J.J. 2002. Controls on old and new water contributions to stream flow at some nested catchments in Vermont, USA. *Hydrological Processes* 16: 589–609.
- Škerlep, M., Steiner, E., Axelsson, A.-L. & Kritzberg, E.S. 2020. Afforestation driving long-term surface water browning. *Global Change Biology* 26: 1390–1399.
- Sobek, S., Tranvik, L.J., Prairie, Y.T., Kortelainen, P. & Cole, J.J. 2007. Patterns and regulation of dissolved organic carbon: An analysis of 7,500 widely distributed lakes. *Limnology and Oceanography* 52: 1208–1219.
- Stekhoven, D.J. & Bühlmann, P. 2012. MissForest--non-parametric missing value imputation for mixed-type data. *Bioinformatics* 28: 112–118.
- Strohmeier, L., Fovet, O., Hrachowitz, M., Salmon-Monviola, J. & Gascuel-Oudoux, C. 2021. Is a simple model based on two mixing reservoirs able to reproduce the intra-annual dynamics of DOC and NO₃ stream

- concentrations in an agricultural headwater catchment? *Science of The Total Environment* 794: 148715.
- Taketani, R.G., Yoshiura, C.A., Dias, A.C.F., Andreote, F.D. & Tsai, S.M. 2010. Diversity and identification of methanogenic archaea and sulphate-reducing bacteria in sediments from a pristine tropical mangrove. *Antonie van Leeuwenhoek* 97: 401–411.
- Tank, S.E., Striegl, R.G., McClelland, J.W. & Kokelj, S.V. 2016. Multi-decadal increases in dissolved organic carbon and alkalinity flux from the Mackenzie drainage basin to the Arctic Ocean. *Environ. Res. Lett.* 11: 054015.
- Teutschbein, C. & Seibert, J. 2012. Bias correction of regional climate model simulations for hydrological climate-change impact studies: Review and evaluation of different methods. *Journal of Hydrology* 456–457: 12–29.
- Thurman, E.M. 1985. Amount of Organic Carbon in Natural Waters, in: Thurman, E.M. (Ed.), *Organic Geochemistry of Natural Waters, Developments in Biogeochemistry*. Springer Netherlands, Dordrecht: pp. 7–65.
- Tipping, E., Corbishley, H.T., Koprivnjak, J.-F., Lapworth, D.J., Miller, M.P., Vincent, C.D. & Hamilton-Taylor, J. 2009. Quantification of natural DOM from UV absorption at two wavelengths. *Environmental Chemistry* 6: 472–476.
- Tipping, E., Hilton, J. & James, B. 1988. Dissolved organic matter in Cumbrian lakes and streams. *Freshwater Biology* 19: 371–378.
- Tipping, E. & Woof, C. 1990. Humic substances in acid organic soils: modelling their release to the soil solution in terms of humic charge. *Journal of Soil Science* 41: 573–586.
- Tiwari, T., Buffam, I., Sponseller, R.A. & Laudon, H. 2017. Inferring scale-dependent processes influencing stream water biogeochemistry from headwater to sea. *Limnology and Oceanography* 62: S58–S70.
- Tiwari, T., Sponseller, R.A. & Laudon, H. 2022. The emerging role of drought as a regulator of dissolved organic carbon in boreal landscapes. *Nat Commun* 13: 5125.
- Tiwari, T., Sponseller, R.A. & Laudon, H. 2018. Extreme Climate Effects on Dissolved Organic Carbon Concentrations During Snowmelt. *Journal of Geophysical Research: Biogeosciences* 123: 1277–1288.
- Tranvik, L.J., Downing, J.A., Cotner, J.B., Loiselle, S.A., Striegl, R.G., Ballatore, T.J., Dillon, P., Finlay, K., Fortino, K., Knoll, L.B., Kortelainen, P.L.,

- Kutser, T., Larsen, Soren., Laurion, I., Leech, D.M., McCallister, S.L., McKnight, D.M., Melack, J.M., Overholt, E., Porter, J.A., Prairie, Y., Renwick, W.H., Roland, F., Sherman, B.S., Schindler, D.W., Sobek, S., Tremblay, A., Vanni, M.J., Verschoor, A.M., von Wachenfeldt, E. & Weyhenmeyer, G.A. 2009. Lakes and reservoirs as regulators of carbon cycling and climate. *Limnology and Oceanography* 54: 2298–2314.
- Ukonmaanaho, L., Starr, M., Lindroos, A.-J. & Nieminen, T.M. 2014. Long-term changes in acidity and DOC in throughfall and soil water in Finnish forests. *Environ Monit Assess* 186: 7733–7752.
- Vargas, R., Baldocchi, D.D., Bahn, M., Hanson, P.J., Hosman, K.P., Kulmala, L., Pumpanen, J. & Yang, B. 2011. On the multi-temporal correlation between photosynthesis and soil CO₂ efflux: reconciling lags and observations. *New Phytologist* 191: 1006–1017.
- Varmuza, K. & Filzmoser, P. 2009. Principal component analysis. Introduction to Multivariate Statistical Analysis in Chemometrics 1–0.
- Villnäs, A. & Norkko, A. 2011. Benthic diversity gradients and shifting baselines: implications for assessing environmental status. *Ecological Applications* 21: 2172–2186.
- Wallage, Z.E. & Holden, J. 2010. Spatial and temporal variability in the relationship between water colour and dissolved organic carbon in blanket peat pore waters. *Science of The Total Environment* 408: 6235–6242.
- Waterloo, M.J., Oliveira, S.M., Drucker, D.P., Nobre, A.D., Cuartas, L.A., Hodnett, M.G., Langedijk, I., Jans, W.W.P., Tomasella, J., Araújo, A.C. de, Pimentel, T.P. & Estrada, J.C.M. 2006. Export of organic carbon in run-off from an Amazonian rainforest blackwater catchment. *Hydrological Processes* 20: 2581–2597.
- Wen, H., Perdrial, J., Bernal, S., Abbott, B.W., Dupas, R., Godsey, S.E., Harpold, A., Rizzo, D., Underwood, K., Adler, T., Hale, R. & Sterle, G., Li, L. 2020. Temperature controls production but hydrology controls export of dissolved organic carbon at the catchment scale.
- Weyhenmeyer, G., Prairie, Y. & Tranvik, L. 2014. Browning of Boreal Freshwaters Coupled to Carbon-Iron Interactions along the Aquatic Continuum. *PLoS ONE* 9.
- Wilken, S., Soares, M., Urrutia-Cordero, P., Ratcovich, J., Ekvall, M.K., Van Donk, E. & Hansson, L.-A. 2018. Primary producers or consumers? Increasing phytoplankton bacterivory along a gradient of lake

- warming and browning. *Limnology and Oceanography* 63: S142–S155.
- Wilson, H.F. & Xenopoulos, M.A. 2008. Ecosystem and Seasonal Control of Stream Dissolved Organic Carbon Along a Gradient of Land Use. *Ecosystems* 11: 555–568.
- Wing, M.K.C. from J., Weston, S., Williams, A., Keefer, C., Engelhardt, A., Cooper, T., Mayer, Z., Kenkel, B., Team, the R.C., Benesty, M., Lescarbeau, R., Ziem, A., Scrucca, L., Tang, Y., Candan, C. & Hunt, T. 2019. caret: Classification and Regression Training.
- Winterdahl, M., Erlandsson, M., Futter, M.N., Weyhenmeyer, G.A. & Bishop, K. 2014. Intra-annual variability of organic carbon concentrations in running waters: Drivers along a climatic gradient. *Global Biogeochemical Cycles* 28: 451–464.
- Worrall, F. & Burt, T.P. 2010. Has the composition of fluvial DOC changed? Spatiotemporal patterns in the DOC-color relationship. *Global Biogeochemical Cycles* 24.
- Worrall, F. & Burt, T.P. 2007. Flux of dissolved organic carbon from U.K. rivers. *Global Biogeochemical Cycles* 21.
- Worrall, F., Harriman, R., Evans, C.D., Watts, C.D., Adamson, J., Neal, C., Tipping, E., Burt, T., Grieve, I., Monteith, D., Naden, P.S., Nisbet, T., Reynolds, B. & Stevens, P. 2004. Trends in Dissolved Organic Carbon in UK Rivers and Lakes. *Biogeochemistry* 70: 369–402.
- Zhu, X., Chen, L., Pumpanen, J., Ojala, A., Zobitz, J., Zhou, X., Laudon, H., Palviainen, M., Neitola, K. & Berninger, F. 2022. The role of terrestrial productivity and hydrology in regulating aquatic dissolved organic carbon concentrations in boreal catchments. *Global Change Biology* 28(8): 2764–2778.

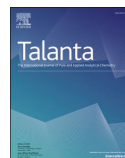
Assessment of a portable UV-Vis spectrophotometer's performance for stream water DOC and Fe content monitoring in remote areas.

Zhu, X., Chen, L., Pumpanen, J., Keinänen, M., Laudon, H., Ojala, A., Palviainen, M., Kiirikki, M., Neitola, K., & Berninger, F.

2021

Talanta, 224: 121919.

Reprinted with the kind permission of ELSEVIER.



Assessment of a portable UV–Vis spectrophotometer's performance for stream water DOC and Fe content monitoring in remote areas

Xudan Zhu^{a,*}, Liang Chen^a, Jukka Pumpanen^b, Markku Keinänen^a, Hjalmar Laudon^c, Anne Ojala^{d,e,f}, Marjo Palviainen^g, Mikko Kiirikki^h, Kimmo Neitolaⁱ, Frank Berninger^a

^a Department of Environmental and Biological Sciences, University of Eastern Finland, 80101, Joensuu, Finland

^b Department of Environmental and Biological Sciences, University of Eastern Finland, 70211, Kuopio, Finland

^c Department of Forest Ecology and Management, Swedish University of Agricultural Sciences, 90183, Umeå, Sweden

^d Faculty of Biological and Environmental Sciences, Ecosystems and Environment Research Programme, University of Helsinki, Lahti, Finland

^e Institute for Atmospheric and Earth System Research/Forest Sciences, Faculty of Agriculture and Forestry, University of Helsinki, 00014, Helsinki, Finland

^f Faculty of Biological and Environmental Sciences, Helsinki Institute of Sustainability Science, University of Helsinki, 00014, Helsinki, Finland

^g Department of Forest Science, University of Helsinki, 00014, Helsinki, Finland

^h Luode Consulting Sinimäentie 10 B, 02630, Espoo, Finland

ⁱ Institute for Atmospheric and Earth System Research (INAR), University of Helsinki, 00014, Helsinki, Finland

ARTICLE INFO

Keywords:

Water quality
UV–Vis spectrophotometer
Spectral absorbance
Dissolved organic matter
Ferric iron

ABSTRACT

Quantification of dissolved organic carbon (DOC) and iron (Fe) in surface waters is critical for understanding the water quality dynamics, brownification and carbon balance in the northern hemisphere. Especially in the remote areas, sampling and laboratory analysis of DOC and Fe content at a sufficient temporal frequency is difficult. Ultraviolet–visible (UV–Vis) spectrophotometry is a promising tool for water quality monitoring to increase the sampling frequency and applications in remote regions. The aim of this study was (1) to investigate the performance of an in-situ UV–Vis spectrophotometer for detecting spectral absorbances in comparison with a laboratory benchtop instrument; (2) to analyse the stability of DOC and Fe estimates from UV–Vis spectrophotometers among different rivers using multivariate methods; (3) to compare site-specific calibration of models to pooled models and investigate the extrapolation of DOC and Fe predictions from one catchment to another. This study indicates that absorbances that were measured by UV–Vis sensor explained 96% of the absorbance data from the laboratory benchtop instrument. Among the three tested multivariate methods, multiple stepwise regression (MSR) was the best model for both DOC and Fe predictions. Accurate and unbiased models for multiple watersheds for DOC were built successfully, and these models could be extrapolated from one watershed to another even without site-specific calibration for DOC. However, for Fe the combination of different datasets was not possible.

1. Introduction

Globally inland waters are a sink for 600 million tn C y^{-1} and deliver an additional ~ 900 million to 1200 million tn C y^{-1} to the oceans of which a majority is in organic forms [1,2]. With estimates of the global land sink to be around 2400 million tn C y^{-1} [3], the C exports via inland waters would account for about half of the net terrestrial C sink. It has been frequently reported that water colour is becoming darker in many lakes and running waters of the Northern hemisphere [4–7]. The drivers behind this trend, sometimes referred to as brownification, are heavily debated and have been ascribed to hydrological factors [8,9] as well as

an increase in temperature, changes in land-use and reduced acid deposition [7]. Although it is difficult to tease out any single factor causing brownification, brownification is directly due to the increased dissolved organic matter (DOM) and iron (Fe) concentrations [4,10]. Much of the export of DOC and Fe occurs during extreme rainfall or snowmelt events [11], which makes the high frequency monitoring of pulse events necessary. However, pulse events are usually of short duration and challenging to capture using physical water sampling.

The development of continuously operating water quality sensors has led to a transition from studying long-term trends and seasonal patterns to the investigation of highly dynamic phenomena, such as

* Corresponding author. Institution: University of Eastern Finland, Natura building 375a, Yliopistokatu 2, FI-80100, Joensuu, Finland.
E-mail address: xudan.zhu@uef.fi (X. Zhu).

<https://doi.org/10.1016/j.talanta.2020.121919>

Received 10 September 2020; Received in revised form 20 November 2020; Accepted 21 November 2020

Available online 3 December 2020

0039-9140/© 2020 Elsevier B.V. All rights reserved.

storm events and diurnal patterns, using high-frequency in situ measurements [12]. With the currently available technology and decreasing costs, in situ sensors are more frequently used for monitoring, especially in remote areas [13–15]. Although large amounts of data present challenges regarding storage, processing, and analysis [16], long-term monitoring datasets provide an opportunity for detailed investigations of hydrological and biogeochemical processes in dynamic systems [15, 17,18].

UV-Vis sensors are an emerging technology to measure and monitor concentrations of dissolved organic carbon (DOC) in situ. These commercially available sensors are spectrophotometers in the UV-visible spectrum. They can be used for in situ real-time measurements at field sites and in the offline mode in the laboratory to determine the spectral absorbance of waters [14]. Thereafter, algorithms calculate solute concentrations based on absorbance at a specific wavelength or multiple wavelengths. UV-Vis sensors can be applied to detect rapid changes in response to environmental conditions. They can also be used for an adaptive sampling approach with higher sampling frequency during high-flow events such as the snowmelt period and a reduced observation frequency during the base flow period [19].

Recent efforts have been made to qualitatively and quantitatively characterise DOM in water bodies for ecological studies, and in-situ UV-Vis spectrophotometer plays an important role in this. Different wavelengths have been used to estimate DOC concentration from spectral absorbances. Laudon et al. found that the absorbance at 254 nm could explain 78%–97% of TOC concentration in seven streams [20]. Waterloo et al. used absorbance at 255 and 350 nm as proxies for estimating DOC with calibration using a TOC analyser [21]. Wallage and Holden tested the robustness of spectrophotometric measurements for DOC content based on absorbance at 400 nm [22]. However, their DOC concentrations differed by up to 50% in comparison to the TOC analyser results. Therefore, methods relying on absorbance at more than one wavelength are suggested by several studies to improve the accuracy of DOC concentration measurements [23–25]. Avagyan et al. concluded that using absorbance values as a proxy for DOC content determination should include 2–5 wavelengths in the absorbance-concentration models [14]. Few estimates of the interference of iron concentrations by UV-Vis have been presented [26]. Iron has been suggested to contribute to the absorption of solar ultraviolet radiation either directly or through interactions with DOC. Maloney et al. found a strong correlation between total Fe and absorbance from wavelength at 320 nm [10].

More widespread use of UV-Vis spectrophotometers raises the question on how relationships between spectral absorbances and concentrations of various substances in water should be build and calibrated. Especially in remote sites, the acquisition of samples is expensive, and it may be difficult to obtain samples during critical high flow periods. In this article, we explore strategies for modelling DOC and Fe concentrations in three northern catchments. We compare the in-situ UV-Vis spectrophotometer to a laboratory benchtop instrument. Then we analyse the accuracy of DOC and Fe estimates from UV-Vis spectrophotometers across different rivers using multivariate methods. Especially we analyse various calibration strategies for the estimation of DOC and Fe concentrations. We compare site-specific calibration of models, to the construction of pooled models and investigate the extrapolation of DOC and Fe predictions from one catchment to another. These questions are of importance when planning the monitoring of water quality using spectral measurements in remote areas with limited calibration data.

2. Material and methods

2.1. Study site

There were three study sites in this research. Two sites locate in Krycklan, approximately 50 km northwest of the city of Umeå in

northern Sweden (64°14' N, 19°46'E), where C4 (Kalkkäls-myren) is a mire-dominated Svartberget sub-catchment and C5 is a lake outlet (Fig. S1). The catchment area of C4 is 0.19 km² and 40% of it is covered by wetlands and the rest is forest. There are no lakes in the catchment. The catchment area of C5 is 0.85 km², of which forest accounts for 59% and wetlands constitute 36%. A small portion (5%) of the catchment is covered by a lake and the measurements were done at the lake outlet [27]. The climate is characterised as a cold temperate humid type with persistent snow cover during the winter season. The 30-year mean annual temperature (1981–2010) is 1.8 °C, January –9.5 °C, and July 14.7 °C, and the mean annual precipitation is 614 mm. During the experimental period, the average DOC and Fe concentrations were 33.01 mg L⁻¹ and 1.56 mg L⁻¹ in C4, 20.72 mg L⁻¹ and 1.69 mg L⁻¹ in C5. The pH values varied in the range of 3.94–5.75, 4.16–6.40 in C4, C5, respectively.

Yli-Nuortti measurement station (Cold station) locates in Yli-Nuortti river (67°44' N, 29°27'E) in Värriö, Finland (Fig. S1). It is about 120 km north of the Arctic Circle close to the northern timberline. The catchment covers about 40 km² with less than 25% of peatlands, which, however, dominating the riparian zone. Less than 5% of the area is covered by alpine vegetation while the rest of the catchment is dominated by pine forests on glacial tills. There are no lakes above the measurement station. According to the statistics of the Finnish Meteorological Institute, the mean annual air temperature is –0.5 °C. The mean temperature in January is –11.4 °C and in July 13.1 °C. The mean annual precipitation is 601 mm. The average DOC and Fe concentrations were 4.96 mg L⁻¹ and 0.21 mg L⁻¹, and the pH values were 6.27–6.95 during the experimental period.

2.2. Sampling and filtration

All sample bottles and reagent containers were made from high-density polyethylene and they were first cleaned in a Deko-2000 washer with detergent, then soaked for at least 24 h in 2% HNO₃, and finally rinsed six times with Milli-Q water. All glassware used in this study was additionally pre-combusted for 4 h at 450 °C before use.

The sampling in Yli-Nuortti river (Cold station) took place during the hydrological year 2018–2019 and in Krycklan (C4 and C5) during the hydrological years 2016–2019. In Cold station, water samples were collected monthly in winter and fall, once a fortnight in spring, and every week in summer. In Krycklan, we sampled monthly during winter, once a fortnight during summer and fall, and every third day during the spring flood. The water samples were filtered through Filtration Assembly with Whatman GF/F Glass Microfibre Filters (pore size 0.45 µm). To precondition the filtration system and avoid contamination from the filter before collecting samples, 30 ml of sample water was filtered and then discarded. The samples for absorbance measurements were preserved using ZnCl₂ and then stored at 4 °C until laboratory analysis. Samples for DOC and Fe measurements were frozen until further analysis.

2.3. Measurement of in-situ and ex-situ spectral absorbances

In site, submersible, portable multi-parameter UV-Vis probes (spectro:lyser, S:CAN Messtechnik GmbH, Austria) were used for absorbance measurements. The spectro:lyser measures absorbance across the UV-Vis range (220–732.5 nm, at 2.5 nm intervals) and saves these values in an internal datalogger. The measurement range of the probe depends on the optical path length, which can range from 2 to 100 mm. In this study, a probe with a path length of 35 mm was used. All of the control unit's electronics, including the data logger, were placed in four tubular anodised aluminium housings. The UV-Vis probe was installed in the Yli-Nuortti river on June 12, 2018 and in the Krycklan catchments on May 9, 2016.

In the laboratory, spectral absorbance was measured with a UV-1800 UV-VIS spectrophotometer (Shimadzu, Kyoto, Japan) between 200 and

800 nm with a 10 mm pathlength quartz cell (acquisition step: 1 nm, scan speed: slow).

2.4. Measurements of DOC and Fe concentration by laboratory techniques

In Finland, dissolved organic carbon (DOC) was determined by thermal oxidation coupled with infrared detection (Multi N/C 2100, Analytik Jena, Germany) following acidification with phosphoric acid, and each sample was measured in triplicate with errors less than 3%. Fe concentrations were determined colorimetrically with ferrozine corresponding to an absorbance at 562 nm by Victor 3 1420 Multilabel Counter (PerkinElmer) [28].

In Sweden, DOC was measured with Shimadzu TOC-5000 using catalytic combustion [20]. Fe was analyzed using Inductively Coupled Plasma Optical Emission Spectroscopy (ICP-OES Varian Vista Pro Ax). To ensure the accuracy of the analysis an external certified standard (Spectrapure Standards SPS-SW1) was analyzed on a regular basis. The uncertainty was always less than 2% [29].

2.5. Multilinear regression methods for estimating DOC and Fe by spectral absorbance

To test for an optimised estimate of DOC and Fe from the absorbance, a set of calibrations based on three different multilinear regression methods was performed with water samples ($n = 183$ for DOC, $n = 142$ for Fe). The absorbance values from 220 nm to 732.5 nm at 2.5 nm intervals (207 variables) were used as input data for Fe analyses, while wavelengths shorter than 250 nm were excluded from the DOC analyses (194 variables) because inorganic substances can lead to interference at the lower end of the UV–Vis range [30]. The multivariate models we are using in this paper rely on splitting the data into a training and testing data set. We tried 5 different splits of the data; 1. The training set contained 75% of observations that were randomly selected from all samples (C4, C5 and Cold station) and the testing set contained the remaining 25% of observations; 2. The training set contained observations from C4 and C5 and the testing set consisted of observations from Cold station; 3. The training set contained 75% of observations randomly selected from C4 and C5 and the testing set consisted of the rest 25% of observations; 4. The training set contained 75% of observations randomly selected from C4 and Cold station and the testing set contained the rest 25% of observations; 5. The training set contained 75% of observations randomly selected from C5 and Cold station and the testing set contained the rest 25%.

The tested three statistical methods were used for the multilinear prediction of DOC and Fe concentration obtained by the laboratory measurements. Measured concentrations were always the dependent variable, and the absorbance values at different wavelengths were the independent variables. We used three methods: multiple stepwise regression (MSR), partial least-squares regression (PLS), and principal component regression (PCR). These methods were selected due to their applicability to data sets containing collinear variables and datasets that may contain a larger number of independent variables than observations. Different approaches were used for the PLS and PCR regressions. These techniques reduce the number of dimensions in the data by computing latent linear variables [31,32]. However, the method by which these linear combinations are constructed differs. In PCR, the principal components are generated to describe the maximum variation in the predictors without considering the strength of the relationship between the predictor and predictand variables [32]. In PLS, the variables exhibiting a high correlation with the response variables are given extra weight [32].

The PCR and PLS analyses were conducted with 'pls' package [33] in R [34]. Coefficients and p-values were estimated by jackknife T-test method using 'jack.test' function in 'pls' package. MSR analyses were performed with 'caret' package [35] in R [34]. The correlation

coefficient (R), root-mean-square deviation (RMSD), standard deviation (STD) and bias were used to check the performance of the models.

3. Results

3.1. Comparison of spectral absorbance measured by two methods

Comparison of the absorbance values measured by S:CAN (average daily absorbance) and the desktop UV-1800 for the same day in 2018–2019 at Cold station reveals that the shape of absorbance curves is very similar in the wavelength range from 220 to 732.5 nm (Fig.S2). Linear regression analysis indicated that absorbances that were measured by S:CAN explained 96% of the absorbances from UV-1800, though the slope of absorbance ratios differed among days (Fig. 1a). There were some exceptions from February to April when the relationships between absorbances of the two methods were not linearly correlated (Fig. 1b).

Environmental factors such as water depth, temperature, turbidity and the voltage of S:CAN be possible reasons for the differences in absorbance ratios (S:CAN/UV-1800) in different days. However, no significant linear correlations between absorbance ratio and water depth (a proxy for discharge), temperature, turbidity or the voltage of S:CAN were found (Fig.S3).

3.2. Comparison of multilinear models for DOC-measurement

When applied to data set 1, the DOC values from the PLS, PCR, MSR calibrations produced accurate estimates for the training set as can be seen from high explanatory power r^2 values of the models (near to 1) (Table S1), as well as for the testing set proved by the models with low root-mean-square deviations (RMSD) and high correlation coefficient values near to 1, as well as the standard deviations (STD) which are close to STD of the laboratory-measured DOC. The MSR produced the model with the highest r^2 (0.971), lowest RMSD values (2.352 mg L⁻¹) and lowest bias in each site. The PLS and PCR models performed similarly (Fig. 2a).

When applied to data set 2, the DOC values from the PLS, PCR, MSR calibrations produced accurate estimates for Krycklan data set (training set) as can be seen from very low bias and high explanatory power r^2 values of the models (near to 1) (Table S2). For the testing set, the correlation coefficients and RMSD of the three models are good and very similar. STD of predicted DOC values from PLS and MSR models are close to the STD of laboratory-measured DOC values. However, the bias showed that the PLS model seemed to underestimate and PCR model over-estimate the DOC concentrations. MSR model was the best one (Fig. 2b).

Different combinations of spectral data from three rivers were applied to develop joint models. In each data set, the DOC values from MSR calibrations produced accurate estimates for the training set as can be seen by very high explanatory power r^2 values of the models (near to 1). For the testing set, the model performances for all data sets were good with r^2 values being higher than 0.8. The MSR calibration for data set 4 demonstrated the highest r^2 , lowest RMSD values and smallest bias (Table 1).

When models were built on data set 1, the normalised coefficients of PLS ($p < 0.05$) showed that the important wavelengths fell in band 250 nm–295 nm, 310 nm–370 nm, 377.5 nm–410 nm, 417.5 nm–427.5 nm and 570 nm–580 nm while in PCR they fell in band 250 nm–297.5 nm, 317.5 nm–412.5 nm, 417.5 nm–490 nm and 537.5 nm–600 nm (Fig. 3a). For data set 2, the coefficients of PLS ($p < 0.05$) showed that the important wavelengths fell in band 275 nm–292.5 nm, 342.5 nm–365 nm, and 570 nm–582.5 nm, while in 250 nm–307.5 nm, 342.5 nm–370 nm and 412.5 nm–440 nm in PCR (Fig. 3b).

MSR method included 7 wavelengths for data set 1 (250, 290, 307.5, 437.5, 447.5, 630, 645 nm), 5 wavelengths for data set 2 (282.5, 302.5, 487.5, 645, 665 nm) and data set 3 (252.5, 255, 257.5, 447.5, 645 nm),

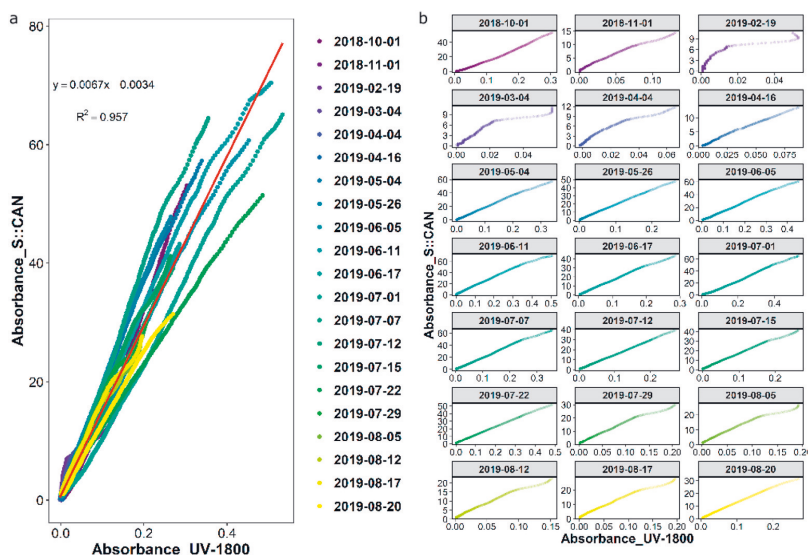


Fig. 1. Relationship between Spectral absorbance measured by UV-1800 and S:CAN in different days.

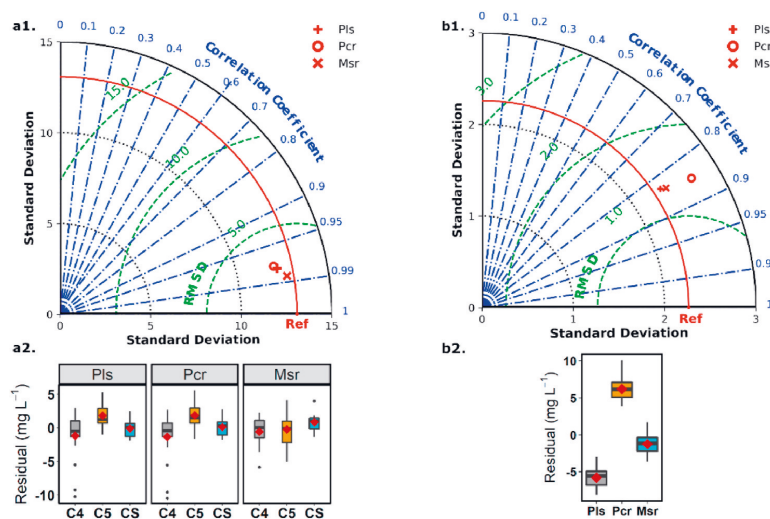


Fig. 2. Statistical parameters (testing set) of partial least-squares (PLS), principal component (PCR) and multiple stepwise (MSR) regressions of estimating DOC concentration by spectral absorbance, “Ref” shows the standard deviation of the laboratory-measured DOC concentration, the diamond symbol in each box plot represents the bias. a1&2 models are based on data set 1, where the training set contains 75% of the observations (n = 140) randomly selected from all samples and the testing set contains the rest 25% of the observations (n = 43). b1&2 models are based on data set 2 where training and testing data are from different locations where the training set contains the observations from C4 and C5 (n = 150) and the testing set contains the observations from the Cold station (n = 33).

4 wavelengths for data set 4 (255, 260, 692.5, 722.5 nm) and data set 5 (257.5, 260, 420, 722.5 nm). In MSR models of all data sets, 645 nm was the most important wavelength, followed by 255 nm, 260 nm and 722.5 nm (Table .2).

3.3. Comparison of multilinear models for Fe -measurement

When applied to data set 1, the Fe concentrations from the PLS, PCR, MSR calibrations produced accurate estimates for the training set as can be seen from good explanatory power (r^2 values) of the models (Table S3). For the testing set, the goodness of fit was evaluated using the RMSD and the correlation coefficient. The MSR calibration method produced the model with the highest correlation coefficient, lowest

RMSD, and the smallest bias in each site. (Fig. 4a).

When applied to data set 2, the Fe concentrations from the PLS, PCR, and MSR calibrations produced good Fe estimates for Krycklan data set (training set) as can be seen by models with explanatory power r^2 higher than 0.45 (Table S4). However, for the Värrio testing data set the measurements applying these three calibration methods showed poor correlation coefficients and high RMSD values. (Fig. 4b).

Different combinations of spectral data from several streams were applied to develop joint models. In each data set, the predicted Fe values from the PLS calibrations produced accurate estimates for the training set as can be seen by high explanatory power r^2 values. For the testing set, the performances were not so good as with the DOC predictions. MSR calibrations by data set 4 produced the model with the highest r^2

Table 1

The goodness of fit statistics of MSR regression estimating DOC by spectral absorbance for different data sets. Data set 3 is observations from C4 and C5; Data set 4 is observations from C4 and Cold station; Data set 5 is observations from C5 and Cold station. The training set contains 75% of observations that were randomly selected from each data set and the testing set contains the rest 25% of observations.

MSR	Statistical Parameters	Data set 3 (C4&C5)	Data set 4 (C4&Cold station)	Data set 5 (C5&Cold station)
Training Set	r^2	0.903	0.973	0.959
	RMSE (mg L ⁻¹)	3.243	2.599	1.787
Testing Set	r^2	0.942	0.976	0.802
	RMSD (mg L ⁻¹)	2.797	2.424	4.177
	Bias (mg L ⁻¹)	-0.288	-0.203	1.369

Table 2

Wavelengths used in MSR models for DOC and Fe prediction by different data sets.

Data sets	Number of wavelengths	Wavelengths used for DOC prediction, nm	Number of wavelengths	Wavelengths used for Fe prediction, nm
Data set 1:				
Training set = 75% randomly from all samples, n = 140	7	250, 290, 307.5, 437.5, 447.5, 630, 645	7	227.5, 297.5, 320, 342.5, 480, 557.5, 635
Testing set = the rest 25%, n = 43				
Data set 2:				
Training set = C4&C5, n = 150	5	305, 307.5, 632.5, 645, 692.5	-	-
Testing set = Cold station, n = 33				
Data set 3:				
Training set = 75% randomly from C4&C5, n = 114	5	252.5, 255, 257.5, 447.5, 645	9	365, 370, 382.5, 397.5, 472.5, 480, 545, 690, 710
Testing set = the rest 25%, n = 36				
Data set 4:				
Training set = 75% randomly from C4&Cold station, n = 86	4	255, 260, 692.5, 722.5	10	252.5, 262.5, 277.5, 327.5, 417.5, 455, 610, 680, 707.5, 722.5
Testing set = the rest 25%, n = 28				
Data set 5:				
Training set = 75% randomly from C5&Cold station, n = 72	4	257.5, 260, 420, 722.5	4	220, 222.5, 225, 230
Testing set = the rest 25%, n = 24				

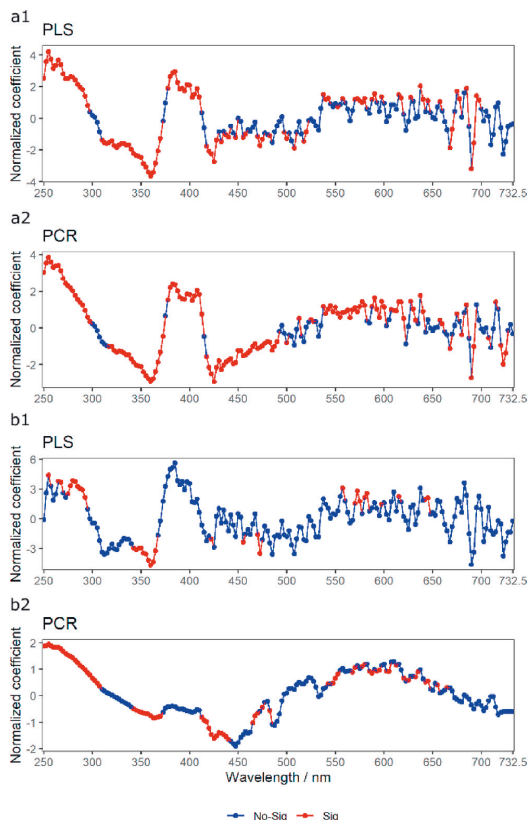


Fig. 3. Normalised regression coefficients of PLS and PCR models from wavelength 250 nm–732.5 nm at 2.5 intervals to show the effects of absorbances on DOC concentration. a1&2 models are based on data set 1 where the training set contains 75% of the observations (n = 140) randomly selected from all samples, and the testing set contains the rest 25% of the observations (n = 43) to check the performance of the models. b1&2 models are based on data set 2 where the training set contains observations from C4 and C5 (n = 150) while the testing set contains observations from the Cold station (n = 33). “Sig” indicates $p < 0.05$; “No-sig” indicates $p > 0.05$.

and lowest RMSD (Table 3).

For data set 1, the normalised coefficients of PLS ($p < 0.05$) showed that the important wavelengths were 225 nm, from 245 nm to 250 nm and 717.5, from 220 nm to 225 nm, from 240 nm to 282.5 nm, from 372.5 nm to 395 nm, from 440 nm to 472.5 nm, from 597.5 nm to 625 nm, from 680 nm to 685 nm and from 715 nm to 732.5 nm in PCR (Fig. 5).

MSR models were based on 7 wavelengths for data set 1 (227.5, 297.5, 320, 342.5, 480, 557.5, 635 nm), 9 wavelengths for data set 3 (365, 370, 382.5, 397.5, 472.5, 480, 545, 690, 710 nm), 10 wavelengths for data set 4 (252.5, 262.5, 277.5, 327.5, 417.5, 455, 610, 680, 707.5, 722.5 nm) and 4 wavelengths for data set 5 (220, 222.5, 225, 230 nm) (Table .2).

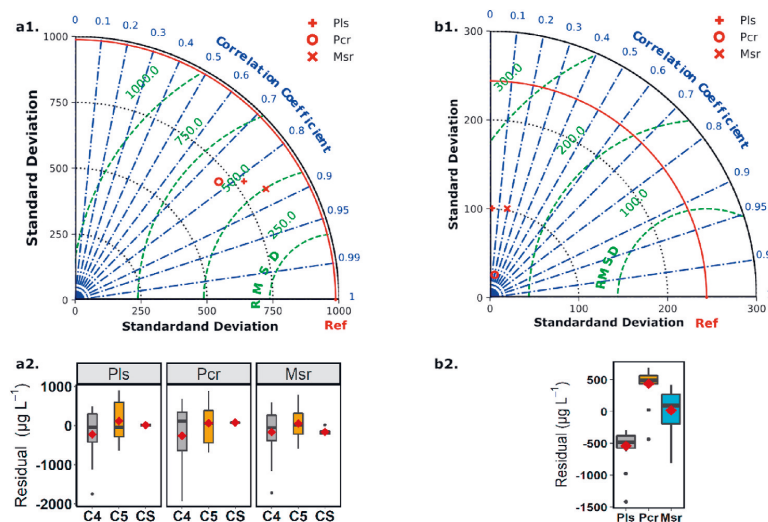


Fig. 4. Statistical parameters (testing set) of partial least-squares (PLS), principal component (PCR) and multiple stepwise (MSR) models for estimating the Fe concentration by spectral absorbance. “Ref” shows the standard deviation of the laboratory-measured Fe concentrations, and the diamond symbol in each box plot represents bias (b). a1&2 models are based on data set 1 where the training set contains 75% of the observations (n = 108) randomly selected from all samples and the testing set contains the rest 25% of the observations (n = 34). b1&2 models are based on data set 2 where the training set contains observations from C4 and C5 (n = 124), and the testing set contains observations from the Cold station (n = 18).

Table 3

The goodness of fit statistics of the MSR regression estimating Fe by spectral absorbance for different data sets. Data set 3 is observations from C4 and C5; Data set 4 is observations from C4 and Cold station; Data set 5 is observations from C5 and Cold station. Training sets are 75% of the observations randomly selected from each data set and testing sets are the rest 25% of the observations.

MSR	Statistical Parameters	Data set 3 (C4&C5)	Data set 4 (C4&Cold station)	Data set 5 (C5&Cold station)
Training Set	r^2	0.868	0.9889	0.672
	RMSE ($\mu\text{g L}^{-1}$)	287.398	108.905	473.997
Testing Set	r^2	0.583	0.876	0.623
	RMSD (mg L^{-1})	619.901	378.814	479.334
	Bias ($\mu\text{g L}^{-1}$)	179.009	-124.951	78.672

4. Discussion

Spectral measurement from the in-situ S: CAN uses different technologies than benchtop spectrophotometers. In situ instruments measure unfiltered water and are subject to variation in temperature. Ambient sunlight could disturb spectral measurements from the open path of the spectrophotometer and power supply is less reliable in situ than under lab conditions. A comparison of the in-situ S: CAN and the UV1800 benchtop spectrophotometer usually showed a good linear correlation between the two instruments while there was some variation in slope. We tested if differences between the ex-situ and in-situ spectra could be caused by the changes in the operating conditions. These variations in the regression slope of ex-situ on in-situ spectral absorbances were not dependent on temperature, water level (as a proxy for water discharge) or other factors like the voltage of the power supply. This shows that in general the in-situ spectral measurements were reliable, unbiased, and not affected by water temperature, discharge or small changes in electricity supply. There were a few occasions on non-linear correlations from February to April which can probably be explained by the ice formation on the instruments. Ice formation was caused by the compressed air used to automatically clean the instrument and not by the freezing of the river. Other possible reasons may be particles on the lenses of the instrument as well as the storage time of water samples before analysing by UV-1800. Avagyan et al. suggest that

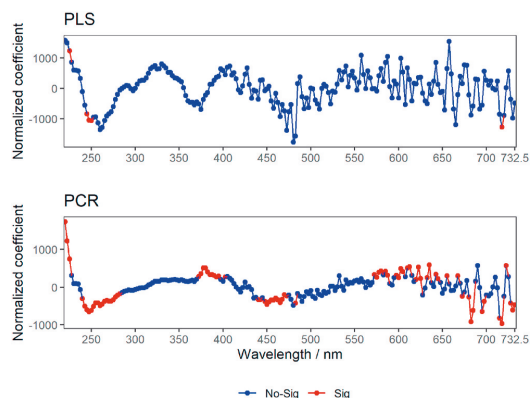


Fig. 5. Normalised regression coefficients of PLS and PCR models from wavelength 220 nm–732.5 nm at 2.5 intervals to show the effects of absorbances on iron (Fe) concentration. Models are built on data set 1, the training set contains 75% observations (n = 108) randomly selected from all samples, and the testing set which was used to check the performance of the models contains the rest 25% (n = 34). “Sig” indicates $p < 0.05$; “No-sig” indicates $p > 0.05$.

spectrophotometric measurements and laboratory method should be performed during the same day, otherwise the spectrophotometric features may change slightly during storage [14]. In our case, the sample plots locate in remote areas which makes the sample storage unavoidable before laboratory analysis. Therefore, samples were protected using ZnCl_2 against microbial decomposition.

Analysis of spectral data for environmental monitoring aims to obtain reconstructions of environmental variables that are general, unbiased and accurate. We compared the performances of the three multivariate methods (PCR, PLS and MSR), and though the MSR analysis included a limited number of wavelengths in the model, it produced a model with the highest explanatory power, the lowest RMSD, and bias when applied to test data sets in different situations for both DOC and Fe predictions. Previous study found that the PCR model failed to produce accurate estimates for the testing set due to its possible over-

parameterisation. In contrast, the differences in the three methods in our study were relatively minor [14].

Wavelengths that have previously been used as proxies for DOC concentration include 254 nm [36,37], 272 nm [36], 320 nm [38], 340 nm [30,36,37,39,40], 365 nm [36], 400 nm [22,40] and 410 nm [36]. Moreover, in addition to the widely used wavelength (254–400 nm), the inclusion of absorbance values at the wavelengths of 600 nm and 740 nm may significantly increase the accuracy of DOC estimates [14]. In our case, according to PCR and PLS loadings, the most important ranges of wavelengths covered most of the widely used wavelengths in previous studies.

DOC primarily controls UV absorbance in aquatic ecosystems. The role of Fe has also been suggested to contribute to UV absorbance either directly or by interaction with DOC [10]. Moreover, Fe can also absorb UV–Vis radiation when present in mineral particles suspended in natural waters [41]. Wavelengths that have previously been used as proxies for Fe concentration include 245 nm [42], 280 nm [42], 320 nm [10] and 410 [26]. In our case, according to PCR loadings, the most important ranges of wavelengths covered most of the widely used wavelengths in previous studies. In MSR models for different data sets, from 4 to 10 wavelengths were identified (Table 2).

Our study demonstrated contrasting results on the use of in situ UV–Vis spectrophotometers to estimate DOC and Fe concentrations from northern catchments. While our catchments were representative for Northern Fennoscandia, relationships between spectral absorbance and DOC (or Fe) may be different in other regions with different pH or turbidities. Spectrophotometric estimates of DOC concentrations were usually in good agreement with laboratory measurements. The spectrophotometric DOC models (PLS, PCR and MSR) explained more than 95% of the variation in DOC in our data when we used DOC measurements from three catchments for the calibration of the relationship. Additionally, our analysis suggests that it is possible to develop joint models by combining spectral and calibration data from several rivers, reducing the need to acquire physical water samples for calibration of new sensor applications. The joint calibration of all three sites resulted in low bias and a high R^2 . Even the spectrophotometric DOC model based only on observations from Krycklan, Sweden did fit to measurements from Lapland, Finland reasonably well. The standard deviation of the predicted data was similar to the standard deviation of measured data indicating that the analysis was able to capture extreme events and that it had a realistic variance of measured values.

In contrast, the spectrophotometric estimates of Fe concentrations were not as good as DOC measurements. The spectrophotometric Fe models (PLS, PCR and MSR) explain about 65% of the variation in Fe concentrations. However, spectrophotometric Fe models based on data from Krycklan, Sweden did not fit to measurements from the catchment in Lapland, Finland. Gledhill et al. found that in waters with $\text{pH} > 5$, the concentration of inorganic free ferric Fe is very low, and the dissolved Fe is primarily associated with dissolved organic ligands such as humic substances and siderophores [43]. In our case, pH in the Cold station (6.27–6.95) was much higher than in C4 (3.94–5.75) and in C5 (4.16–6.4). Additionally, the difference of soil redox conditions from one site to another could affect the results as well. In our study, the Krycklan catchments are more peatland dominated than the catchment in Finland. In peatland environments redox processes are predominant and they are the main source of terrestrial Fe in surface waters. The effect of Fe on watercolour varies depending on its oxidation state, hydration, and chemical complexation [44]. Furthermore, the reason why Krycklan spectrophotometric Fe models do not fit to the estimates from Finnish Lapland could also be explained by the huge difference in Fe concentrations. In C4 and C5 of Krycklan, the concentration were 155–3730 $\mu\text{g L}^{-1}$, and in Cold station of Lapland 32–539 $\mu\text{g L}^{-1}$.

The results indicate that our model was successful for building accurate and unbiased models for multiple watersheds for DOC. The models were, at a certain loss of precision, appropriate to be extrapolated from one watershed to another even without site-specific

calibration for DOC. However, for Fe the combination of different datasets was not possible. This means that the remote DOC sensors based on spectrophotometry could operate with a low number of samples and that a set of DOC sensors could be calibrated jointly with little loss of accuracy, but the same approach seems to be not working well for Fe.

5. Conclusions

The in-situ S: CAN worked well except for February to April when the ice formation on the instruments may have somehow reduced the accuracy. Eventhough, this did not affect successfully using absorbance from S: CAN to build accurate and unbiased models for multiple watersheds for DOC, and these models could be extrapolated from one watershed to another even without site-specific calibration for DOC. For Fe the combination of different datasets was not possible. This means that the remote DOC sensors based on spectrophotometry could be calibrated with a low number of samples but the same approach is not working well for Fe. Comparison of the performance of the three multivariate methods (PCR, PLS and MSR) indicated that MSR lead to the best model for both DOC and Fe predictions. Same research in different regions around the world should be conducted in the future to prove the versatility of our proposed models.

Credit author statement

Xudan Zhu: Conceptualization, Methodology, Formal analysis, Writing – original draft, Visualization. Liang Chen: Methodology, Software, Writing – review & editing, Jukka Pumpanen: Supervision, Writing – review & editing, Markku Keinänen: Resources, Writing – review & editing, Hjalmar Laudon: Data curation, Writing – review & editing. Anne Ojala: Writing – review & editing. Marjo Palviainen: Writing – review & editing, Mikko Kiirikki: Validation, Kimmo Neitola: Data curation, Frank Berninger: Conceptualization, Supervision, Project administration, Funding acquisition, Writing – review & editing.

Declaration of competing interest

The authors declare that they have no known competing financial interests or personal relationships that could have appeared to influence the work reported in this paper.

Acknowledgement

This work was supported through Kone project (201906598) - ‘The role of terrestrial productivity on fluxes of dissolved organic carbon in watersheds (Maaekosysteemien tuottavuuden merkitys liukoisien orgaanisen hiilen virtoihin valuma-alueilla)’ and the Water JPI and Academy of Finland project REFORMWATER (Academy of Finland project number 326818). The Krycklan Catchment Study is funded by the Swedish Infrastructure for Ecosystem Science (SITES), the VR extreme event project, the Swedish Research Council for Sustainable Development (FORMAS) and SKB, while the high frequency work is supported by the European Union’s Horizon 2020 Research and Innovation Programme under the Marie Skłodowska-Curie Grant Agreement No 734317.

Appendix A. Supplementary data

Supplementary data to this article can be found online at <https://doi.org/10.1016/j.talanta.2020.121919>.

References

- [1] J.J. Cole, Y.T. Prairie, N.F. Caraco, W.H. McDowell, L.J. Tranvik, R.G. Striegl, C. M. Duarte, P. Kortelainen, J.A. Downing, J.J. Middelburg, J. Melack, Plumbing the global carbon cycle: integrating inland waters into the terrestrial carbon budget, *Ecosystems* 10 (2007) 172–185, <https://doi.org/10.1007/s10021-006-9013-8>.

- [2] A.K. Aufdenkampe, E. Mayorga, P.A. Raymond, J.M. Melack, S.C. Doney, S.R. Alin, R.E. Aalto, K. Yoo, Riverine coupling of biogeochemical cycles between land, oceans, and atmosphere, *Front. Ecol. Environ.* 9 (2011) 53–60, <https://doi.org/10.1890/100014>.
- [3] L.M. Mercado, N. Bellouin, S. Sitch, O. Boucher, C. Huntingford, M. Wild, P.M. Cox, Impact of changes in diffuse radiation on the global land carbon sink, *Nature* 458 (2009) 1014–1017, <https://doi.org/10.1038/nature07949>.
- [4] S. Haaland, D. Hongve, H. Laudon, G. Riise, R.D. Vogt, Quantifying the drivers of the increasing colored organic matter in boreal surface waters, *Environ. Sci. Technol.* 44 (2010) 2975–2980, <https://doi.org/10.1021/es903179j>.
- [5] M. Erlandsson, N. Cory, J. Fölster, S. Köhler, H. Laudon, G.A. Weyhenmeyer, K. Bishop, Increasing dissolved organic carbon redefines the extent of surface water acidification and helps resolve a classic controversy, *Bioscience* 61 (2011) 614–618, <https://doi.org/10.1525/bio.2011.61.8.7>.
- [6] E. Peitooma, A. Ojala, A.-L. Holopainen, K. Salonen, Changes in Phytoplankton in a Boreal Lake during a 14-year Period, *vol. 18*, 2014, p. 14.
- [7] E. Asmala, J. Carstensen, A. Räike, Multiple anthropogenic drivers behind upward trends in organic carbon concentrations in boreal rivers, *Environ. Res. Lett.* 14 (2019) 124018, <https://doi.org/10.1088/1748-9326/ab4fa9>.
- [8] D. Hongve, G. Riise, J.F. Kristiansen, Increased colour and organic acid concentrations in Norwegian forest lakes and drinking water – a result of increased precipitation? *Aquat. Sci.* 66 (2004) 231–238, <https://doi.org/10.1007/s00027-004-0708-7>.
- [9] M. Erlandsson, I. Buffam, J. Fölster, H. Laudon, J. Temmerud, G.A. Weyhenmeyer, K. Bishop, Thirty-five years of synchrony in the organic matter concentrations of Swedish rivers explained by variation in flow and sulphate, *Global Change Biol.* 14 (2008) 1191–1198, <https://doi.org/10.1111/j.1365-2486.2008.01551.x>.
- [10] K.O. Maloney, D.P. Morris, C.O. Moses, C.L. Osburn, The role of iron and dissolved organic carbon in the absorption of ultraviolet radiation in humic lake water, *Biogeochemistry* 75 (2005) 393–407, <https://doi.org/10.1007/s10533-005-1675-3>.
- [11] P.A. Raymond, J.E. Saiers, W.V. Sobczak, Hydrological and biogeochemical controls on watershed dissolved organic matter transport: pulse-shunt concept, *Ecology* 97 (2016) 5–16, <https://doi.org/10.1890/141684.1>.
- [12] S.R. Jacobs, B. Weeser, M.C. Rufino, L. Breuer, Diurnal patterns in solute concentrations measured with in situ UV-vis sensors: natural fluctuations or artefacts? *Sensors* 20 (2020) 859, <https://doi.org/10.3390/s20030859>.
- [13] G. Langergraber, N. Fleischmann, F. Hofstätter, A multivariate calibration procedure for UV/VIS spectrometric quantification of organic matter and nitrate in wastewater, *Water Sci. Technol.* 47 (2003) 63–71.
- [14] A. Avagyan, B.R.K. Runkle, L. Kutzbach, Application of high-resolution spectral absorbance measurements to determine dissolved organic carbon concentration in remote areas, *J. Hydrol.* 517 (2014) 435–446, <https://doi.org/10.1016/j.jhydrol.2014.05.060>.
- [15] M. Rode, A.J. Wade, M.J. Cohen, R.T. Hensley, M.J. Bowes, J.W. Kirchner, G. B. Arhonditsis, P. Jordan, B. Kronvang, S.J. Halliday, R.A. Skeffington, J. C. Rozemeijer, A.H. Aubert, K. Rinke, S. Jomaa, Sensors in the stream: the high-frequency wave of the present, *Environ. Sci. Technol.* 50 (2016) 10297–10307, <https://doi.org/10.1021/acs.est.6b02155>.
- [16] W.H. McDowell, NEON and STREON: opportunities and challenges for the aquatic sciences, *Freshw. Sci.* 34 (2015) 386–391, <https://doi.org/10.1086/679489>.
- [17] J.W. Kirchner, X. Feng, C. Neal, A.J. Robson, The fine structure of water-quality dynamics: the (high-frequency) wave of the future, *Hydrol. Process.* 18 (2004) 1353–1359, <https://doi.org/10.1002/hyp.5537>.
- [18] S. Krause, J. Lewandowski, C.N. Dahm, K. Tockner, Frontiers in real-time ecohydrology – a paradigm shift in understanding complex environmental systems, *Ecohydrology* 8 (2015) 529–537, <https://doi.org/10.1002/eco.1646>.
- [19] B.A. Pellerin, J.F. Saraceno, J.B. Shanley, S.D. Sebestyen, G.R. Aiken, W. M. Wollheim, B.A. Bergamaschi, Taking the pulse of snowmelt: in situ sensors reveal seasonal, event and diurnal patterns of nitrate and dissolved organic matter variability in an upland forest stream, *Biogeochemistry* 108 (2012) 183–198, <https://doi.org/10.1007/s10533-011-9589-8>.
- [20] H. Laudon, S. Köhler, I. Buffam, Seasonal TOC export from seven boreal catchments in northern Sweden, *Aquat. Sci. - Res. Boundaries.* 66 (2004) 223–230, <https://doi.org/10.1007/s00027-004-0700-2>.
- [21] M.J. Waterloo, S.M. Oliveira, D.P. Drucker, A.D. Nobre, L.A. Cuartas, M. G. Hodnett, I. Langedijk, W.W.P. Jans, J. Tomasella, A.C. de Araújo, T.P. Pimentel, J.C.M. Estrada, Export of organic carbon in run-off from an Amazonian rainforest blackwater catchment, *Hydrol. Process.* 20 (2006) 2581–2597, <https://doi.org/10.1002/hyp.6217>.
- [22] Z.E. Wallage, J. Holden, Spatial and temporal variability in the relationship between water colour and dissolved organic carbon in blanket peat pore waters, *Sci. Total Environ.* 408 (2010) 6235–6242, <https://doi.org/10.1016/j.scitotenv.2010.09.009>.
- [23] E. Tipping, H.T. Corbhisley, J.-F. Koprivnjak, D.J. Lapworth, M.P. Miller, C. D. Vincent, J. Hamilton-Taylor, Quantification of natural DOM from UV absorption at two wavelengths, *Environ. Chem.* 6 (2009) 472–476, <https://doi.org/10.1071/EN09090>.
- [24] R.C. Sandford, R. Bol, P.J. Worsfold, In situ determination of dissolved organic carbon in freshwaters using a reagentless UV sensor, *J. Environ. Monit.* 12 (2010) 1678, <https://doi.org/10.1039/c0em00060d>.
- [25] C.G. Fichot, R. Benner, A novel method to estimate DOC concentrations from CDOM absorption coefficients in coastal waters: DOC estimates from cdom absorption coefficients, *Geophys. Res. Lett.* 38 (2011), <https://doi.org/10.1029/2010GL046152> n/a-n/a.
- [26] Y.-H. Xiao, T. Sara-Aho, H. Hartikainen, A.V. Vähätalo, Contribution of ferric iron to light absorption by chromophoric dissolved organic matter, *Limnol. Oceanogr.* 58 (2013) 653–662, <https://doi.org/10.4319/lo.2013.58.2.0653>.
- [27] H. Laudon, I. Taberman, A. Ågren, M. Futter, M. Ottosson-Löfvenius, K. Bishop, The Krycklan Catchment Study—a flagship infrastructure for hydrology, biogeochemistry, and climate research in the boreal landscape, *Water Resour. Res.* 49 (2013) 7154–7158, <https://doi.org/10.1002/wrcr.20520>.
- [28] E. Viollier, P.W. Inglett, K. Hunter, A.N. Roychoudhury, P. Van Cappellen, The ferrozine method revisited: Fe(II)/Fe(III) determination in natural waters, *Appl. Geochem.* 15 (2000) 785–790, [https://doi.org/10.1016/S0883-2927\(99\)00097-9](https://doi.org/10.1016/S0883-2927(99)00097-9).
- [29] L. Björkvald, I. Buffam, H. Laudon, C.-M. Mörth, Hydrogeochemistry of Fe and Mn in small boreal streams: the role of seasonality, landscape type and scale, *Geochim. Cosmochim. Acta* 72 (2008) 2789–2804, <https://doi.org/10.1016/j.gca.2008.03.024>.
- [30] E. Tipping, J. Hilton, B. James, Dissolved organic matter in Cumbrian lakes and streams, *Freshw. Biol.* 19 (1988) 371–378, <https://doi.org/10.1111/j.1365-2427.1988.tb00358.x>.
- [31] K. Varmuza, P. Filzmoser, *Introduction to Multivariate Statistical Analysis in Chemometrics*, 2016. CRC press.
- [32] J.N. Miller, J.C. Miller, *Statistics and Chemometrics for Analytical Chemistry*, sixth ed., 2010.
- [33] B.-H. Mevik, R. Wehrens, K.H. Liland, Pls: Partial Least Squares and Principal Component Regression, 2019. <https://CRAN.R-project.org/package=pls>.
- [34] R Core Team, R, A Language and Environment for Statistical Computing, R Foundation for Statistical Computing, Vienna, Austria, 2019. <https://www.R-project.org/>.
- [35] M.K. C. J. Wing, S. Weston, A. Williams, C. Keefer, A. Engelhardt, T. Cooper, Z. Mayer, B. Kenkel, , the R.C. Team, M. Benesty, R. Lescarbeau, A. Ziem, L. Scrucca, Y. Tang, C. Candan, T. Hunt, Caret: Classification and Regression Training, 2019. <https://CRAN.R-project.org/package=caret>.
- [36] A. Baker, L. Bolton, M. Newson, R.G.M. Spencer, Spectrophotometric properties of surface water dissolved organic matter in an afforested upland peat catchment, *Hydrol. Process.* 22 (2008) 2325–2336, <https://doi.org/10.1002/hyp.6827>.
- [37] E. Tipping, H.T. Corbhisley, J.-F. Koprivnjak, D.J. Lapworth, M.P. Miller, C. D. Vincent, J. Hamilton-Taylor, Quantification of natural DOM from UV absorption at two wavelengths, *Environ. Chem.* 6 (2009) 472–476, <https://doi.org/10.1071/EN09090>.
- [38] J. Pastor, J. Solin, S.D. Bridgman, K. Updegraff, C. Harth, P. Weishampel, B. Dewey, Global warming and the export of dissolved organic carbon from boreal peatlands, *Oikos* 100 (2003) 380–386, <https://doi.org/10.1034/j.1600-0706.2003.11774.x>.
- [39] A. Baker, R.G.M. Spencer, Characterization of dissolved organic matter from source to sea using fluorescence and absorbance spectroscopy, *Sci. Total Environ.* 333 (2004) 217–232, <https://doi.org/10.1016/j.scitotenv.2004.04.013>.
- [40] R. Grayson, J. Holden, Continuous measurement of spectrophotometric absorbance in peatland streamwater in northern England: implications for understanding fluvial carbon fluxes, *Hydrol. Process.* 26 (2012) 27–39, <https://doi.org/10.1002/hyp.8106>.
- [41] M. Babin, D. Stramski, Variations in the mass-specific absorption coefficient of mineral particles suspended in water, *Limnol. Oceanogr.* 49 (2004) 756–767, <https://doi.org/10.4319/lo.2004.49.3.0756>.
- [42] J.L. Weishaar, G.R. Aiken, B.A. Bergamaschi, M.S. Fram, R. Fujii, K. Mopper, Evaluation of specific ultraviolet absorbance as an indicator of the chemical composition and reactivity of dissolved organic carbon, *Environ. Sci. Technol.* 37 (2003) 4702–4708, <https://doi.org/10.1021/es030360x>.
- [43] M. Gledhill, P. McCormack, S. Ussher, E.P. Achterberg, R.F.C. Mantoura, P. J. Worsfold, Production of siderophore type chelates by mixed bacterioplankton populations in nutrient enriched seawater incubations, *Mar. Chem.* 88 (2004) 75–83, <https://doi.org/10.1016/j.marchem.2004.03.003>.
- [44] S. Sarkkola, M. Nieminen, H. Koivusalo, A. Laurén, P. Kortelainen, T. Mattsson, M. Palviainen, S. Piirainen, M. Starr, L. Finér, Iron concentrations are increasing in surface waters from forested headwater catchments in eastern Finland, *Sci. Total Environ.* 463–464 (2013) 683–689, <https://doi.org/10.1016/j.scitotenv.2013.06.072>.

II

The role of terrestrial productivity and hydrology in regulating aquatic dissolved organic carbon concentrations in boreal catchments.

Zhu, X., Chen, L., Pumpanen, J., Ojala, A., Zobitz, J., Zhou, X., Laudon, H., Palviainen, M., Neitola, K., & Berninger, F.











2022

Global Change Biology, 28(8), 2764–2778.

Reprinted with the kind permission of WILEY

RESEARCH ARTICLE

The role of terrestrial productivity and hydrology in regulating aquatic dissolved organic carbon concentrations in boreal catchments

Xudan Zhu¹  | Liang Chen¹  | Jukka Pumpanen²  | Anne Ojala³  | John Zobitz⁴  | Xuan Zhou¹  | Hjalmar Laudon⁵  | Marjo Palviainen⁶  | Kimmo Neitola⁷  | Frank Berninger¹ 

¹Department of Environmental and Biological Sciences, Joensuu Campus, University of Eastern Finland, Joensuu, Finland

²Department of Environmental and Biological Sciences, Kuopio Campus, University of Eastern Finland, Kuopio, Finland

³Natural Resources Institute Finland (LUKE), Helsinki, Finland

⁴Department of Mathematics, Statistics, and Computer Science, Augsburg University, Minneapolis, Minnesota, USA

⁵Department of Forest Ecology and Management, Swedish University of Agricultural Science, Umeå, Sweden

⁶Department of Forest Sciences, University of Helsinki, Helsinki, Finland

⁷Institute for Atmospheric Earth System Research (INAR), University of Helsinki, Helsinki, Finland

Correspondence

Xudan Zhu, Department of Environmental and Biological Sciences, Joensuu Campus, University of Eastern Finland, 80101 Joensuu, Finland.
Email: xudan.zhu@uef.fi

Funding information

the VR extreme event project; Academy of Finland, Grant/Award Number: 304460, 323997, 326818, 337549 and 337550; European Commission-Horizon 2020 Research and innovation programme, Grant/Award Number: 689443; Koneen Säätiö, Grant/Award Number: 201906598; European Union's Horizon 2020 Research and Innovation Programme, Grant/Award Number: 734317; the Swedish Research Council for Sustainable Development (FORMAS); the Fulbright Finland Foundation and Saastamoinen Foundation Grant in Health and Environmental Sciences; Swedish Infrastructure for Ecosystem Science (SITES)

Abstract

The past decades have witnessed an increase in dissolved organic carbon (DOC) concentrations in the catchments of the Northern Hemisphere. Increasing terrestrial productivity and changing hydrology may be reasons for the increases in DOC concentration. The aim of this study is to investigate the impacts of increased terrestrial productivity and changed hydrology following climate change on DOC concentrations. We tested and quantified the effects of gross primary production (GPP), ecosystem respiration (RE) and discharge on DOC concentrations in boreal catchments over 3 years. As catchment characteristics can regulate the extent of rising DOC concentrations caused by the regional or global environmental changes, we selected four catchments with different sizes (small, medium and large) and landscapes (forest, mire and forest-mire mixed). We applied multiple models: Wavelet coherence analysis detected the delay-effects of terrestrial productivity and discharge on aquatic DOC variations of boreal catchments; thereafter, the distributed-lag linear models quantified the contributions of each factor on DOC variations. Our results showed that the combined impacts of terrestrial productivity and discharge explained 62% of aquatic DOC variations on average across all sites, whereas discharge, gross primary production (GPP) and RE accounted for 26%, 22% and 3%, respectively. The impact of GPP and discharge on DOC changes was directly related to catchment size: GPP dominated DOC fluctuations in small catchments (<1 km²), whereas discharge controlled

This is an open access article under the terms of the Creative Commons Attribution-NonCommercial-NoDerivs License, which permits use and distribution in any medium, provided the original work is properly cited, the use is non-commercial and no modifications or adaptations are made.

© 2022 The Authors. *Global Change Biology* published by John Wiley & Sons Ltd.

DOC variations in big catchments (>1 km²). The direction of the relation between GPP and discharge on DOC varied. Increasing RE always made a positive contribution to DOC concentration. This study reveals that climate change-induced terrestrial greening and shifting hydrology change the DOC export from terrestrial to aquatic ecosystems. The work improves our mechanistic understanding of surface water DOC regulation in boreal catchments and confirms the importance of DOC fluxes in regulating ecosystem C budgets.

KEYWORDS

boreal catchments, catchment size, discharge, DOC, GPP, landscape, RE, terrestrial productivity

1 | INTRODUCTION

Dissolved organic carbon (DOC) concentrations in freshwater ecosystems have increased in large areas of the northern hemisphere over the past few decades (Filella & Rodríguez-Murillo, 2014), which is called 'aquatic browning' (Roulet & Moore, 2006). From an ecological point of view, rising DOC has important implications on aquatic ecosystems. First, rising DOC may reduce aquatic primary production and affect predator-prey interactions (Kritzberg et al., 2020) due to the changes in the light climate. Second, it may also contribute to eutrophication in coastal ecosystems, further leading to hypoxia (Conley et al., 2011) and loss of biodiversity (Villnäs & Norkko, 2011). Additionally, societal impacts of rising DOC include increasing costs for purifying drinking water and reducing the aesthetic and recreational value of aquatic landscapes (Ekström, 2013; Freeman et al., 2004). Finally, DOC exports play an essential role in ecosystem carbon (C) budgets (Cole et al., 2007; Nilsson et al., 2008). Since much of terrestrial derived DOC that reaches surface waters will be converted to CO₂ by biotic and abiotic processes, increased DOC has the potential to mobilize large terrestrial C pools and affect C fluxes in both the atmosphere and the ocean (Mann et al., 2012; Öquist et al., 2014).

Proposed mechanisms behind rising DOC concentrations include decreasing acidification (Kang et al., 2018), land-use changes (Wilson & Xenopoulos, 2008) and climate change (Asmala et al., 2019; Ekström, 2013). Decreasing acidification has been identified as a significant driver behind the long-term DOC increases in catchments, either by itself (Ekström, 2013; Monteith et al., 2007; Vuorenmaa et al., 2006) or coupled with climate change (Burns et al., 2006; Evans et al., 2005). In addition, land management, such as the drainage of peatlands, may transform the hydrochemistry and hydrology (Holden et al., 2004), and DOC loads are typically high from the drained boreal peatlands (Asmala et al., 2019; Nieminen et al., 2021). However, the land-use changes or recovery from acid deposition do not always explain changing DOC concentrations. For example, increased DOC has also occurred in areas with low acid deposition and with increasing forest biomass, such as Krycklan in Sweden (Laudon & Sponseller, 2018).

Climate change impacts such as permafrost thaw (Tank et al., 2016), increased precipitation alone (Hongve et al., 2004) or in combination with higher temperature (Keller et al., 2008) have contributed to rising DOC concentrations. However, Freeman et al. (2004) stated that neither warming, increased discharge or the shifting trends in the proportion of annual rainfall arriving in summer can offer satisfactory explanations. However, the CO₂-mediated stimulation of primary productivity is responsible for increasing exported DOC from peatlands. Schlesinger and Andrews (2000) also confirmed that elevated CO₂ concentrations could potentially increase primary productivity leading to increased DOC inputs from terrestrial to aquatic systems. On the contrary, Ellis et al. (2009) found that elevated atmospheric CO₂ treatment decreased DOC concentrations, in environments where the concentrations of labile C limit decomposition. Ombrotrophic bogs were such environments. Finstad et al. (2016) and Pumpanen et al. (2014) brought forward the hypothesis that browning could be linked to changes in the productivity of forests. To a large extent, DOC in water bodies is derived from the microbial decomposition of organic matter (Schimel et al., 1994; Xu & Guo, 2018). Increases in the productivity of vegetation could then increase DOC via gradual increases in soil organic matter (SOM) or via a process called priming (He et al., 2020). Priming denotes changes in recalcitrant local soil C decomposition after new fresh C is available. Changes in decomposition due to priming can be positive or negative. Positive priming effects mean that increases in production lead to increasing decomposition of SOM and consequently increased DOC concentrations. Positive priming is attributed to increased microbial growth and activity (Kuzakov, 2010; Linkosalmi et al., 2015). However, it is often associated to nutrient-poor conditions, under which microbes use the energy from rhizodeposition 'to mine nutrients in SOM', thereby releasing extra CO₂ (Sullivan & Hart, 2013). A negative priming effect means that increased production leads to a decrease in native SOM decomposition and subsequently DOC concentrations. Competition between the plant roots and rhizosphere organisms for mineral N and nutrient limitation of the rhizosphere have been proposed as reasons for negative priming (Dijkstra et al., 2013; Kuzakov, 2002). Additionally, the so-called preferential substrate utilization may lead to a decrease in the decomposition of old C in the short term, since the microbes tend to utilize the fresh organic matter initially (Kuzakov et al., 2000). Priming will lead to more rapid changes in DOC

since microbial biomass and functions change over days to weeks after a change in the supply of easily available carbon.

Studies by Pumpanen et al. (2014) and Finstad et al. (2016) examined the role of direct priming on DOC concentrations using proxy measurements. Finstad et al. (2016) showed that increasing Normalized Difference Vegetation Index (NDVI), a remote sensing-derived indicator of plant leaf area and productivity, was associated with DOC concentrations. Increases in NDVI led to increasing DOC concentrations. Pumpanen et al. (2014) showed that the average yearly DOC concentration depended on the forest GPP of the previous year. Both analyses suggest a role of priming, but the evidence presented is at a time scale that exceeds the response of microbial communities to changes in resources (years instead of days to weeks). Additionally, the effects of increasing soil organic carbon cannot be excluded in both studies.

The connections between primary production and DOC concentrations in surface waters are not easy to detect. In large monitoring data sets, surface DOC concentrations may be caused by changes in vegetation and its management. For example, in the study of (Pumpanen et al., 2014), changes in forest age are easily confounded with changes in productivity. However, direct regressions of DOC concentrations and photosynthetic production are not reasonable since changes in productivity will affect changes in DOC concentrations at a delay of several days to several weeks. The delay is caused by the transport of fresh photosynthates to the roots, changes in decomposition and microbial biomass after a change in root exudation and hydraulic delays required to transport DOC from the soil to water bodies (Wen et al., 2020). This study tested the effects of variation in terrestrial productivity from eddy covariance (EC) data with high-frequency measurements of DOC concentrations in four Northern boreal watersheds. We used cross-spectral wavelet analyses as well as distributed-lag linear models (DLMs) to test and quantify the effects of GPP, ecosystem respiration (RE), net ecosystem production (NEP) and discharge on aquatic DOC concentrations.

2 | MATERIALS AND METHODS

2.1 | Study site

Four catchments with different sizes (small, medium and large) and landscapes (forest, mire and forest-mire mixed) were studied. The size and landscape of catchment were noted after site name.

Hereafter, the letters 'S', 'M' and 'L' signify the catchment sizes (small, medium and large), whereas the symbols 'forest', 'mire' and 'mix' reflect the land cover types (forest, mire and forest-mire mixed). Three sub-catchments locate in Krycklan, about 50 km northwest of the city of Umeå in northern Sweden (64°14'N, 19°46'E) (Figure S1). In Krycklan, C2[S-forest] is covered by forest with the size of 0.14 km²; C4[S-mire] of 0.19 km² is covered by 40.4% of wetlands and the remainder is forest; C6[M-mix] of 1.3 km² is constituted by 72.8% of forest, 24.1% of wetland and 3.1% of lakes (Table 1). The climate is characterized as a cold temperate humid type with persistent snow cover during the winter season. The 30-year mean annual temperature (1981–2010) is 1.8°C, January −9.5°C, and July 14.7°C. The mean annual precipitation is 614 mm and mean annual runoff 311 mm, giving annual average evapotranspiration of 303 mm (Laudon et al., 2013). The 40-year average duration of winter snow cover is 167 days, but this has been decreasing over time (Laudon et al., 2021). Yli-Nuortti (NT[L-mix]) is a catchment nearby Nuorttiaapa measuring station and located in Värriö, Finland (67°44'N, 29°27'E) approximately 120 km north of the Arctic Circle close to the northern timberline (Figure S1). NT[L-mix] covers about 40 km² with 25% of peatlands, and 5% of the area is covered by alpine vegetation on the top of the fells while the rest of the catchment is dominated by pine forests on glacial tills (Table 1). There are no lakes above the measurement station. According to the statistics of the Finnish Meteorological Institute (1981–2012), the mean annual air temperature is −0.5°C. The mean temperature in January is −11.4°C and in July 13.1°C. The mean annual precipitation is 601 mm, mean annual runoff 212 mm and annual average evapotranspiration is 389 mm. The average number of days with snow cover is 205–225 days (Pohjonen et al., 2008).

2.2 | Sampling and laboratory dissolved organic carbon measurement

All water samples were sampled in the surface water (25 cm) by acid-washed LDPE bottles. In Finland (NT[L-mix]), we sampled monthly in winter and fall, fortnightly in spring and every week in summer (2018–2020). In Sweden (C2[S-forest], C4[S-mire] and C6[M-mix]), water samples were collected monthly during winter, every 2 weeks during summer and fall, and every third day during the spring flood (2016–2018). Water samples were filtered immediately after

TABLE 1 Site information

Site ID.	Site name	Size (km ²)	Land cover %				Alpine vegetation	Land-use type	EC tower
			Forest	Wetland	Lake				
C2[S-forest]	Västrabäcken	0.14	100	0	0	0	Forest	Rosinedal	
C4[S-mire]	Kalkkälsmyren	0.19	59.6	40.4	0	0	Wetland	Degerö	
C6[M-mix]	Stortjärnsbäcken	1.30	72.8	24.1	3.1	0	Mixed	Rosinedal	
NT[L-mix]	Nuorttiaapa station	40.0	70.0	25.0	0	5.0	Mixed	SMEAR I	

sampling by a filtration system made of glass using Whatman GF/F Glass Microfiber Filters (pore size 0.45 μm), which had been rinsed by the sample water before filtration. All samples were frozen until further DOC analysis.

In Finland, DOC concentrations were determined by thermal oxidation coupled with infrared detection (Multi N/C 2100, Analytik Jena, Germany) following acidification with phosphoric acid. In Sweden, after all samples were acidified with H_3PO_4 , DOC concentrations were measured by catalytic oxidation combustion (Shimadzu TOC-5000, Kyoto, Japan) (Laudon et al., 2011).

2.3 | Prediction of dissolved organic carbon based on real-time spectral absorbance

To monitor the real-time spectral absorbance, in situ portable multi-parameter UV-Vis probes (spectro:lyser, S:CAN Messtechnik GmbH, Austria) were installed in Yli-Nuortti river on June 12, 2018, and in the Krycklan catchments on May 9, 2016. The spectro:lyser measures absorbance across the wavelengths from 220 to 732.5 nm at 2.5 nm intervals with a path length of 35 mm. The benefits of in-situ UV-Vis probe is to make high-frequency aquatic monitoring possible, especially during short-duration events or in remote areas (Avagyian et al., 2014; Rode et al., 2016; Zhu et al., 2020).

Principal component regression (PCR) was used to model the relationship between DOC concentration and absorbance. In the PCR model, absorbance values from 250 nm to 732.5 nm at 2.5 nm intervals (194 variables) were the independent variables. The dependent variables were the DOC concentrations measured in the lab from water samples collected in the respective days. The observations were split into a training and testing data set. The training set contained 75% of observations that were randomly selected from all samples (C2[S-forest], C4[S-mire], C6[M-mix] and NT[L-mix]), and the testing set contained the remaining 25% of observations. The PCR analyses were conducted with the 'pls' package (Mevik et al., 2019) in R (R Core Team, 2019). After the PCR model was built, hourly real-time spectral absorbances were used as input to predict hourly DOC concentrations. The hourly predicted DOC concentrations were aggregated into daily data for further analysis. The outlier values were automatically detected and corrected using the 'tsclean' function of package 'forecast' (Hyndman & Khandakar, 2008) in R (R Core Team, 2019).

2.4 | Water discharge

In Finland, water discharge was determined based on the continuous water depth measurements carried out by pressure sensors measuring the hydrostatic pressure (Levellogger, Solinst, Georgetown, Canada) in the bottom of the river, which was corrected by barometric pressure measurements (Barologger, Solinst, Georgetown, Canada). The water depth measurements were converted to flow

rates using channel cross-section, water depth and manual flow rate measurements (Flow Tracker Handheld ADV, SonTek, CA, USA) carried out at sampling locations.

In Sweden, water discharge was computed hourly from water level measurements (using pressure transducers connected to Campbell Scientific dataloggers, USA, or duplicate WT-HR water height data loggers, Trutrack Inc., New Zealand). Rating curves were derived based on discharge measurements using salt dilution or time-volume methods (Laudon et al., 2011).

2.5 | Carbon fluxes

There are three measuring stations nearby our study sites where the C exchange between the terrestrial ecosystem and the atmosphere is continuously recorded by the EC technology (Medlyn et al., 2005). The EC data included GPP, RE and NEP. We assumed that $\text{NEP} = -\text{NEE}$ (Black et al., 2007), and the value for RE and GPP was taken from day-time measurements (Aubinet et al., 2012).

In Finland, the Värriö measuring station SMEAR I (67°45'N, 29°36'E, 390 m asl) is close to NT[L-mix]. Most of the area is dominated by 60-year-old Scots pine (*Pinus sylvestris* L.) forests, in addition to which there are also large wetlands and deep gorges in the surroundings (Vehkamäki et al., 2004a, b). Flux data from SMEAR I was applied to NT[L-mix]. The flux data were collected from the Dynamic Ecological Information Management System (<https://deims.org/b471311f-e819-4f6f-bbae-1ac86cd9777f>). The processing pipeline differed from the two Swedish sites due to polar day (24 h sunlight) during the growing season. More details about the whole process for data quality control are presented in Kulmala et al. (2019).

In Sweden, the Rosinedalsheden station (64°10'N, 19°45'E, 145 m asl) is located in a forest stand that consists of naturally regenerated 80-year-old Scots pine (*P. sylvestris* L.), and the soil is a deep deposit of sand and fine sand. The ground vegetation is dominated by blueberries (*Vaccinium myrtillus* L.) and lingonberries (*Vaccinium vitis-idaea* L.). Degerö station (64°11'N, 19°33'E, 270 m asl) is situated on a highland between two major rivers, Umeälven and Vindelälven. The site is a nutrient-poor minerogenic mire dominated by flat mire lawn plant communities with bog mosses (*Sphagnum balticum*, *Sphagnum majus* and *Sphagnum lindbergii*) dominating the bottom layer. The field layer is dominated by the cottongrass (*Eriophorum vaginatum* L.) and cranberry (*Vaccinium oxycoccos* L.), bog-rosemary (*Andromeda polifolia* L.) and deergrass (*Trichophorum cespitosum* L.). Sedges (*Carex* spp.) occur more sparsely. C fluxes data from Rosinedalsheden were applied to C2[S-forest], and C6[M-mix] and C fluxes data from Degerö were used in C4[S-mire] (Table S1). C fluxes data from the two EC towers were obtained from the ICOS data portal (Drought 2018 Team & ICOS Ecosystem Thematic Centre, 2020). The data had been subjected to standardized quality control using the ONEFlux processing pipeline (<https://github.com/icos-etc/ONEFlux>), including spike detection, data flagging and friction velocity filtering (Papale et al., 2006). ONEFlux processing pipeline is described in more detail in Pastorello et al. (2020).

2.6 | Wavelet coherence analysis

To test the hypothesis that discharge, GPP, NEP and RE influence DOC concentration in catchments, we investigated the temporal correlations between discharge, GPP, NEP, RE and DOC concentration by wavelet coherence analysis during the growing season and whole experimental period. Wavelet analysis has been effectively applied in the geosciences and ecology, showing good localization properties in the time and frequency domain (Grinsted et al., 2004; Kumar & Foufoula-Georgiou, 1997; Vargas et al., 2011). Wavelet analysis aims to quantify the variance of a specific time series and correlations between different time series across multiple frequencies in time (Grinsted et al., 2004). We applied continuous wavelet transforms (CWTs) to show frequency-dependent behaviour for exploring the relationship between discharge, GPP, RE, NEP and aquatic DOC concentration. In the CWT, it is possible to detect if two time series tend to oscillate simultaneously, rising and falling together within a given time period (in phase, and therefore showing no time lags), or rise and fall out of phase within a given time period (therefore showing a time lag between them) (Vargas et al., 2011). A 95% confidence level for the CWT was done through Monte-Carlo simulation using 1000 times. In this study, wavelet analysis was done using 'WaveletComp' package (Schmidbauer & Roesch, 2018) in R (R Core Team, 2019).

2.7 | Distributed lag models

DLMs (Gasparrini, 2011) were applied to quantify the lag effects of discharge, GPP, NEP and RE on DOC in each site (C2[S-forest], C4[S-mire], C6[M-mix] and NT[L-mix]) separately. DLMs are linear regressions between weighted lagged values of independent variables and dependent variables. In our case, we assumed that lag times are long, and the values of the weights were specified using polynomial transformations of lags of the independent variables by building so-called cross-basis functions. In DLMs, fourth-degree polynomial cross-basis functions were built for each factor GPP, RE and NEP and second-degree for discharge. Then, DOC variations were predicted by linear combinations of the cross-basis of each factor. We used explorative analysis to determine the optimal length of the lags. Lag time for each variable was determined by the results of wavelet coherence analysis and adjustments of DLMs, 0–7 days lag time was chosen for discharge and 4–30 days for GPP and RE. Since our variables exhibit an annual cycle, we also added year as a factor variable and did not consider longer time lags. This part was done using the 'DLNM' package (Gasparrini, 2011) in R (R Core Team, 2019). The Akaike information criterion (AIC) and explanatory power (R^2) were used to select the best DLM model across all sites (Table 3). Finally, the distributed lag models (DLM 1–6) applied across all sites were defined as follows:

$$\text{DOC} = \beta_1 \text{DIS}_{\text{lag}} + \alpha \text{Year} \quad (1)$$

$$\text{DOC} = \beta_1 \text{GPP}_{\text{lag}} + \alpha \text{Year} \quad (2)$$

$$\text{DOC} = \beta_1 \text{RE}_{\text{lag}} + \alpha \text{Year} \quad (3)$$

$$\text{DOC} = \beta_1 \text{NEP}_{\text{lag}} + \alpha \text{Year} \quad (4)$$

$$\text{DOC} = \beta_1 \text{DIS}_{\text{lag}} + \beta_2 \text{GPP}_{\text{lag}} + \alpha \text{Year} \quad (5)$$

$$\text{DOC} = \beta_1 \text{DIS}_{\text{lag}} + \beta_2 \text{GPP}_{\text{lag}} + \beta_3 \text{RE}_{\text{lag}} + \alpha \text{Year} \quad (6)$$

where β is the lag effect of discharge (DIS), GPP, RE and NEP on DOC concentrations, DIS_{lag} , GPP_{lag} , RE_{lag} and NEP_{lag} are the mean cross-basis of discharge, GPP, RE and NEP during their lag times, respectively. We also tested the different effects caused by discharge, baseflow and direct runoff on DOC variations by DLM 1 across the sites, and the results showed that DOC is more related to discharge than baseflow or direct runoff (Table S2). Therefore, discharge was set as the effect of hydrology to DOC variations in DLM 5–6.

3 | RESULTS

3.1 | Prediction of dissolved organic carbon by principal component regression model

We chose the first six components as the input variables into the PCR model. When applied to the training set, the DOC values from PCR calibration produced accurate estimates, as can be seen from the high explanatory power values of the model ($R^2 = 0.93$) and low root-mean-square deviation (RMSD = 3.38). PCR model showed even better performance when applied to the testing set, proved by the high explanatory power ($R^2 = 0.95$), low RMSD (RMSD = 2.95) and low mean bias error (0.12) (Table S3).

Daily DOC concentrations were predicted by PCR model based on the real-time spectral absorbances measurements in the field. Across all the sites, DOC concentrations were usually more stable and lower in the snow cover period compared with the growing season (Table S4). During the snow melt period, sudden increases are visible each year in C2[S-forest], C6[M-mix] and NT[L-mix], while there was a clear decrease in C4[S-mire] (Figure 1a). C4[S-mire] had the highest mean DOC concentrations ($33.83 \pm 7.95 \text{ mg l}^{-1}$) and the lowest coefficient of variation (CV = 23.49%) across 2016 to 2018. The lowest mean DOC values ($4.51 \pm 2.85 \text{ mg l}^{-1}$) and highest CV (63.12%) was found in NT[L-mix] from 2018 to 2020. The mean values of DOC were $18.95 \pm 6.36 \text{ mg l}^{-1}$ in C2[S-forest] (CV = 33.58%) and $17.80 \pm 5.57 \text{ mg l}^{-1}$ in C6[M-mix] (CV = 31.31%) across 2016 to 2018, respectively (Figure 1b).

3.2 | Wavelet coherence analysis between dissolved organic carbon and environmental factors

There was temporal synchrony between discharge (Figure 2a) and DOC during 1 to 30 days and 4 to 30 days between GPP (Figure 2b), NEP (Figure 2c), RE (Figure 2d) and DOC. However, the temporal synchrony was not continuous, and it was mainly restricted to the growing

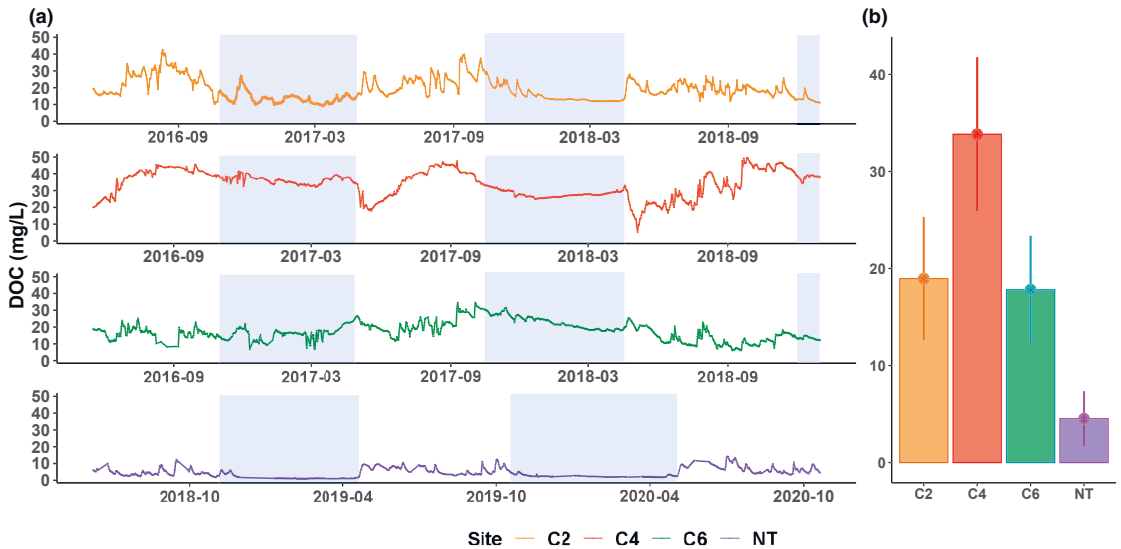


FIGURE 1 Daily dissolved organic carbon (DOC) variations (predicted by principal component regression model) across 2016 to 2019 in C2[S-forest], C4[mire], C6[mix], 2018 to 2020 in Nuorttiaapa Station (NT[mix]) (a) and the mean DOC concentration with standard deviation in each site during the whole experimental period (b). The different colours (orange, red, green and purple) represent different sites (C2[S-forest], C4[mire], C6[mix] and NT[mix]). The blue shades represent the snow cover periods

season. The temporal relations between discharge, GPP, NEP, RE and DOC concentration were unstable and varied between summers in different years and sites, and sometimes the temporal synchrony was not visible for all of them (Figure S2). The wavelet coherence analysis revealed that the environmental predictors affected DOC concentration and the effects always had a lag time (Figure 2).

3.3 | Relationships between dissolved organic carbon and environmental factors by distributed-lag linear models

The performances of DLMs improved with more time-lagged environmental factors, as shown by the increase of R^2 and decrease of AIC across all the sites. Among all the DLMs, DLM6 turned out to be the best one across all the sites, and it explained on average 62% of DOC variations. DLM6 in NT[L-mix] performed best with the highest R^2 (0.73), followed by C2[S-forest] ($R^2 = 0.69$) and C4[S-mire] ($R^2 = 0.65$), while C6[M-mix] had the lowest R^2 (0.42) (Table 2).

The cumulative responses of DOC concentration to a 10-unit increase of discharge were similar in C6[M-mix] (Figure 3c) and NT[L-mix] (Figure 3d). DOC concentration reached the first peak at 2 days lag, then decreased slightly and became the highest at 7 days lag (Figure 3c and d). In C2[S-forest], DOC concentration reached the peak at 3 days lag and then stayed relatively stable (Figure 3a). In C4[S-mire], DOC concentration responded negatively to the increase of discharge during the whole lag period (Figure 3b).

In C4[S-mire] (Figure 3f), C6[M-mix] (Figure 3g) and NT[L-mix] (Figure 3h), DOC concentration decreased immediately after a 10-unit increase of GPP and turned to revive slowly from 20, 25, 7 days lag, respectively. After a month lag, DOC concentration in NT[L-mix] (Figure 3h) returned to the original level but in C4[S-mire] (Figure 3f) and C6[M-mix] (Figure 3g) to lower than the initial level. Unlike the other three sites, DOC concentration in C2[S-forest] stayed relatively stable during the first half month, then started to rise and showed higher than the original level at a month lag (Figure 3e).

After a 10-unit increase of RE, DOC concentrations in C2[S-forest] (Figure 3i), C6[M-mix] (Figure 3k) increased immediately. In comparison, DOC concentrations in C4[S-mire] decreased slightly at the initial stage and turned to increase at 10 days lag (Figure 3g). These three sites then showed much higher than the original level at a month lag (Figure 3g,i,k). DOC variations in NT[L-mix] were much smaller than in the other sites, and DOC concentration was slightly higher than the initial level after a month lag (Figure 3l).

3.4 | Contributions of environmental variables to dissolved organic carbon concentrations

Comparing all the sites, the independent contribution of discharge and GPP to DOC concentrations in DLM6 behaved differently as catchment size increased (discharge increased whereas GPP decreased; Table 3). The separated contributions of the environmental factors to the DOC variations (in DLM6) across the experimental period are visualized in Figure 4. Unlike the other

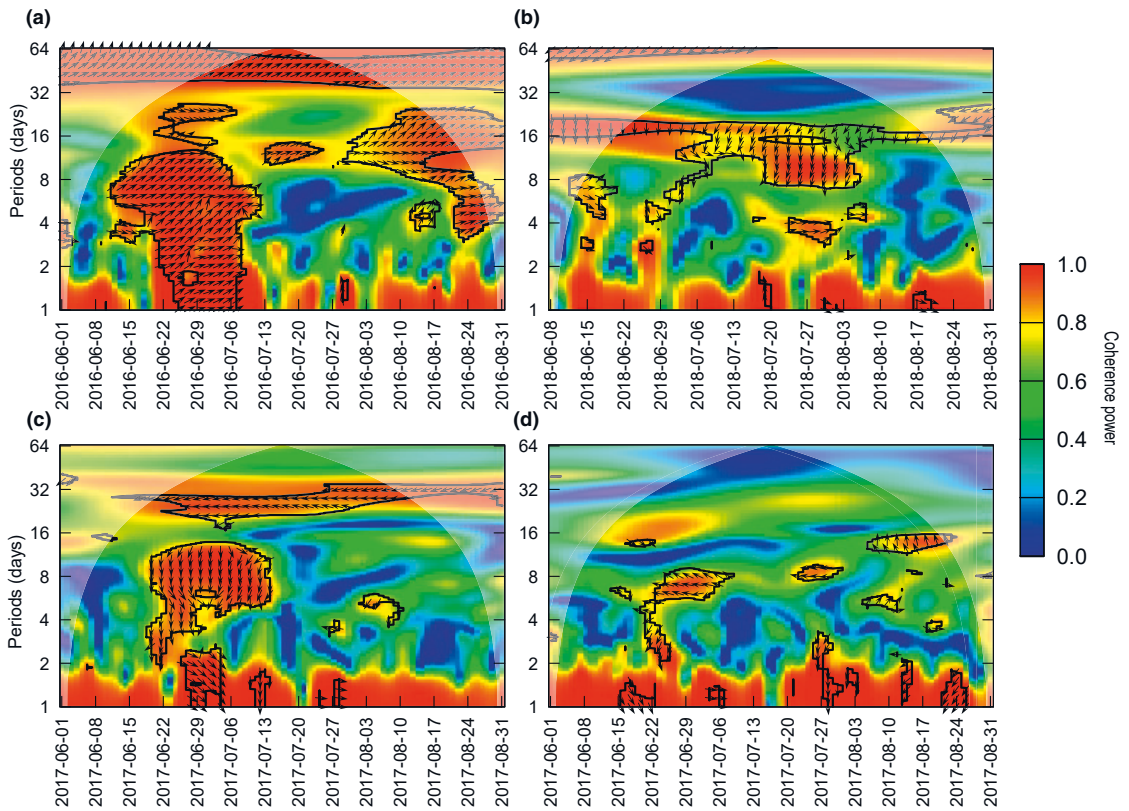


FIGURE 2 Wavelet coherence analysis between dissolved organic carbon concentrations and discharge (a), gross primary production (b), net ecosystem production (c), ecosystem respiration (d) in summer 2016, 2018, 2017 and 2017, respectively. The colours of power values range from blue (low values) to green (intermediate) to red (high values). The red parts inside the black border indicate significantly temporal coherence between the studied parameters ($p < .05$). The arrows show the leading and lagging relationship between the variables. The y-axis indicates the length of the time window in the wavelet coherence analysis (in days)

three sites, DOC variations in NT[L-mix] (Figure 4g) were controlled mainly by discharge leading to the negligible contributions of GPP and RE. In C2[S-forest] (Figure 4a), C4[S-mire] (Figure 4c) and C6[M-mix] (Figure 4e), RE contributed positively to DOC variations, but GPP and discharge acted differently among sites. GPP and discharge both contributed positively to DOC variations in C2[S-forest] (Figure 4a) but negatively in C4[S-mire] (Figure 4c), while in C6[M-mix] (Figure 4e), the former acted negatively and the latter positively. The dynamics of discharge, GPP and RE across years in each site are shown in Figure 4b,d,f,h. The mean values of discharge, GPP and RE during the experimental period were listed in Table 4.

4 | DISCUSSION

Our findings indicated that the contributions of GPP and discharge to aquatic DOC concentrations were closely related to catchment size. In small catchments ($<1 \text{ km}^2$), GPP dominated DOC variations,

whereas in bigger rivers ($>1 \text{ km}^2$), discharge is the most important driver of DOC concentrations. Additionally, GPP and discharge can have either positive or negative effects on DOC concentrations depending on the landcover type. RE was always positively related to DOC concentrations. The impacts of GPP, RE and discharge on DOC variations were always detected with delays from days to weeks.

The best distributed-lag linear model (DLM6) could explain on average 62% of aquatic DOC variations across the four catchments. In DLM6, discharge, GPP and RE accounted for 26%, 22% and 3% of DOC variations, respectively. The relationship between GPP and DOC concentration could be controlled by the priming mechanism (Guenet et al., 2010). While a meta-analysis showed only a small potential for a significant priming effect in aquatic ecosystems (Bengtsson et al., 2018; Catalán et al., 2015), here we mainly focused on the priming effect in the soil. As plants are usually nitrogen-limited in boreal ecosystems, they mostly rely on mycorrhiza for nutrient acquiring. Enhanced forest productivity results in more root exudates (more C) for mycorrhizal fungi to grow, increasing nutrients supply feeding back on trees (Heinonsalo et al., 2010; Pumpanen

TABLE 2 Performance of distributed-lag linear models (DLMs) showing the relationship between dissolved organic carbon (DOC) and environmental predictors across C2[S-forest], C4[S-mire], C6[Mix] and NT[L-mix]

DLMs	DIS Lag\day	GPP	RE	NEP	C2[S-forest]		C4[S-mire]		C6[M-mix]		NT[L-mix]	
					AIC	R ²	AIC	R ²	AIC	R ²	AIC	R ²
1. DOC = DIS _{lag} + year	0-7				6051.4	0.22	6374.8	0.25	5339.5	0.36	2693.6	0.72
2. DOC = GPP _{lag} + year		4-30			5464.7	0.52	5980.9	0.41	5337.2	0.28	3387.6	0.17
3. DOC = RE _{lag} + year			4-30		5415.3	0.55	5807.8	0.51	5352.8	0.26	3390.8	0.17
4. DOC = NEP _{lag} + year				4-30	5712.6	0.38	6187.3	0.27	5925.2	0.28	3405.0	0.15
5. DOC = DIS _{lag} + GPP _{lag} + year	0-7	4-30			5130.6	0.67	5778.1	0.53	5201.9	0.38	2621.4	0.72
6. DOC = DIS _{lag} + GPP _{lag} + RE _{lag} + year	0-7	4-30	4-30		5069.0	0.69	5531.9	0.65	5155.3	0.42	2608.6	0.73

Note: DOC concentrations were predicted by principal component regression (PCR) model; DIS means discharge.

et al., 2009). In most northern headwaters, the link between terrestrial and aquatic environments is dominated by riparian zone with high SOC and water content (Laudon & Sponseller, 2018; Lidman et al., 2017; McGlynn et al., 1999; Wen et al., 2020). Our results demonstrated that although the riparian organic C pool can continue to sustain DOC export at the present rate for several hundred years without supplement (Ledesma et al., 2015), new C input due to increased GPP does affect the export of DOC from riparian zone to aquatic systems.

In this study, we found that GPP dominated the DOC variations in small catchments (C2[S-forest] and C4[S-mire]) but not in the larger catchments. The importance of GPP was masked by discharge in medium- and large-scale catchments (C6[M-mix] and NT[L-mix]). The faded impact of GPP with increased catchment size may be due to several reasons. Firstly, as groundwater moves from uphill mineral soils through the riparian zone with large stores of SOM, major biogeochemical transformations occur within meters of the stream (Laudon & Sponseller, 2018). These transformations mean that the active area affecting the DOC export is limited and does not change as much with increased catchment size. Thus, with the same amount of DOC export, the dynamics of aquatic DOC concentrations must be more evident in small-scale catchments than in larger ones. Secondly, Tiwari et al. (2017) stated that biogeochemical transitions from small to mesoscale catchments are partially mediated by the increased relative contribution of deep groundwater inflow with increased drainage area. The principal hydrological pathway shifts from mainly surface flow paths in small streams to deeper organic-poor groundwater in larger-scale catchments. These changes in the flow path also explain why discharge masked the effect of GPP in C6[M-mix] and NT[L-mix]. Finally, during the spring flood which typically occurs in the months of May and June over 60% of the annual DOC flux may occur (Mann et al., 2012). Large-scale rivers have a larger contribution of their flow from groundwater and their DOC concentrations are buffered against changes of DOC inputs from soils (Shanley et al., 2002; Strohmenger et al., 2021). These differences further explain why the proportion of DOC driven by GPP decreases when catchment size increase.

The roles of GPP in controlling DOC variations among sites were also complicated. We would have expected a mostly positive contribution of GPP on DOC concentrations due to the priming effect. The idea is that increased GPP leads, with a lag, to higher microbial biomass and, with a longer lag, to an increase in DOC production. However, apart from C2[S-forest] catchment, our results showed GPP was negatively correlated with DOC contents in C4[S-mire], C6[M-mix] and NT[L-mix], which does not support our hypothesis that GPP has a positive priming effect on aquatic DOC concentrations. Especially in C-rich ecosystems, increases in labile C supply may lead to increases in microbial biomass that consumes most organic materials. In these ecosystems, DOC consumption by an increasing microbial biomass exceeds the production of DOC (Qiao et al., 2014). Ding et al. (2018) emphasized the role of the C/N ratio for priming and demonstrated that priming often requires sufficient N supply. When the two small-scale catchments (C2[S-forest] and

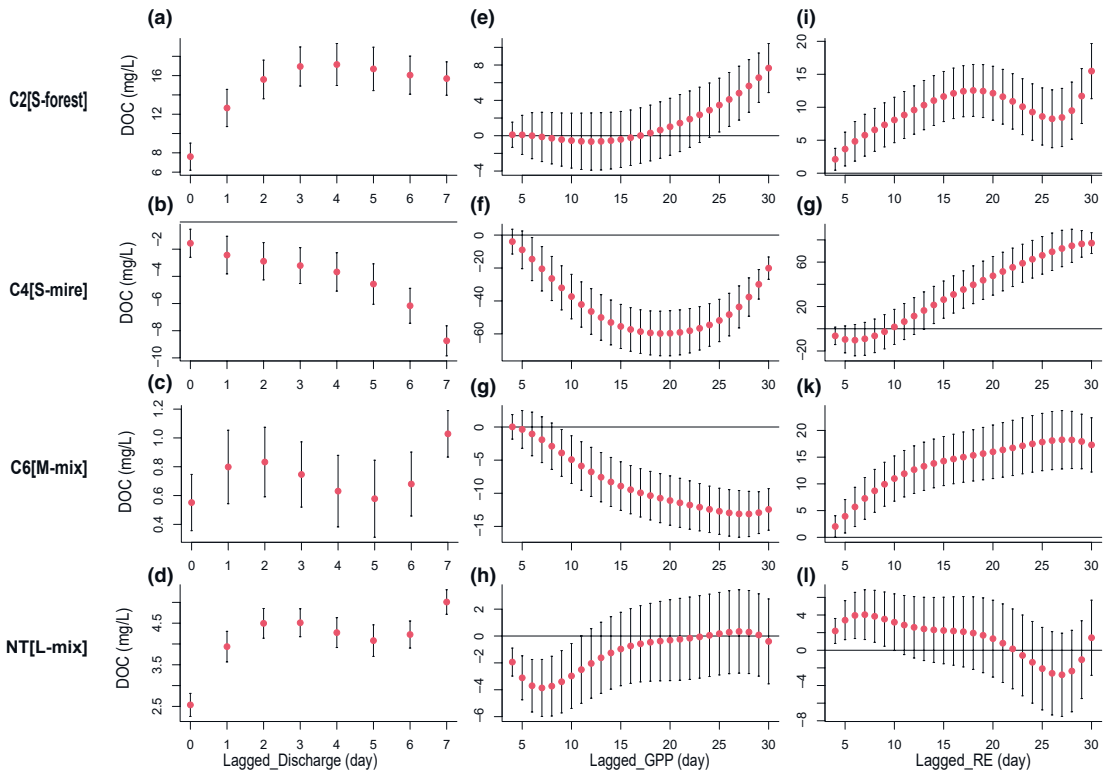


FIGURE 3 Cumulative lag-response of DOC concentrations to 10-unit increase in discharge (a–d), gross primary production (GPP) (e–h), ecosystem respiration (RE) (i–l) in C2[S-forest], C4[S-mire], C6[M-mix] and NT[L-mix] based on DLM6. The horizontal line at 0 represents the mean DOC concentrations

C4[S-mire]) were compared, the effect of forest GPP on catchment DOC was positive, while that of mire was negative. Laudon and Sponseller (2018) confirmed that the landscape always plays a vital role in downstream biogeochemical patterns. Liu et al. (2017) found a positive linear relationship between C input and priming, that priming increased from negative or no priming at low C input to strong positive priming at high C input. In our case, when comparing these two small catchments, the mean GPP values in C2[S-forest] ($3.01 \text{ g C m}^{-2} \text{ d}^{-1}$) are much higher than in C4[S-mire] ($0.78 \text{ g C m}^{-2} \text{ d}^{-1}$), which may also explain the positive contribution of GPP to DOC variations in C2[S-forest] and the negative contribution in C4[S-mire]. Bastida et al. (2019) suggested that priming effects tend to be negative in more mesic sites with higher SOC contents and positive in more arid locations with low SOC contents. Our results also support the association between SOC content and priming. Moreover, the large difference of aboveground plant biomass between C2[S-forest] and C4[S-mire] could be the third reason, as it has been noted that the level of rhizosphere priming effect is positively correlated with aboveground plant biomass (Huo et al., 2017). In our case, C2[S-forest] was totally dominated by forest while C4[S-mire] was covered mainly by wetland, and there is much more aboveground biomass in the former than the latter.

Unlike GPP, RE was consistently positively correlated with DOC exports. These correlations fit the idea that below-ground microbial activity leads to decomposition of complex organic substances into monomers which form the bulk of the DOC (Schimel et al., 1994). The catchment essentially stores the produced DOC in soil water and on soil surfaces, leading to the continued accumulation of DOC until the next precipitation event occurs and flushes out the stored DOC. Hence, low hydrological connectivity implies a delay of DOC export such that the DOC we see today in the stream may often be the DOC produced a while ago (Wen et al., 2020).

The importance of discharge as a carrier of DOC from terrestrial ecosystems cannot be ignored. Approximately 80% of watersheds in the USA and France show significant relationships between the stream DOC concentration and discharge, either positive or negative. Whereas, the remaining watersheds show negligible concentration change with discharge (Wen et al., 2020). In our case, discharge alone could contribute from 9.9% to 68.7% of DOC variations across years in both positive and negative patterns. Dawson et al. (2002) found that the relationship between discharge and DOC can be strengthened if the data was split seasonally, and then discharge could predict from 58% to 81% of DOC values in different seasons. Clark et al. (2007) showed that discharge could explain 72% of DOC

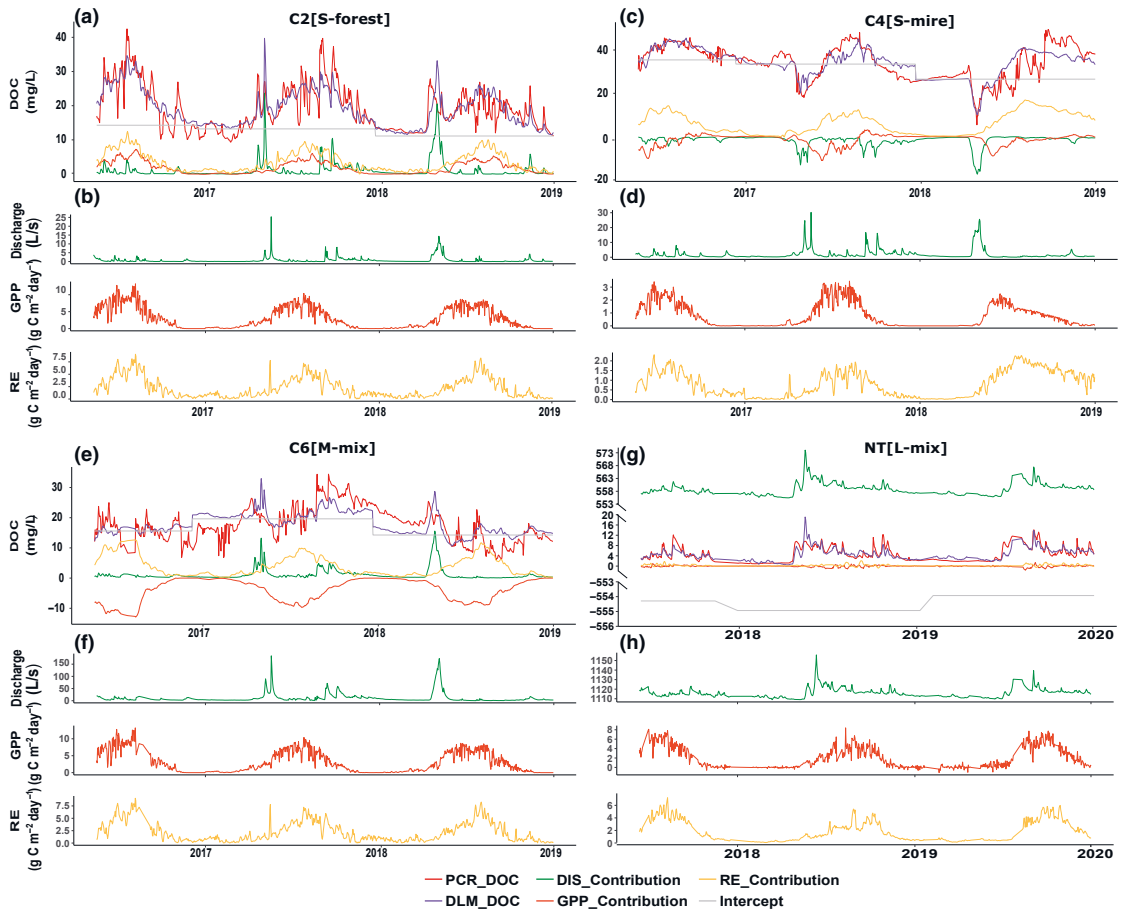


FIGURE 4 The independent contributions of discharge, gross primary production (GPP) and ecosystem respiration (RE) to dissolved organic carbon (DOC) based on DLM6 model in C2[S-forest] (a), C4[S-mire] (c), C6[M-mix] (e), NT[L-mix] (g). PCR_DOC was predicted by the PCR model as the response of DLM6, DLM6 model predicted DLM_DOC; DIS_Contribution was the independent contribution of discharge in DLM6 model; GPP_Contribution was the independent contribution of GPP in DLM6 model; RE_Contribution was the independent contribution of RE in DLM6 model. Continuously measured environmental predictors (discharge, GPP and RE) across years in C2[S-forest] (b), C4[S-mire] (d), C6[M-mix] (f), NT[L-mix] (h)

Site	Size (km ²)	Discharge	GPP	RE	Year	R ²
C2[S-forest]	0.14	9.9% +	53.2% +	2.5% +	3.6%	69.3%
C4[S-mire]	0.19	14.3% -	30.8% -	3.9% +	15.6%	64.5%
C6[M-mix]	1.3	15.0% +	2.2% -	6.1% +	18.6%	41.9%
NT[L-mix]	40	68.7% +	1.0% ns	1.1% ns	2.3%	73.1%

Note: '+'/'-' indicate positive or negative relations with DOC concentrations, respectively.

TABLE 3 Contributions of time-lagged environmental variables (discharge, [GPP] and ecosystem respiration [RE]) to dissolved organic carbon (DOC) concentrations across four catchments based on DLM6

concentrations during autumn storm events, but they also showed a poor relationship during other seasons. Instead of grouping data by season to remove this component of the annual variation (Clark et al., 2007; Dawson et al., 2008), in our DLM models, we included 'year'

as a factor variable without splitting data to keep the continuity and concerned the delay effect of discharge on DOC concentration.

It has been well documented that the hydrological connectivity to the stream versus the distribution of SOC ultimately dictates the

TABLE 4 Mean values and ranges of discharge, gross primary production (GPP) and ecosystem respiration (RE) during the experimental period across four sites

Site ID.	Size (km ²)	Discharge (l s ⁻¹)		GPP (gC m ⁻² d ⁻¹)		RE (gC m ⁻² d ⁻¹)	
		Mean	Range	Mean	Range	Mean	Range
C2[S-forest]	0.14	0.73 ± 1.67	0–25.36	3.01 ± 3.11	0–13.22	2.19 ± 2.00	0–9.05
C4[S-mire]	0.19	1.87 ± 3.24	0.06–30.23	0.78 ± 0.91	0–3.47	0.79 ± 0.66	0–2.32
C6[M-mix]	1.3	10.88 ± 19.95	0.41–184.09	2.94 ± 3.10	0–12.59	2.13 ± 1.97	0–8.95
NT[L-mix]	40	1115.71 ± 4.99	1109–1156	1.94 ± 2.25	0–8.40	1.83 ± 1.65	0.08–7.21

dynamic of DOC concentrations in soil and stream water, leading to different discharge-DOC relationships (Covino, 2017; Wen et al., 2020). In our study, the discharge-DOC relationship shifted from dilution pattern in wetland dominated catchment (C4[S-mire]) to flushing pattern in forest and mixed catchment (C2[S-forest], C6[M-mix] and NT[L-mix]), which is in line with Laudon et al. (2011). The transport of DOC losses from the bulk soil has been linked to hydrological processes in response to precipitation events and changing flow paths through different soil horizons containing contrasting amounts of organic matter (Dawson et al., 2008; Hinton et al., 1998). The contrasts in hydrological functioning of these sites (C4[S-mire] vs. C2[S-forest], C6[M-mix] and NT[L-mix]) is demonstrated by different flow paths. In wetland-dominated streams (C4[S-mire]), event water at the rising stage of hydrograph runoff as overland flow due to frozen wetland surface or saturation, leading to a dilution in DOC concentrations (Laudon et al., 2004). In the other three sites (C2[S-forest], C6[M-mix] and NT[L-mix]), SOC is enriched in uplands, and most of the runoff from forested areas reaches the stream via sub-surface flow paths carrying new activated SOC (Bishop et al., 2004). Therefore, DOC concentrations were high at high flow.

Seasonal variations of DOC concentrations were also observed across the sites in our study. DOC concentrations were usually more stable and lower during the snow cover period compared with the growing season. We assumed that there are several mechanisms driving the low wintertime DOC concentrations. Firstly, DOC sources (litterfall) are relatively limited during winter which partially caused the low wintertime DOC (Jutras et al., 2011; Liu et al., 2014). Worrall et al. (2004) found a pulse of DOC from senescing vegetation at the end of the growing season, which further supports this idea. Secondly, the lower temperatures lead to decreased biological activity, lower decomposition of available organic matter and lower solubility of DOC in wintertime (Dawson et al., 2008). Finally, frozen soil during the wintertime may have reduced the movement of terrestrial organic matter from upland zones and riparian areas to streams, consequently resulting in large fluctuations of DOC concentrations during the snow melt season. (Pacific et al., 2010).

This study demonstrated the importance of terrestrial productivity interacting with discharge in controlling the variations of DOC concentrations in boreal catchments. Forest productivity dramatically promotes DOC contents in small-sized catchments (<1 km²), while the importance of GPP is masked by discharge with increased catchment size. Moreover, our statistical analysis indicated that

priming and the land cover (proportion of forest) should be included in process-based DOC models. Overall, our investigation revealed that terrestrial greening and altering hydrology following climate change may have a major impact on DOC concentration in aquatic ecosystems, as well as reaffirming the importance of DOC fluxes in controlling ecosystem C budgets, which is generally disregarded.

ACKNOWLEDGEMENTS

This work was mainly funded by Kone project (201906598)—‘The role of terrestrial productivity on fluxes of DOC in watersheds (Maaekosysteemien tuottavuuden merkitys liukoisien orgaanisen hiilen virtoihin valuma-alueilla)’ and also supported from the Water JPI and Academy of Finland project REFORMWATER (Academy of Finland Project No. 326818), CASCAS (Academy of Finland Project No. 323997) and the Atmosphere and Climate Competence Center (ACCC) (Academy of Finland Project No. 337550). The Krycklan Catchment Study is funded by the Swedish Infrastructure for Ecosystem Science (SITES), the VR extreme event project, the Swedish Research Council for Sustainable Development (FORMAS) and SKB, while the high-frequency work is supported by the European Union’s Horizon 2020 Research and Innovation Programme under the Marie Skłodowska-Curie (Grant Agreement No. 734317). Research in Varriö station is supported by European Commission-Horizon 2020 Research and innovation programme under Integrative and Comprehensive Understanding on Polar Environments (ICUPE) (Grant Agreement No. 689443) and Flagship funding (Academy of Finland Grant No. 337549) as well as INAR RI Ecosystems (Academy of Finland Grant No. 304460). Funding for co-author Zobitz was provided by the Fulbright Finland Foundation and Saastamoinen Foundation Grant in Health and Environmental Sciences.

DATA AVAILABILITY STATEMENT

Data openly available in a public repository that issues datasets with DOIs.

ORCID

Xudan Zhu  <https://orcid.org/0000-0002-8540-384X>

Liang Chen  <https://orcid.org/0000-0002-1811-5717>

Jukka Pumpanen  <https://orcid.org/0000-0003-4879-3663>

Anne Ojala  <https://orcid.org/0000-0002-7211-4053>

John Zobitz  <https://orcid.org/0000-0002-1830-143X>

Xuan Zhou  <https://orcid.org/0000-0002-3602-5870>
 Hjalmar Laudon  <https://orcid.org/0000-0001-6058-1466>
 Marjo Palviainen  <https://orcid.org/0000-0001-9963-4748>
 Kimmo Neitola  <https://orcid.org/0000-0003-1983-5772>
 Frank Berninger  <https://orcid.org/0000-0001-7718-1661>

REFERENCES

- Asmala, E., Carstensen, J., & Raike, A. (2019). Multiple anthropogenic drivers behind upward trends in organic carbon concentrations in boreal rivers. *Environmental Research Letters*, 14(12), 124018. <https://doi.org/10.1088/1748-9326/ab4fa9>
- Aubinet, M., Vesala, T., & Papale, D. (2012). *Eddy covariance: A practical guide to measurement and data analysis*. Springer Science & Business Media.
- Avagyian, A., Runkle, B. R. K., & Kutzbach, L. (2014). Application of high-resolution spectral absorbance measurements to determine dissolved organic carbon concentration in remote areas. *Journal of Hydrology*, 517, 435–446. <https://doi.org/10.1016/j.jhydrol.2014.05.060>
- Bastida, F., Garca, C., Fierer, N., Eldridge, D. J., Bowker, M. A., Abades, S., Alfaro, F. D., Asefaw Berhe, A., Cutler, N. A., Gallardo, A., Garca-Velazquez, L., Hart, S. C., Hayes, P. E., Hernandez, T., Hseu, Z.-Y., Jehmlich, N., Kirchmair, M., Lambers, H., Neuhauser, S., ... Delgado-Baquerizo, M. (2019). Global ecological predictors of the soil priming effect. *Nature Communications*, 10(1), 3481. <https://doi.org/10.1038/s41467-019-11472-7>
- Bengtsson, M. M., Attermeyer, K., & Catalan, N. (2018). Interactive effects on organic matter processing from soils to the ocean: Are priming effects relevant in aquatic ecosystems? *Hydrobiologia*, 822(1), 1–17. <https://doi.org/10.1007/s10750-018-3672-2>
- Bishop, K., Seibert, J., Kohler, S., & Laudon, H. (2004). Resolving the double paradox of rapidly mobilized old water with highly variable responses in runoff chemistry. *Hydrological Processes*, 18(1), 185–189. <https://doi.org/10.1002/hyp.5209>
- Black, K., Bolger, T., Davis, P., Nieuwenhuis, M., Reidy, B., Saiz, G., Tobin, B., & Osborne, B. (2007). Inventory and eddy covariance-based estimates of annual carbon sequestration in a Sitka spruce (*Picea sitchensis* (Bong.) Carr.) forest ecosystem. *European Journal of Forest Research*, 126(2), 167–178. <https://doi.org/10.1007/s10342-005-0092-4>
- Burns, D. A., McHale, M. R., Driscoll, C. T., & Roy, K. M. (2006). Response of surface water chemistry to reduced levels of acid precipitation: Comparison of trends in two regions of New York, USA. *Hydrological Processes*, 20(7), 1611–1627. <https://doi.org/10.1002/hyp.5961>
- Catalan, N., Kellerman, A. M., Peter, H., Carmona, F., & Tranvik, L. J. (2015). Absence of a priming effect on dissolved organic carbon degradation in lake water. *Limnology and Oceanography*, 60(1), 159–168. <https://doi.org/10.1002/lno.10016>
- Clark, J. M., Lane, S. N., Chapman, P. J., & Adamson, J. K. (2007). Export of dissolved organic carbon from an upland peatland during storm events: Implications for flux estimates. *Journal of Hydrology*, 347(3), 438–447. <https://doi.org/10.1016/j.jhydrol.2007.09.030>
- Cole, J. J., Prairie, Y. T., Caraco, N. F., McDowell, W. H., Tranvik, L. J., Striegl, R. G., Duarte, C. M., Kortelainen, P., Downing, J. A., Middelburg, J. J., & Melack, J. (2007). Plumbing the global carbon cycle: Integrating inland waters into the terrestrial carbon budget. *Ecosystems*, 10(1), 172–185. <https://doi.org/10.1007/s10021-006-9013-8>
- Conley, D. J., Carstensen, J., Aigars, J., Axe, P., Bonsdorff, E., Eremina, T., Haahti, B.-M., Humborg, C., Jonsson, P., Kotta, J., Lannegren, C., Larsson, U., Maximov, A., Medina, M. R., Lysiak-Pastuszak, E., Remeikaitė-Nikiėnė, N., Walve, J., Wilhelms, S., & Zillen, L. (2011). Hypoxia is increasing in the coastal zone of the Baltic sea. *Environmental Science & Technology*, 45(16), 6777–6783. <https://doi.org/10.1021/es201212r>
- Covino, T. (2017). Hydrologic connectivity as a framework for understanding biogeochemical flux through watersheds and along fluvial networks. *Geomorphology*, 277, 133–144. <https://doi.org/10.1016/j.geomorph.2016.09.030>
- Dawson, J. J. C., Billelt, M. F., Neal, C., & Hill, S. (2002). A comparison of particulate, dissolved and gaseous carbon in two contrasting upland streams in the UK. *Journal of Hydrology*, 257(1), 226–246. [https://doi.org/10.1016/S0022-1694\(01\)00545-5](https://doi.org/10.1016/S0022-1694(01)00545-5)
- Dawson, J. J. C., Soulsby, C., Tetzlaff, D., Hrachowitz, M., Dunn, S. M., & Malcolm, I. A. (2008). Influence of hydrology and seasonality on DOC exports from three contrasting upland catchments. *Biogeochemistry*, 90(1), 93–113. <https://doi.org/10.1007/s10533-008-9234-3>
- Dijkstra, F., Carrillo, Y., Pendall, E., & Morgan, J. (2013). Rhizosphere priming: A nutrient perspective. *Frontiers in Microbiology*, 4, 216. <https://doi.org/10.3389/fmicb.2013.00216>
- Ding, F., Van Zwieten, L., Zhang, W., Weng, Z., Shi, S., Wang, J., & Meng, J. (2018). A meta-analysis and critical evaluation of influencing factors on soil carbon priming following biochar amendment. *Journal of Soils and Sediments*, 18(4), 1507–1517. <https://doi.org/10.1007/s11368-017-1899-6>
- Drought 2018 Team & ICOS Ecosystem Thematic Centre. (2020). Drought-2018 ecosystem eddy covariance flux product for 52 stations in FLUXNET-Archive format. <https://doi.org/10.18160/YVRO-4898>
- Ekstrom, S. (2013). Brownification of freshwaters—The role of dissolved organic matter and iron [Thesis/doccomp, Lund University]. <http://lup.lub.lu.se/record/4076293>
- Ellis, T., Hill, P. W., Fenner, N., Williams, G. G., Godbold, D., & Freeman, C. (2009). The interactive effects of elevated carbon dioxide and water table draw-down on carbon cycling in a Welsh ombrotrophic bog. *Ecological Engineering*, 35(6), 978–986. <https://doi.org/10.1016/j.ecoleng.2008.10.011>
- Evans, C. D., Monteith, D. T., & Cooper, D. M. (2005). Long-term increases in surface water dissolved organic carbon: Observations, possible causes and environmental impacts. *Environmental Pollution*, 137(1), 55–71. <https://doi.org/10.1016/j.envpol.2004.12.031>
- Filella, M., & Rodriguez-Murillo, J. C. (2014). Long-term trends of organic carbon concentrations in freshwaters: Strengths and weaknesses of existing evidence. *Water*, 6(5), 1360–1418. <https://doi.org/10.3390/w6051360>
- Finstad, A. G., Andersen, T., Larsen, S., Tominaga, K., Blumentrath, S., de Wit, H. A., Tømmervik, H., & Hessen, D. O. (2016). From greening to browning: Catchment vegetation development and reduced S-deposition promote organic carbon load on decadal time scales in Nordic lakes. *Scientific Reports*, 6(1), 31944. <https://doi.org/10.1038/srep31944>
- Freeman, C., Fenner, N., Ostle, N. J., Kang, H., Dowrick, D. J., Reynolds, B., Lock, M. A., Sleep, D., Hughes, S., & Hudson, J. (2004). Export of dissolved organic carbon from peatlands under elevated carbon dioxide levels. *Nature*, 430(6996), 195–198. <https://doi.org/10.1038/nature02707>
- Gasparrini, A. (2011). Distributed Lag Linear and Non-Linear models in R: The package dlm. *Journal of Statistical Software*, 43(1), 1–20. <https://doi.org/10.18637/jss.v043.i08>
- Grinsted, A., Moore, J. C., & Jevrejeva, S. (2004). Application of the cross wavelet transform and wavelet coherence to geophysical time series. *Nonlinear Processes in Geophysics*, 11(5/6), 561–566. <https://doi.org/10.5194/npg-11-561-2004>
- Guenet, B., Danger, M., Abbadie, L., & Lacroix, G. (2010). Priming effect: Bridging the gap between terrestrial and aquatic ecology. *Ecology*, 91(10), 2850–2861. <https://doi.org/10.1890/09-1968.1>
- He, Y., Cheng, W., Zhou, L., Shao, J., Liu, H., Zhou, H., Zhu, K., & Zhou, X. (2020). Soil DOC release and aggregate disruption mediate rhizosphere priming effect on soil C decomposition. *Soil Biology and Biochemistry*, 144, 107787. <https://doi.org/10.1016/j.soilbio.2020.107787>

- Heinonsalo, J., Pumpanen, J., Rasilo, T., Hurme, K.-R., & Ilvesniemi, H. (2010). Carbon partitioning in ectomycorrhizal Scots pine seedlings. *Soil Biology and Biochemistry*, 42(9), 1614–1623. <https://doi.org/10.1016/j.soilbio.2010.06.003>
- Hinton, M. J., Schiff, S. L., & English, M. C. (1998). Sources and flowpaths of dissolved organic carbon during storms in two forested watersheds of the precambrian shield. *Biogeochemistry*, 41(2), 175–197. <https://doi.org/10.1023/A:1005903428956>
- Holden, J., Chapman, P. J., & Labadz, J. C. (2004). Artificial drainage of peatlands: Hydrological and hydrochemical process and wetland restoration. *Progress in Physical Geography: Earth and Environment*, 28(1), 95–123. <https://doi.org/10.1191/0309133304pp403ra>
- Hongve, D., Riise, G., & Kristiansen, J. F. (2004). Increased colour and organic acid concentrations in Norwegian forest lakes and drinking water—A result of increased precipitation? *Aquatic Sciences*, 66(2), 231–238. <https://doi.org/10.1007/s00027-004-0708-7>
- Huo, C., Luo, Y., & Cheng, W. (2017). Rhizosphere priming effect: A meta-analysis. *Soil Biology and Biochemistry*, 111, 78–84. <https://doi.org/10.1016/j.soilbio.2017.04.003>
- Hyndman, R. J., & Khandakar, Y. (2008). Automatic time series forecasting: The forecast package for R. *Journal of Statistical Software*, 27(3). <https://doi.org/10.18637/jss.v027.i03>
- Jutras, M.-F., Nasr, M., Castonguay, M., Pit, C., Pomeroy, J. H., Smith, T. P., Zhang, C., Ritchie, C. D., Meng, F.-R., Clair, T. A., & Arp, P. A. (2011). Dissolved organic carbon concentrations and fluxes in forest catchments and streams: DOC-3 model. *Ecological Modelling*, 222(14), 2291–2313. <https://doi.org/10.1016/j.ecolmodel.2011.03.035>
- Kang, H., Kwon, M. J., Kim, S., Lee, S., Jones, T. G., Johncock, A. C., Haraguchi, A., & Freeman, C. (2018). Biologically driven DOC release from peatlands during recovery from acidification. *Nature Communications*, 9(1), 3807. <https://doi.org/10.1038/s41467-018-06259-1>
- Keller, B. W., Paterson, A. M., Somers, K. M., Dillon, P. J., Heneberry, J., & Ford, A. (2008). Relationships between dissolved organic carbon concentrations, weather, and acidification in small Boreal Shield lakes. *Canadian Journal of Fisheries and Aquatic Sciences*, 65(5), 786–795. <https://doi.org/10.1139/f07-193>
- Kritzberg, E. S., Hasselquist, E. M., Škerlep, M., Löfgren, S., Olsson, O., Stadmark, J., Valinia, S., Hansson, L.-A., & Laudon, H. (2020). Browning of freshwaters: Consequences to ecosystem services, underlying drivers, and potential mitigation measures. *Ambio*, 49(2), 375–390. <https://doi.org/10.1007/s13280-019-01227-5>
- Kulmala, L., Pumpanen, J., Kolari, P., Dengel, S., Berninger, F., Köster, K., Matkala, L., Vanhatalo, A., Vesala, T., & Bäck, J. (2019). Inter- and intra-annual dynamics of photosynthesis differ between forest floor vegetation and tree canopy in a subarctic Scots pine stand. *Agricultural and Forest Meteorology*, 271, 1–11. <https://doi.org/10.1016/j.agrformet.2019.02.029>
- Kumar, P., & Fofoula-Georgiou, E. (1997). Wavelet analysis for geophysical applications. *Reviews of Geophysics*, 35(4), 385–412. <https://doi.org/10.1029/97RG00427>
- Kuzyakov, Y. (2002). Review: Factors affecting rhizosphere priming effects. *Journal of Plant Nutrition and Soil Science*, 165(4), 382–396.
- Kuzyakov, Y. (2010). Priming effects: Interactions between living and dead organic matter. *Soil Biology and Biochemistry*, 42(9), 1363–1371. <https://doi.org/10.1016/j.soilbio.2010.04.003>
- Kuzyakov, Y., Friedel, J. K., & Stahr, K. (2000). Review of mechanisms and quantification of priming effects. *Soil Biology and Biochemistry*, 32(11), 1485–1498. [https://doi.org/10.1016/S0038-0717\(00\)00084-5](https://doi.org/10.1016/S0038-0717(00)00084-5)
- Laudon, H., Berggren, M., Ågren, A., Buffam, I., Bishop, K., Grabs, T., Jansson, M., & Köhler, S. (2011). Patterns and dynamics of dissolved organic carbon (DOC) in boreal streams: The role of processes, connectivity, and scaling. *Ecosystems*, 14(6), 880–893. <https://doi.org/10.1007/s10021-011-9452-8>
- Laudon, H., Hasselquist, E. M., Peichl, M., Lindgren, K., Sponseller, R., Lidman, F., Kuglerová, L., Hasselquist, N. J., Bishop, K., Nilsson, M. B., & Ågren, A. M. (2021). Northern landscapes in transition: Evidence, approach and ways forward using the Krycklan Catchment Study. *Hydrological Processes*, 35(4), e14170. <https://doi.org/10.1002/hyp.14170>
- Laudon, H., Köhler, S., & Buffam, I. (2004). Seasonal TOC export from seven boreal catchments in northern Sweden. *Aquatic Sciences—Research across Boundaries*, 66(2), 223–230. <https://doi.org/10.1007/s00027-004-0700-2>
- Laudon, H., & Sponseller, R. A. (2018). How landscape organization and scale shape catchment hydrology and biogeochemistry: Insights from a long-term catchment study. *Wires Water*, 5(2), e1265. <https://doi.org/10.1002/wat2.1265>
- Laudon, H., Taberman, I., Ågren, A., Futter, M., Ottosson-Löfvenius, M., & Bishop, K. (2013). The Krycklan Catchment Study—A flagship infrastructure for hydrology, biogeochemistry, and climate research in the boreal landscape. *Water Resources Research*, 49(10), 7154–7158. <https://doi.org/10.1002/wrcr.20520>
- Ledesma, J. L. J., Grabs, T., Bishop, K. H., Schiff, S. L., & Köhler, S. J. (2015). Potential for long-term transfer of dissolved organic carbon from riparian zones to streams in boreal catchments. *Global Change Biology*, 21(8), 2963–2979. <https://doi.org/10.1111/gcb.12872>
- Lidman, F., Boily, Å., Laudon, H., & Köhler, S. J. (2017). From soil water to surface water—How the riparian zone controls element transport from a boreal forest to a stream. *Biogeochemistry*, 14(12), 3001–3014. <https://doi.org/10.5194/bg-14-3001-2017>
- Linkosalmi, M., Pumpanen, J., Biasi, C., Heinonsalo, J., Laiho, R., Lindén, A., Palonen, V., Laurila, T., & Lohila, A. (2015). Studying the impact of living roots on the decomposition of soil organic matter in two different forestry-drained peatlands. *Plant and Soil*, 396(1–2), 59–72. <https://doi.org/10.1007/s11104-015-2584-4>
- Liu, W., Xu, X., McGoff, N. M., Eaton, J. M., Leahy, P., Foley, N., & Kiely, G. (2014). Spatial and seasonal variation of dissolved organic carbon (DOC) concentrations in Irish streams: Importance of soil and topography characteristics. *Environmental Management*, 53(5), 959–967. <https://doi.org/10.1007/s00267-014-0259-1>
- Liu, X.-J. A., Sun, J., Mau, R. L., Finley, B. K., Compson, Z. G., van Gestel, N., Brown, J. R., Schwartz, E., Dijkstra, P., & Hungate, B. A. (2017). Labile carbon input determines the direction and magnitude of the priming effect. *Applied Soil Ecology*, 109, 7–13. <https://doi.org/10.1016/j.apsoil.2016.10.002>
- Mann, P. J., Davydova, A., Zimov, N., Spencer, R. G. M., Davydov, S., Bulygina, E., Zimov, S., & Holmes, R. M. (2012). Controls on the composition and lability of dissolved organic matter in Siberia's Kolyma River basin. *Journal of Geophysical Research: Biogeosciences*, 117(G1). <https://doi.org/10.1029/2011JG001798>
- McGlynn, B. L., McDonnell, J. J., Shanley, J. B., & Kendall, C. (1999). Riparian zone flowpath dynamics during snowmelt in a small headwater catchment. *Journal of Hydrology*, 222(1), 75–92. [https://doi.org/10.1016/S0022-1694\(99\)00102-X](https://doi.org/10.1016/S0022-1694(99)00102-X)
- Medlyn, B. E., Robinson, A. P., Clement, R., & McMurtrie, R. E. (2005). On the validation of models of forest CO₂ exchange using eddy covariance data: Some perils and pitfalls. *Tree Physiology*, 25(7), 839–857. <https://doi.org/10.1093/treephys/25.7.839>
- Mevik, B.-H., Wehrens, R., & Liland, K. H. (2019). pls: Partial least squares and principal component regression. <https://CRAN.R-project.org/package=pls>
- Monteith, D. T., Stoddard, J. L., Evans, C. D., de Wit, H. A., Forsius, M., Högåsen, T., Wilander, A., Skjelkvåle, B. L., Jeffries, D. S., Vuorenmaa, J., Keller, B., Kopáček, J., & Vesely, J. (2007). Dissolved organic carbon trends resulting from changes in atmospheric deposition chemistry. *Nature*, 450(7169), 537–540. <https://doi.org/10.1038/nature06316>
- Nieminen, M., Sarkkola, S., Sallantausta, T., Hasselquist, E. M., & Laudon, H. (2021). Peatland drainage—A missing link behind increasing TOC concentrations in waters from high latitude forest catchments? *Science of the Total Environment*, 774, 145150. <https://doi.org/10.1016/j.scitotenv.2021.145150>

- Nilsson, M., Sagerfors, J., Buffam, I., Laudon, H., Eriksson, T., Grelle, A., Klemetsson, L., Weslien, P., & Lindroth, A. (2008). Contemporary carbon accumulation in a boreal oligotrophic minerogenic mire—A significant sink after accounting for all C-fluxes. *Global Change Biology*, 14(10), 2317–2332. <https://doi.org/10.1111/j.1365-2486.2008.01654.x>
- Öquist, M. G., Bishop, K., Grelle, A., Klemetsson, L., Köhler, S. J., Laudon, H., Lindroth, A., Ottosson Löfvenius, M., Wallin, M. B., & Nilsson, M. B. (2014). The full annual carbon balance of boreal forests is highly sensitive to precipitation. *Environmental Science & Technology Letters*, 1(7), 315–319. <https://doi.org/10.1021/ez500169j>
- Pacific, V. J., Jencso, K. G., & McGlynn, B. L. (2010). Variable flushing mechanisms and landscape structure control stream DOC export during snowmelt in a set of nested catchments. *Biogeochemistry*, 99(1), 193–211. <https://doi.org/10.1007/s10533-009-9401-1>
- Papale, D., Reichstein, M., Aubinet, M., Canfora, E., Bernhofer, C., Kutsch, W., Longdoz, B., Rambal, S., Valentini, R., Vesala, T., & Yakir, D. (2006). Towards a standardized processing of net ecosystem exchange measured with eddy covariance technique: Algorithms and uncertainty estimation. *Biogeosciences*, 3(4), 571–583. <https://doi.org/10.5194/bg-3-571-2006>
- Pastorello, G., Trotta, C., Canfora, E., Chu, H., Christianson, D., Cheah, Y.-W., Poindexter, C., Chen, J., Elbashandy, A., Humphrey, M., Isaac, P., Polidori, D., Reichstein, M., Ribeca, A., van Ingen, C., Vuichard, N., Zhang, L., Amiro, B., Ammann, C., ... Papale, D. (2020). The FLUXNET2015 dataset and the ONEFlux processing pipeline for eddy covariance data. *Scientific Data*, 7(1), 225. <https://doi.org/10.1038/s41597-020-0534-3>
- Pohjonen, V., Mönkkönen, P., & Hari, P. (2008). Test of northern timber line. *Boreal Forest and Climate Change*, 472–475.
- Pumpanen, J. S., Heinonsalo, J., Rasilo, T., Hurme, K.-R., & Ilvesniemi, H. (2009). Carbon balance and allocation of assimilated CO₂ in Scots pine, Norway spruce, and Silver birch seedlings determined with gas exchange measurements and ¹⁴C pulse labelling. *Trees*, 23(3), 611–621. <https://doi.org/10.1007/s00468-008-0306-8>
- Pumpanen, J., Lindén, A., Miettinen, H., Kolari, P., Ilvesniemi, H., Mammarella, I., Hari, P., Nikinmaa, E., Heinonsalo, J., Bäck, J., Ojala, A., Berninger, F., & Vesala, T. (2014). Precipitation and net ecosystem exchange are the most important drivers of DOC flux in upland boreal catchments. *Journal of Geophysical Research: Biogeosciences*, 119(9), 1861–1878. <https://doi.org/10.1002/2014JG002705>
- Qiao, N., Schaefer, D., Blagodatskaya, E., Zou, X., Xu, X., & Kuzyakov, Y. (2014). Labile carbon retention compensates for CO₂ released by priming in forest soils. *Global Change Biology*, 20(6), 1943–1954. <https://doi.org/10.1111/gcb.12458>
- R Core Team. (2019). *R: A language and environment for statistical computing*. R Foundation for Statistical Computing. <https://www.R-project.org/>
- Rode, M., Wade, A. J., Cohen, M. J., Hensley, R. T., Bowes, M. J., Kirchner, J. W., Arhonditsis, G. B., Jordan, P., Kronvang, B., Halliday, S. J., Skeffington, R. A., Rozemeijer, J. C., Aubert, A. H., Rinke, K., & Jomaa, S. (2016). Sensors in the stream: The high-frequency wave of the present. *Environmental Science & Technology*, 50(19), 10297–10307. <https://doi.org/10.1021/acs.est.6b02155>
- Roulet, N., & Moore, T. R. (2006). Browning the waters. *Nature*, 444(7117), 283–284. <https://doi.org/10.1038/444283a>
- Schimel, D. S., Braswell, B. H., Holland, E. A., McKeown, R., Ojima, D. S., Painter, T. H., Parton, W. J., & Townsend, A. R. (1994). Climatic, edaphic, and biotic controls over storage and turnover of carbon in soils. *Global Biogeochemical Cycles*, 8(3), 279–293. <https://doi.org/10.1029/94GB00993>
- Schlesinger, W. H., & Andrews, J. A. (2000). Soil respiration and the global carbon cycle. *Biogeochemistry*, 48(1), 7–20. <https://doi.org/10.1023/A:1006247623877>
- Schmidbauer, H., & Roesch, A. (2018). WaveletComp 1.1: A guided tour through the R package.
- Shanley, J. B., Kendall, C., Smith, T. E., Wolock, D. M., & McDonnell, J. J. (2002). Controls on old and new water contributions to stream flow at some nested catchments in Vermont, USA. *Hydrological Processes*, 16(3), 589–609. <https://doi.org/10.1002/hyp.312>
- Strohmenger, L., Fovet, O., Hrachowitz, M., Salmon-Monviola, J., & Gascuel-Odoux, C. (2021). Is a simple model based on two mixing reservoirs able to reproduce the intra-annual dynamics of DOC and NO₃ stream concentrations in an agricultural headwater catchment? *Science of the Total Environment*, 794, 148715. <https://doi.org/10.1016/j.scitotenv.2021.148715>
- Sullivan, B. W., & Hart, S. C. (2013). Evaluation of mechanisms controlling the priming of soil carbon along a substrate age gradient. *Soil Biology and Biochemistry*, 58, 293–301. <https://doi.org/10.1016/j.soilbio.2012.12.007>
- Tank, S. E., Striegl, R. G., McClelland, J. W., & Kokelj, S. V. (2016). Multi-decadal increases in dissolved organic carbon and alkalinity flux from the Mackenzie drainage basin to the Arctic Ocean. *Environmental Research Letters*, 11(5), 54015. <https://doi.org/10.1088/1748-9326/11/5/054015>
- Tiwari, T., Buffam, I., Sponseller, R. A., & Laudon, H. (2017). Inferring scale-dependent processes influencing stream water biogeochemistry from headwater to sea. *Limnology and Oceanography*, 62(S1), S58–S70. <https://doi.org/10.1002/lno.10738>
- Vargas, R., Baldocchi, D. D., Bahn, M., Hanson, P. J., Hosman, K. P., Kulmala, L., Pumpanen, J., & Yang, B. (2011). On the multi-temporal correlation between photosynthesis and soil CO₂ efflux: Reconciling lags and observations. *New Phytologist*, 191(4), 1006–1017. <https://doi.org/10.1111/j.1469-8137.2011.03771.x>
- Vehkamäki, H., Dal Maso, M., Hussein, T., Flanagan, R., Hyvärinen, A., Lauros, J., Merikanto, P., Mönkkönen, M., Pihlatie, K., Salminen, K., Sogacheva, L., Thum, T., Ruuskanen, T. M., Keronen, P., Aalto, P. P., Hari, P., Lehtinen, K. E. J., Rannik, Ü., & Kulmala, M. (2004a). Atmospheric particle formation events at Värrö measurement station in Finnish Lapland 1998–2002. *Atmospheric Chemistry and Physics*, 4(7), 2015–2023. <https://doi.org/10.5194/acp-4-2015-2004>
- Vehkamäki, H., Dal Maso, M., Hussein, T., Flanagan, R., Hyvärinen, A., Lauros, J., Merikanto, P., Mönkkönen, M., Pihlatie, K., Salminen, K., Sogacheva, L., Thum, T., Ruuskanen, T. M., Keronen, P., Aalto, P. P., Hari, P., Lehtinen, K. E. J., Rannik, Ü., & Kulmala, M. (2004b). Atmospheric particle formation events at Värrö measurement station in Finnish Lapland 1998–2002. *Atmospheric Chemistry and Physics*, 4(7), 2015–2023. <https://doi.org/10.5194/acp-4-2015-2004>
- Villnäs, A., & Norkko, A. (2011). Benthic diversity gradients and shifting baselines: Implications for assessing environmental status. *Ecological Applications*, 21(6), 2172–2186. <https://doi.org/10.1890/10-1473.1>
- Vuorenmaa, J., Forsius, M., & Mannio, J. (2006). Increasing trends of total organic carbon concentrations in small forest lakes in Finland from 1987 to 2003. *Science of the Total Environment*, 365(1), 47–65. <https://doi.org/10.1016/j.scitotenv.2006.02.038>
- Wen, H., Perdrial, J., Bernal, S., Abbott, B. W., Dupas, R., Godsey, S. E., Harpold, A., Rizzo, D., Underwood, K., Adler, T., Hale, R., Sterle, G., & Li, L. (2020). Temperature controls production but hydrology controls export of dissolved organic carbon at the catchment scale. *Hydrology and Earth System Sciences*, 24, 1–22. <https://digital.csic.es/handle/10261/199199>
- Wilson, H. F., & Xenopoulos, M. A. (2008). Ecosystem and seasonal control of stream dissolved organic carbon along a gradient of land use. *Ecosystems*, 11(4), 555–568. <https://doi.org/10.1007/s10021-008-9142-3>

- Worrall, F., Harriman, R., Evans, C. D., Watts, C. D., Adamson, J., Neal, C., Tipping, E., Burt, T., Grieve, I., Monteith, D., Naden, P. S., Nisbet, T., Reynolds, B., & Stevens, P. (2004). Trends in dissolved organic carbon in UK rivers and lakes. *Biogeochemistry*, 70(3), 369–402. <https://doi.org/10.1007/s10533-004-8131-7>
- Xu, H., & Guo, L. (2018). Intriguing changes in molecular size and composition of dissolved organic matter induced by microbial degradation and self-assembly. *Water Research*, 135, 187–194. <https://doi.org/10.1016/j.watres.2018.02.016>
- Zhu, X., Chen, L., Pumpanen, J., Keinänen, M., Laudon, H., Ojala, A., Palviainen, M., Kiirikki, M., Neitola, K., & Berninger, F. (2020). Assessment of a portable UV-Vis spectrophotometer's performance for stream water DOC and Fe content monitoring in remote areas. *Talanta*, 224, 121919. <https://doi.org/10.1016/j.talanta.2020.121919>

SUPPORTING INFORMATION

Additional supporting information may be found in the online version of the article at the publisher's website.

How to cite this article: Zhu, X., Chen, L., Pumpanen, J., Ojala, A., Zobitz, J., Zhou, X., Laudon, H., Palviainen, M., Neitola, K., & Berninger, F. (2022). The role of terrestrial productivity and hydrology in regulating aquatic dissolved organic carbon concentrations in boreal catchments. *Global Change Biology*, 00, 1–15. <https://doi.org/10.1111/gcb.16094>

III

Several mechanisms drive the heterogeneity in browning across a boreal stream network.

Zhu, X., Berninger, F., Chen, L., Larson, J., Sponseller, R. A., & Laudon, H.

2023

Submitted manuscript.



XUDAN ZHU

Recent decades have witnessed a notable increase in dissolved organic carbon (DOC) concentrations across many boreal catchments, called aquatic browning. This phenomenon has far-reaching ecological, social and global carbon cycle implications. This thesis improves our mechanistic understanding of short-term variations and long-term trends in surface water DOC. It highlights the significance of considering multifaceted, spatially structured, and non-stationary drivers into predicting future trends of browning.



UNIVERSITY OF
EASTERN FINLAND

uef.fi

**PUBLICATIONS OF
THE UNIVERSITY OF EASTERN FINLAND**
Dissertations in Science, Forestry and Technology

ISBN 978-952-61-5175-5
ISSN 2954-131X